A Study of Topological Defects in Gauge Field Theories

By

Rimsha Tariq

Department of Physics

Quaid-i-Azam University Islamabad, Pakistan

(2021-2023)

A Study of Topological Defects in Gauge Field Theories

By

Rimsha Tariq

Department of Physics

Quaid-i-Azam University Islamabad, Pakistan

(2021-2023)

A DISSERTATION SUBMITTED IN PARTIAL FULFILLMENT OF THE REQUIREMENTS FOR THE DEGREE OF MASTERS OF PHILOSOPHY IN PHYSICS AT THE QUAID-I-AZAM UNIVERSITY, ISLAMABAD 45320, PAKISTAN. SEPTEMBER ,2023.

DECLARATION

I, Ms. **Rimsha Tariq** Roll No.**02182111014**, student of M.Phil., in the subject of Physics session 2021-23, hereby declare that the matter printed in the thesis titled **"A Study of Topological Defects in Gauge Field Theories"** is my review work and has not been printed, published or submitted as research work, thesis or publication in any form in any University, Research Institution etc. in Pakistan.

Dated 13th September, 2023

RESEARCH COMPLETION CERTIFICATE

Certified that the research work contained in the thesis titled A Study of Topological Defects in Gauge Field Theories has been carried out and completed by Ms. Rimsha Tariq Roll No. 02182111014 under my supervision.

Supervised by:

_____

Prof. Dr. Mansoor-Ur-Rehman
Department of Physics
Quaid-i-Azam University Islamabad

Submitted through:

_____

Prof. Dr. Kashif Sabeeh
Chairperson
Department of Physics
Quaid-i-Azam University Islamabad

To

My ***Nano****(Late),*

My Beloved ***Parents****,*

My Supportive ***Siblings***

and

Honorable Mentor

Prof. Dr. Mansoor-Ur-Rehman*.*

Acknowledgments

All praises and gratitude to Allah Almighty — the Supreme-Creator, the All-Knowing, the All-Praise-Worthy — for bestowing upon me the knowledge, wisdom, and courage to achieve my ambitions. All of my achievements, from drawing my first breath to the submission of this dissertation, are only possible because of His providence, constant help, and guidance. Many thanks and Durood-o-Salam to our Holy Prophet Muhammad(SAW) — the Perfect Mentor — who brought humanity from utter darkness to light and encouraged them to pursue and cherish knowledge.

I offer my deepest regard and respect to my supervisor Prof. Dr. Mansoor-Ur-Rehman for the encouragement, kindness, and forbearance. It is a great honor and pleasure for me to work under his supervision and to learn from him. His belief enabled me in broadening and improving my capabilities in physics and in accomplishing this task.

My heartfelt thanks to my beloved Mama and Papa, whose ever-present love, support, upbringing, faith and encouragement has made me what I am today. Special thanks to my Papa for being the guiding star whose constant presence and enlightenment helped me in achieving so much throughout my life. After my parents, my siblings — Ali, Wardah, and Ahmed — are the reason behind my motivation to strive for the best. Their love, friendship, and support proved to be a booster. I am eternally grateful to my Nano(late) for providing me with the sense of love and belongingness that shaped me as a person.

A special bow of honor to all my teachers specially Ma'am Shabnum, Ma'am Rukhsana, and Ma'am Gohar, who worked on me, believed in me and enabled me to come this far. My profound regards to all my seniors and research colleagues specially Adeela Afzal and Rajaab Khan for providing a good environment to learn and absorb knowledge. I am also very grateful to my friends Maria Rasheed, Huma Arshad, Rafeha Farooq, and Fareeha Malik, for making this journey worth remembering.

A special mention would be Maria Mehmood for being the loveliest elder sister whom I bothered the most and the relationship with whom I will cherish forever. Words are not enough to express my feelings, but still Thank you Aapi for being always there for me, pampering me, encouraging me, and guiding me. Lastly, I would like to acknowledge my best friend Sania Asghar, who is always there for me through every thick and thin and whose friendship is priceless to me.

Rimsha Tariq

Have they not observed the sky above them:
how We have structured it and adorned it,
and how there are no rifts therein?
Al-Quran, 50:6.

Abstract

Topological defects — remnants of the early universe — are produced during the spontaneous symmetry breaking of a gauge field theory. These relics have a significant role in explaining many cosmic phenomena. Magnetic monopoles are, in particular, intriguing as they preserve electromagnetic symmetry. The mass and structure of monopoles are model-dependent factors, varying from grand unified scale to electroweak scale. Therefore, we will try to develop thorough understanding of the magnetic monopoles starting from Dirac's prediction to considering them as topological solitons. Afterwards, we will discuss different theories that provide an insight into monopoles of TeV range; they can be detected through the current energy range colliders and help to verify the complete correctness of the standard model. While the discovery of these particles remains elusive, we will still look into experimental bounds that are placed on their flux, masses, and charges. The existence of monopoles cannot be ruled out, as there are systems in which they appear as emergent particles. So, we will try to shed some light on these condensed matter systems. However, the prediction of monopoles in the standard model poses a problem as they don't remain topologically stable during the electroweak symmetry breaking. Hence, our prime focus in this manuscript is to achieve homotopically stable, finite-energy light monopoles for their immense importance.

Contents

List of Figures

List of Tables

Chapter 1

Introduction

In winter, with every decline in temperature, the surface of a pond swiftly turns into ice. The fact is that this surface layer will not evolve in a uniform or featureless fashion. Instead, the icy plates formed independently at multiple locations(as seen in figure 1.1) join up and create zig-zag borders between them due to random merging. Physicists refer to these erratic boundaries as "**Topological Defects**." The reason for calling it a defect is that these are remnants of the creation of uncorrelated domains during phase transition, which thenceforth merges [1]. Since topological factors are the basis of their existence and their proper explanation entails symmetry concepts found in topology (a branch of Mathematics in which smooth deformations do not affect a particular property of a system), they are termed topological.

Figure 1.1: Formation of ice plates on the surface of a pond[2].

The study of these classical, non-dissipative solutions (defects) dates back to the 1830s when J. Scott Russell gave us the concept of "**Solitary Wave**" which he spotted in a small canal as a wave having quite different properties from other known waves. These waves were later named solitons by mathematical physicists. What is more interesting is that particle physicists regarded them as potential new "particles" in the spectrum of non-linear field theories. And recently, condensed matter physicists probing superconductivity and astro-physicists researching galaxy formation have also delved into them [3].

One might wonder ***what significance may cosmology derive from such solutions***. The response is that many theories in particle physics inevitably lead to the conclusion that the early universe underwent several phase transitions. Nevertheless, it is conceivable that these cosmic phase transitions might have resulted in topological defects that are possibly still roving in our universe. But, still they are only speculative in the early cosmos although widespread in condensed matter physics. Therefore, the discovery of these fossils from the early universe not only proves the universe's temperature history but also gives crucial knowledge about particle physics and insight into cosmic phenomena. And the absence of these undiscovered topological defects places significant limitations on our particle physics knowledge and may infer novel cosmology.

1.1 Motivation for research in Monopoles

From now on, among all other topological defects, our prime focus will be magnetic monopoles. The credit of first written account of magnetism is actually given to Thales of Miletus (a Greek Mathematician) because he noticed

the odd properties of lodestone (the natural form of magnetite). And about a millennium ago, the Chinese made the first compass by observing that it always points south or north. Over time, our knowledge about electricity and magnetism started building up e.g. quite contrary to electric charges, magnetic charges do not exist, changing electric field produces a magnetic field, etc. Eventually, in 1846, James Clerk Maxwell unified electricity and magnetism and epitomized classical electrodynamics in his famous four equations as,

$$\begin{aligned} \vec{\nabla}.\vec{E} &= \rho_e. \\ \vec{\nabla}.\vec{B} &= 0. \\ \vec{\nabla} \times \vec{E} &= -\partial_o \vec{B}. \\ \vec{\nabla} \times \vec{B} &= \vec{j_e} + \partial_o \vec{E}. \end{aligned} \tag{1.1}$$

The covariant form of above equation in terms of field tensor is given as

$$\partial_\nu F^{\mu\nu} = j^\mu. \tag{1.2}$$

$$\partial_\nu G^{\mu\nu} = 0. \tag{1.3}$$

where j^μ is electric current density 4-vector and is given as $j^\mu = (\rho_e \ , \ j_x \ , \ j_y \ , \ j_z)$. Apart from the inclusion of electric source terms, there is a clear symmetry between roles played by electricity and magnetism in above equations. This becomes immediately visible in case of free Maxwell's equations

if we put $\rho_e = \vec{j_e} = 0$ as shown below

$$\begin{aligned} \vec{\nabla}.\vec{E} &= 0. \\ \vec{\nabla}.\vec{B} &= 0. \\ \vec{\nabla} \times \vec{E} &= -\partial_o \vec{B}. \\ \vec{\nabla} \times \vec{B} &= \partial_o \vec{E}. \end{aligned} \tag{1.4}$$

In tensor form, current density 4-vector (j^μ) will be zero so,

$$\partial_\nu F^{\mu\nu} = 0. \tag{1.5}$$

$$\partial_\nu G^{\mu\nu} = 0. \tag{1.6}$$

From above equations, it is obvious that the electromagnetic (EM) symmetry remains intact in vacuum. Even if we switches the role of $\vec{E}$ and $\vec{B}$ under the following duality transformation, (known as electromagnetic duality)

$$\vec{E} \to \vec{B} \qquad , \qquad \vec{B} \to -\vec{E}$$

there will be no effect on equations mentioned above. However, EM symmetry is broken if electric source terms are not zero and as a result, the invariance of Maxwell's equations no longer persists. For symmetry restoration, we have to consider magnetic source terms (ρ_g , $\vec{j_g}$) as

$$\begin{aligned} \vec{\nabla}.\vec{E} &= \rho_e. \\ \vec{\nabla}.\vec{B} &= \rho_g. \\ \vec{\nabla} \times \vec{E} &= -\vec{j_g} - \partial_o \vec{B}. \\ \vec{\nabla} \times \vec{B} &= \vec{j_e} + \partial_o \vec{E}. \end{aligned} \tag{1.7}$$

which will be symmetric under the action of following duality transformation

$$\begin{aligned} \vec{E} \to \vec{B} \qquad &, \qquad (\rho_e, \vec{j_e}) \to (\rho_g, \vec{j_g}) \\ \vec{B} \to -\vec{E} \qquad &, \qquad (\rho_e, \vec{j_e}) \to (-\rho_g, -\vec{j_g}) \end{aligned}$$

In tensorial form

$$\partial_\nu F^{\mu\nu} = j^\mu. \tag{1.8}$$

$$\partial_\nu G^{\mu\nu} = -k^\mu. \tag{1.9}$$

which remains invariant under the following duality transformation,

$$j^\mu \to k^\mu \qquad , \qquad k^\mu \to -j^\mu \tag{1.10}$$

Here k^μ represents magnetic current density 4-vector and is given as $k^\mu = (\rho_g\ ,\ k_x\ ,\ k_y\ ,\ k_z)$.Hence, it becomes evident that magnetic monopoles cannot be ruled out for the EM symmetry to remain intact when we include source terms.

Okay, for the time being, let's set the debate over the existence of monopoles aside and think for a while, ***why do we have to exclude the magnetic monopoles?*** Do they violate any fundamental laws? Will they be the cause of breaking any symmetry? Does their existence result in any instability in the universe? The answer to all these questions is indeed, **no**. Infact, many Grand Unified Theories (GUTs) predict their formation during phase transition. Not only this, but they also play an essential role in catalyzing proton decay, are a candidate for dark matter, etc. Therefore, the existence of monopoles, whenever detected, will not only be the gateway to new era of

physics, but will also be a hallmark for GUTs. And thus, eventually leads to glory.

In chapter 2, first there will be discussion about different types of topological defects. Then, a brief description of GUTs specifically $SU(5)$ and $SO(10)$ will be given. Afterwards, homotopy theory will be discussed because whenever a symmetry breaks, the topology of vacuum manifold is determined by using this theory. In the end, we will apply homotopy theory to the GUT group $SO(10)$ in order to find which types of defects are possible.

Chapter 3 encapsulates the scientific quest to bridge the gap between electric and magnetic forces. In bottom-up approach, a through description of Dirac's Theory of magnetic monopoles will be provided and the quantization condition given by Dirac will be proven from both classical and quantum mechanical approaches. After this, we will jump to the soliton theory as monopoles have topological characteristics.

Chapter 4 comprises on detailed discussion of monopoles from every aspect: Theoretical, experimental and in condensed matter systems. In top-down approach, a theoretical overview of magnetic monopoles will be provided in detail based on following monopole theories:

1. 't Hooft-Polyakov Theory

2. Nambu Theory

Afterwards, the experimental work that have been done yet will be discussed briefly covering all three known possibilities to dectect magnetic monopoles. To crunch this chapter, light will be shed on condensed matter systems in which monopoles appear as emergent particles, not as elementary particles.

Lastly, in chapter 5, our focus will be on monopoles with electroweak scale mass due to their immense importance. For this, a brief description

of electroweak scale right-handed neutrino model will be given to understand, how this model leads to non-trivial topology required for monopole production. Validating it through Dirac quantization, we will jump to predict topological charge and structure of monopoles in this model. It is worth mentioning here that throughout the manuscript, we will proceed in natural units $h = c = \epsilon_0 = \mu_0 = 1$

Chapter 2

Topological Defects: A Gauge Twist

Topological defects — the hidden threads of gauge theories — are enigmatic, elusive and intriguing fundamental structures, arising from the fundamental forces and symmetries of the cosmos, leaving a profound impact on the fabric of space-time. They are fingerprints of fundamental processes that occurred during the early stages of the universe or during phase transitions in condensed matter systems. From cosmic strings that span billions of light-years to cosmic textures that shape the distribution of matter, all the defects are of immense importance because of their ability to reveal profound insights into the underlying symmetries and dynamics of the universe and matter. So, the thought that occurs to mind is, *How do these defects form at a cosmic scale*? But before jumping into it, let's first explore cosmic phase transitions which will ultimately enable us to comprehend how defects originate.

2.1 Cosmological Phase Transitions

A basic symmetry breaks spontaneously to cause cosmological phase transitions. They are known to happen in the early cosmos when a large symmetry group breaks into a subgroup, further to the Standard Model(SM). Every time a phase transition takes place, a portion of this symmetry is lost, which causes the symmetry group to alter. This can be mathematically expressed as:

$$G \to H \to SU(3)_c \times SU(2)_L \times U(1)_Y \to SU(3)_c \times U(1)_{EM}.$$

Phase transitions might have had a significant impact on how our universe evolved and what is its content including the gravitational wave background, defect formation, baryogenesis, production of primordial magnetic fields, etc. Nevertheless, particle physicists still assess their quantum properties like effective mass, effective coupling and finite temperature effects that control all physical behaviors like the order parameter, the latent heat, the amount of super-cooling, etc[4]. The nature of phase transitions is of two kinds:

1. **1^{st} order phase transition**(dramatic): This phase transition occurs through bubble nucleation in which new phase's bubble nucleate until the old phase or false vacuum completely vanishes, signaling the end of the phase transition as shown in Figure 2.1. Its everyday analogy is the formation of ice on the surface of a pond.

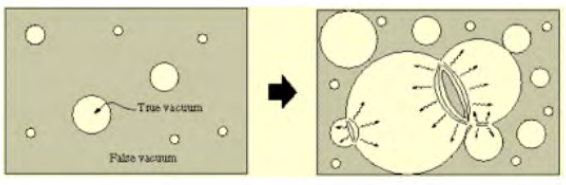

Figure 2.1: In **1^{st}** order phase transition, new phase's bubble(true vacuum) nucleate until the old phase(false vacuum) completely vanishes[5].

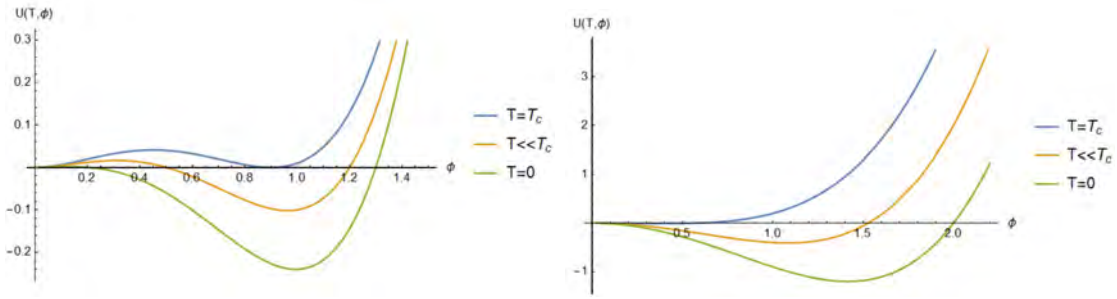

(a) (b)

Figure 2.2: Comparison of the evolution of potential with temperature for phase transitions, mediated by Higgs field (2.2a) 1^{st} order phase transition (2.2b) 2^{nd} order phase transition

2. **2nd order phase transition**: In this phase transition, the old phase continually changes into the new phase just like magnetization of the ferromagnetic materials e.g. iron.[3]

The graphical representations of both the phase transitions can be seen in Figure 2.2 where the phase transition mediated by Higgs field is plotted against the temperature dependent potential. In Figure 2.2a, it can be observed that between a local minimum and the ground state, there is a barrier in the event of 1st order phase transition which occurs due to quantum tunneling. While in Figure 2.2b for 2nd order phase transition, the evolution of ground state is smooth.

The nature of a particular phase transition influences the observable remnant traces and their utility. For instance, it may be a hint that the electroweak phase transition caused baryonic asymmetry in the universe if a fossil of gravitational background signals that it happened through bubble nucleation. Similarly, the production of primordial magnetic fields is attributed to the turbulence stage of the plasma undergoing bubble nucleation, etc[4].

The examples of cosmic phase transitions include the GUTs phase transition at $10^{-16}GeV$ (and the age of universe was around 10^{-37}s), the elec-

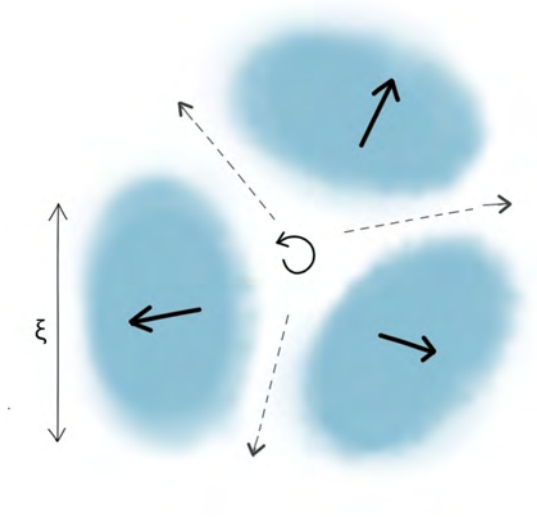

Figure 2.3: A $2D$ illustration of Kibble mechanism. Here ξ represents correlation length.

troweak phase transition at approximately $250GeV$ (occurred when our universe's age was 10^{-12}) and the quark-hadron confinement predicted by QCD at around $1GeV$ (when our universe was about a 10^{-6}s old) along with many others [1].

2.2 Mechanism of Defect Formation

In 1976, T.W.B. Kibble became the first to explain the mechanism behind the defect formation in the early universe, later known as Kibble mechanism after him. He claimed that with every decline in the universe's temperature, the Higgs field, which permeates all of space, may have taken different vacuum states or ground states. By the way, this is how symmetry is often broken. An everyday analogy of it would be domains in ferromagnetic materials that got randomly oriented as soon as the magnetic field vanished. Note that the Higgs field is constant far and wide in a symmetrical ground state. And

when the Higgs field attains a finite value, the symmetry is broken. All orientations are equally likely because distanced points cannot interact during the transition as information cannot move faster than the speed of light. Consequently, it is reasonable to assume that distinct areas ultimately had varied Higgs field alignments, and when they amalgamated, it was difficult for domains with drastically different preferred orientations to amend and fit seamlessly. So, defects arose at the interface of these areas [6].

2.3 Classification of Topological Defects

Depending on the pattern of symmetry breaking and topology of coset space, topological defects are of four types whose details are as follows:

1. **Monopoles**: Magnetic Monopole(MM) is point defect generated by the spontaneous breaking of a spherical symmetry. Almost in every natural GUT model, they are ineluctable. The key idea is that monopole production is associated with $U(1)$ symmetry which must constantly be intact in any symmetry breaking transition. This, coupled with the selection of any simpler GUT model ($SU(5), SO(10)$, etc) inevitably leads to MMs production. Interestingly, MMs are stable defects having a well-defined core and their winding number is also quantized. Furthermore,the monopole field necessarily has hedgehog configuration of the field which means that is directed radially outward from the core as visualized in Figure 2.4. And the mass of the MMs is of the order of symmetry breaking scale, represented by 'M_{mon}'. For the GUT scale,

$$M_{mon} = M_G = 10^{16} GeV.$$

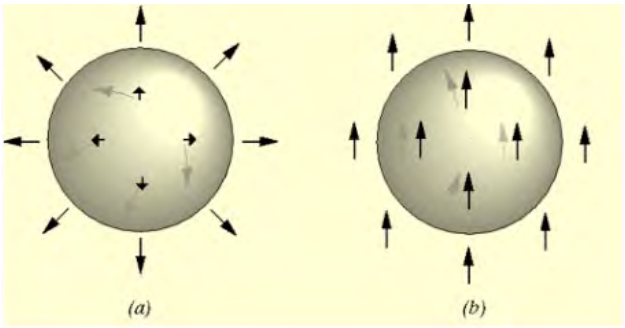

Figure 2.4: Configuration of field for monopole(left) and for vacuum(right)[5].

The Kibble mechanism predicts that per Hubble volume, the probability of the emergence of MMs is the order of unity since the number density of monopole is given as

$$n_{mon} \simeq H^3 \simeq \left(\frac{T_c^2}{m_p}\right)^3.$$

where'm_p' is mass at Planck scale and is equal to $10^{19}GeV$ while T_c where 'm_p' is mass at Planck scale and is equal to $10^{19}GeV$ while 'T_c' is critical temperature of the phase transition whose typical value is approximately $10^{14}GeV$. Since entropy density is given as

$$S = T_c^3.$$

Thus, the ratio of monopole number density and entropy density is

$$\begin{aligned} \frac{n_{mon}}{S} &= \frac{T_c^6/m_p^3}{T_c^3}, \\ \frac{n_{mon}}{S} &= 100\left(\frac{T_c}{m_p}\right)^3, \end{aligned}$$

Putting values, we get

$$\frac{n_{mon}}{S} = 10^{-13} GeV. \tag{2.1}$$

The mass density of monopole is given as

$$\rho_{mon} = M_{mon} n_{mon} \left(\frac{T_0}{T_c}\right)^2. \tag{2.2}$$

Since $M_{mon} = M_G$, then by simplifying above equation, we get

$$\begin{aligned} \rho_{mon} &= M_G \left(\frac{T_c^2}{m_p}\right)^3 \left(\frac{T_0}{T_c}\right)^2, \\ &= M_G \left(\frac{T_c T_0}{m_p}\right)^3, \\ &\sim M_G. \end{aligned} \tag{2.3}$$

Hence, MMs are superheavy. The energy density can be calculated as

$$\Omega_{mon} = \frac{\rho_{mon}}{\rho_c}. \tag{2.4}$$

here 'Ω_{mon}' denotes the energy density of the MM, 'ρ_c' represents the critical density of the universe, the value of which is equal to $10^{-5} GeV$. Thus, we have

$$\begin{aligned} \Omega_{mon} &\simeq \frac{M_G}{\rho_c} = \frac{10^{16}}{10^5}, \\ \Omega_{mon} &\sim 10^{11}. \end{aligned} \tag{2.5}$$

This is not acceptable as it indicates that the universe's matter is dominated by monopoles which is disastrous. We call this monopole overabundance problem. The primary driver behind the notion of the infla-

tionary universe, where monopoles are eliminated by the exponential growth, was this monopole dilemma. Other approaches to prevent the monopole issue include:

- Langacker-Pi Mechanism:
- It has also been proposed in 1998 by Dvali and others that monopoles melt during their encounter with domain walls if the transition generates both defects. In the end, domain walls deteriorate because of slight asymmetries and hence, sweep MMs away [7].

Keep in mind that global monopoles are an exception to above mention rules since they have long-range forces that reduce their number density in the absence of gauge fields. There is a substantial likelihood of annihilation due to the strong attraction force between global monopoles and antimonopoles which indicates that there is no over-abundance problem in case of global monopoles. Hence, global monopoles are not cosmologically disastrous but may be a seed of matter clustering [1].

2. **Cosmic Strings**: When axial symmetry is broken, line-like defects called cosmic strings are produced. Cosmic strings are related to models where the vacuum manifold includes holes or where the minima are not simply connected and will only form strings when results in a circle as seen in Figure 2.5. Extensive researches have been done on cosmic strings not only in cosmology but also in solid state physics. Though cosmologically intriguing, cosmic strings have not yet been found and are subject to strong constraints from the millisecond pulsar and other observations. Cosmic strings are stable defects having a well-defined core and quantized winding number. The mass density of cosmic strings

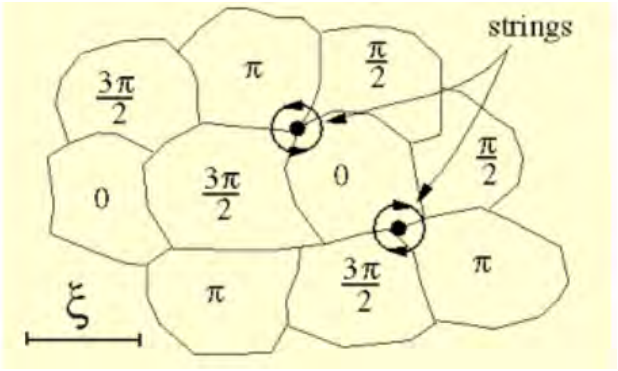

Figure 2.5: Cosmics strings' formation via Kibble mechanism[5].

is given as

$$\rho_s = \eta^2 t^{-2}. \tag{2.6}$$

Thus, mass per unit length of GUT scale strings is $10^{16} tons/cm$. And the energy density can be calculated as

$$\begin{aligned} \Omega_s &\sim \frac{\rho_s}{\rho_c}, \\ &= \left(\frac{\eta}{m_p}\right)^2, \\ &= 10^{-6}. \end{aligned} \tag{2.7}$$

Hence, strings are not cosmologically disastrous and due to gravitational accretion, can seed structure formation [1]. Following processes make them loose their energy due to which they do not dominate the matter of the universe.

(a) String inter-commutation: In this process, two strings can switch partners at the point of intersection while they are crossing. This causes a loop to be chopped off when a string folds back on itself. Also, due to repeated inter-commutation, strings lose their straightness and form wavy structures as shown in Fig. 2.6 which

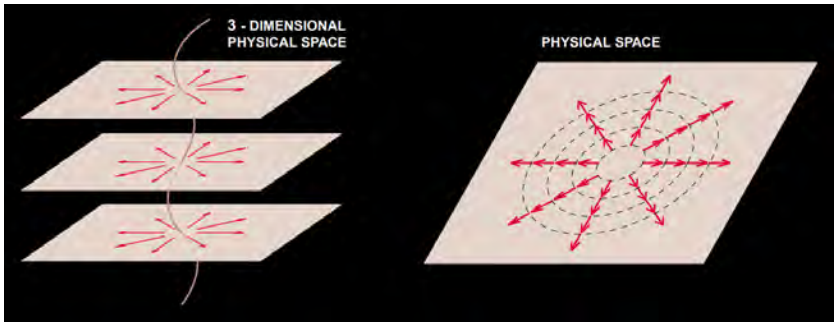

Figure 2.6: Wiggly structure of cosmics strings[1].

attract matter to them but straight strings do not.

(b) Oscillating loops gradually dissipate after emitting radiation, mostly gravitational radiation for gauge strings.

The above mentioned reasons lead strings to continue deteriorating. The ultimate result is a scaling solution where a fixed amount of loops and long strings are present at any time in a Hubble volume [8]. Simulations reveal that around 80% energy is composed of infinite strings in the string network.

3. **Domain Walls**: Domain walls(DWs) are result of spontaneous breaking of discrete symmetry. The disconnection of the vacuum manifold causes these 2-D defects to appear as shown in figure 2.7. Note that it is impossible to gauge discrete symmetries since they are not continuous. Therefore, domain walls are invariably global defects. Because of their enormous mass, domain walls are often catastrophic for cosmology at GUT scale as,

$$M_{DW} = 10^{46} tons/cm^2$$

while

$$M_{galaxy} = 10^{39} tonnes$$

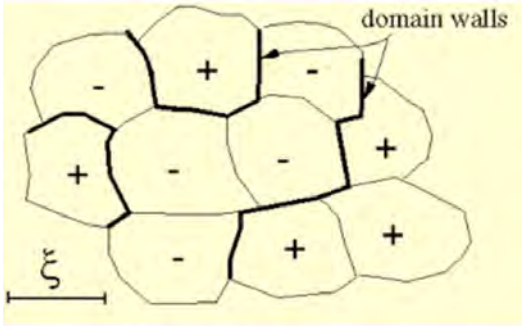

Figure 2.7: Domain walls' generation via the Kibble mechanism [5].

Therefore, a domain wall of 10^{-6} m size has a mass equivalent to that of a galaxy. However, inflation can solve the domain wall problem produced at GUT scale. As a result of the horizon providing an upper bound on any associated domain, the Kibble mechanism predicts one domain wall per horizon. Thus, at GUT scale,

$$\frac{\Omega_{dw}}{\Omega_c} = \frac{m_{GUT}^3 \times t^{-1}}{m_p^2 \times t^{-2}} = 10^{51} \tag{2.8}$$

where "m_{GUT}" is mass at GUT scale and is equal to 10^{16}GeV while "m_p" is mass at Planck scale and is equal to 10^{19}GeV .

Domain walls at GUT scale are, therefore, excluded. The only walls that are acceptable are those that may emerge very late in the universe's history. Interestingly, constricting axion models have proven to be the most successful application of the domain wall constraint.[8]

4. **Textures**: A higher, more complex, non-abelian global symmetry breaks entirely and spontaneously to produce textures. Note that the partial breaking of this global symmetry gives rise to other defects rather than global textures like global monopoles or non-topological textures. They are delocalized defects because, in contrast to other defects, the field

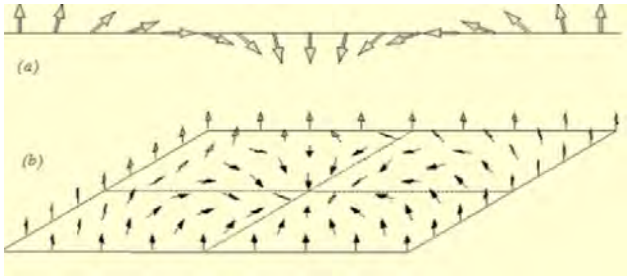

Figure 2.8: Textures (a) in 1-D and (b) in 2-D [5].

is not limited only to the defect core, as all the energy is in the form of spatial gradients as seen in figure 2.8. Even if gauge fields A_ν try to redirect for a local theory, then $D_\nu\phi = 0$. Thus they only exist in theories having global symmetry.

Textures' susceptibility to collapsing is another intriguing phenomenon. Because of this instability, the defect gradually collapses in on itself as its actual size shrinks over the passage of time to the order of the horizon. Up until the magnitude of it reaches the scale $\frac{1}{\eta}$, the collapse persists. By this time, the core will have accumulated enough energy to induce the field to quit this vacuum state. It asserts that textures unwind, leaving a trivial configuration of the field in their wake, and the winding number is not quantized. In light of all this, it is logical to consider them as peculiar topological defects[1].

Two terminologies, local and global defects, are frequently used in the above description and are based on whether the gauge symmetry is involved or not. As far as **local defects** are concerned, the gauge fields offset gradients thus, there is little gradient energy. It has two significant repercussions i.e. local defects do not interact across large distances after they form and have a well-defined core where the energy is confined. Contrary to it in **global defects**, no gauge fields are involved and the gradient energy which is ev-

Topological defect	Widely acceptable	Reason
Monopoles	Global	Local leads to over-abundance issue
Cosmic string	Both local and global	-
Domain walls	Both are not acceptable	Cosmologically disastrous
Textures	Only global textures exist	Rapid disappearance

Table 2.1: Classification of topological defects on the basis of gauge symmetry.

erywhere throughout the horizon scale, dominates. The interaction among defects is quite powerful and meager defects per horizon scale will be present due to the annihilation of opposing-charge defects. Since we know that

$$\Omega_{defect} = \eta^2 \times t^{-2}$$

Therefore

$$\frac{\Omega_{defect}}{\Omega_{matter}} = 4\pi G = E \tag{2.9}$$

Thus, the defect's energy represents a stable, negligible portion of the universe's overall energy density and this is referred as scaling. Only strings undergo scaling among local defects. And if we talk about global defects,they cause geometrical perturbations due to gradient energy. Hence, global defects and local strings can seed formation of large scale structure [9].

2.4 Grand Unified Theory

As physicists continue to explore the mysteries of the cosmos, GUTs remain a captivating avenue for unraveling the complexities of particle physics and

the fundamental nature of our universe. GUT groups are attempts to unify the three fundamental forces of the Standard Model(SM) into a single, larger unified force at high energy scales. These GUT groups aim to describe the interactions of elementary particles beyond the energy range that current particle accelerators can probe. There are many GUT models like $SU(5)$, Pati-Salam, Trinification, $SO(10)$, E_6, etc. However, here we will discuss $SU(5)$ and $SO(10)$. To comprehend the gauge unification, we need to understand unitary group and special unitary groups which are briefly described in appendix A.

2.4.1 Insight into $SU(3)_c \times SU(2)_L \times U(1)_Y$

The story begin with fermions, collection of quarks and leptoons, as the building blocks of matter existing in our universe are fermions i.e. protons, neutrons, and electrons. Deeper analysis shows that proton comprises of two up quarks and a down quark(d), and the neutron made up of two down quarks and an up quark(u). A down quark within a neutron undergoes β-decay(weak interaction), converting it to u, e^{-1}, and antielectron-neutrino($\bar{v_e}$). In order to yield the well-known and adored electromagnetic interaction, the photon couples to different fermions, leaving the $\bar{v_e}$ alone.

Further studies by Gell-Mann unveiled that quarks have a quantum number known as color quantum number. The three color variants for each quarks are represented by red(r), blue(b), and green(g) which explains the gluing of quarks within proton and neutron. And due to strong interaction, these quarks can scatter off each other i.e. $u^r + d^b \rightarrow u^b + d^r$. So, in a way, strong interaction is responsible for the formation of the universe.

Later on, physicists discovered that the universe is actually composed of three generations of fermions with u, d, e, and ν_e constituting the 1^{st}

generation of fermions. With the discovery of the charm quark(c), strange quark(s), muon(μ), and muon-neutrino(v_μ) — the 2^{nd} generation of fermions — scientists were astounded and incredulous. Even more unexpected was the 3^{rd} generation, which included top quark(t), bottom quark(b), tau(τ), and tau-neutrino(v_τ) [10].

Since fermions are spin $\frac{1}{2}$ particles so, two Weyl fields are used to describe them— the Left-Handed(LH) field and Right-Handed(RH) field. Parity conservation ensures that both fields are placed in the same representation($\mathcal{R}$) of the gauge group(G). For instance, the three color variants of up quark having two sets of fields($u_L^r, u_L^b, u_L^g; u_R^r, u_R^b, u_R^g$) are put into the fundamental representation 3 of $SU(3)$. As is well-known that a conjugate LH field translates like a RH field, making it convenient for grand unified theorists to recast all RH fields as conjugate of the LH fields in the gauge theory($\Psi_R \rightarrow \Psi_L^c$). This enables us to describe how gauge bosons interact with fermions, explaining the coupling of eight gauge bosons A_μ^a $(a = 1, ..., 8)$ to the generators T^a of the representation $\mathcal{R}$ to which the fermions belong. This can be expressed in the form of Lagrangian using the up quark as

$$\mathcal{L} = gA_\mu^a(\bar{u}\lambda_a\gamma^\mu\, u + \bar{u}^c\lambda_a^*\gamma^\mu\, u^c). \tag{2.10}$$

Here λ_a represents the Gell-Mann matrices. Have a pause here. One might think that, *Why are we using $SU(3)$ gauge group, not any other one*? So, the recipe to construct a gauge group is

- Choose a compact Lie group G. Just focus on $SU(N)$ for the sake of our goals.
- The $\frac{1}{2}N(N-1)$ gauge bosons A_μ^a transform like the adjoint representation.

- Different representations $\mathcal{R}$ of G are used to represent fermions with a $d_{\mathcal{R}}$-dimensional representation being able to include $d_{\mathcal{R}}$ fermion fields. Following that, the representation to which each fermion belongs fixes the interactions between the gauge bosons and the fermions.

Strong Interaction

Alright, now our aim is to allocate 1^{st} generations's fermion fields— given below

$$u^r, u^b, u^g, u^{cr}, u^{cb}, u^{cg}, d^r, d^b, d^g, d^{cr}, d^{cb}, d^{cg}, e^-, e_+, v_e \tag{2.11}$$

to various $SU(3)$ representations used to describe the strong interaction. The 15 Weyl fields mention above have representations

$$u \sim 3\,,\; u^c \sim \bar{3}\,,\; d \sim 3\,,\; d^c \sim \bar{3}\,,\; e^- \sim 1\,,\; e^+ \sim 1\,,\; v_e \sim 1 \tag{2.12}$$

Note that the singlet representation of SU(3), which does not undergo transformation under the group, is home to the leptons, electrons, anti-electrons, and neutrinos. These leptons receive the cold shoulder from the gluons, who disregard them. In Lagrangian, the symbol for the term representing electron-gluon coupling(λ_a) is a 0 for the singlet representation.

In conclusion, identifying the non-trivial irreducible representations of $SU(3)$

$$(u^r, u^b, u^g), (u^{cr}, u^{cb}, u^{cg}), (d^r, d^b, d^g), (d^{cr}, d^{cb}, d^{cg}) \tag{2.13}$$

allows one to specify the strong interaction. In simpler words, the three fields contained inside each set of parenthesis are transferred into one another by the gluons. Beware, e^-, e^+, and v_e are not included and neutrino has no conjugate partner. According to group theory, the 1^{st} generation of fermion fields are attributed to the reducible representation $3 \oplus 3^* \oplus 3 \oplus 3^* \oplus 1 \oplus 1 \oplus 1$

of $SU(3)$ [11].

Inclusion of Weak interaction

Let's move on to the weak interaction now, denoted by $SU(2)$ gauge theory, which explains the transformation of u and d as doublet $\sim \begin{pmatrix} \mathrm{u} \\ \mathrm{d} \end{pmatrix}$. In the $SU(2)$ gauge theory, there are three gauge bosons($N^2 - 1 = 2^2 - 1 = 3$) denoted by $\mathcal{W}_\mu^a$ which couple to the $SU(2)$ generators T^a(replaced by Pauli matrices τ_a). Thus, the linear combination $\mathcal{W}_\mu^{1\pm\iota 2}$ which got coupled to $\tau^\mp = \frac{1}{2}(\tau_1 \mp \iota\tau_2)$, result in the transformation of the up quark into the down quark and vice versa. The same gauge bosons are responsible for the transformation of the neutrino and electron as a doublet, schematically $\sim \begin{pmatrix} v_e \\ e^- \end{pmatrix}$.

Surprisingly, the neutrino has no conjugate partner. So, the neutrino's left-handed nature requires a left-handed e^- field in the doublet, while the right-handed e^- field lacks sharing the spotlight with the neutrino field. Also, experiments done to study weak interaction, especially parity violation, demonstrated that the right-handed up and down quarks fields have no other to partner with. All this results in singlet representations that transforms like 1 of $SU(2)$. The lack of contact between the weak interaction bosons and the color of the quarks suggests a direct product structure between the strong and weak interactions as $SU(3) \times SU(2)$.

So the 15 Weyl field given in (2.11) are sorted into $SU(3) \times SU(2)$ as

$$\left(\begin{pmatrix} \mathrm{u}^r \\ \mathrm{d}^r \end{pmatrix}, \begin{pmatrix} \mathrm{u}^b \\ \mathrm{d}^b \end{pmatrix}, \begin{pmatrix} \mathrm{u}^g \\ \mathrm{d}^g \end{pmatrix} \right), \begin{pmatrix} v_e \\ e^- \end{pmatrix}, (u^{cr}, u^{cb}, u^{cg}), (d^{cr}, d^{cb}, d^{cg}), e^c \tag{2.14}$$

In simple words, 1^{st} generation fields comprise of reducible representation $(3,2)\oplus(1,2)\oplus(\bar{3},1)\oplus(\bar{3},1),(1,1)$ summing up to 3.2+1.2+3.1+3.1+1.1 = 15 [11].

Inclusion of Electromagnetism

Now, let's talk about the leftover $\mathcal{W}_{\mu}^{3}$ gauge boson. Because this gauge boson — associated with T^3 generator — couples with neutrino, it can't be the photon. This gauge boson can also be coupled to both up quark and neutrino with strength equal to $\frac{1}{2}$,to down quark and electron with strength equal to $-\frac{1}{2}$, and can't be coupled to u^c,d^c,e^c. Hence, at least one more gauge boson must be introduced, as suggested by the Gell-Mann Nishijima formula given below

$$Q = I_3 + \frac{1}{2}Y.$$

In terms of T^3 generator, the above equation can be re-written as

$$Q = T^3 + \frac{1}{2}Y. \tag{2.15}$$

The gauge group, which has the generator $\frac{1}{2}Y$, is $U(1)$. By definition, the total of T^3 generator for each of the fields in an $SU(2)$ representation must equal zero. Therefore, (2.15) informs us that the average electric charge Q of all the fields in a representation is equal to $\frac{1}{2}Y$ of the representation. For example, for the fields $\begin{pmatrix} \mathrm{u} \\ \\ \mathrm{d} \end{pmatrix}$ and $\begin{pmatrix} v_e \\ \\ e^- \end{pmatrix}$, the hypercharge($Y$) is equal to $\frac{1}{2}\left[\frac{+2}{3}+\left(\frac{-1}{3}\right)\right] = \frac{1}{2}\left[\frac{2}{3}-\left(\frac{1}{3}\right)\right] = \frac{1}{6}$ and $\frac{1}{2}[0+(-1)] = -\frac{1}{2}$ respectively. This results in an extension of the gauge group underpinning the strong, weak, and electromagnetic interactions to $SU(3)\times SU(2)\times U(1)$. The irreducible

representation of the 15 Weyl field is as follows

$$\left(3, 2, \frac{1}{6}\right) \oplus \left(\bar{3}, 1, -\frac{2}{3}\right) \oplus \left(\bar{3}, 1, \frac{1}{3}\right) \oplus \left(1, 2, -\frac{1}{2}\right) \oplus (1, 1, 1). \qquad (2.16)$$

The gauge bosons's interaction with $U(1)$ is denoted as $\mathcal{B}_\mu$. The photon turns out to be a specific linear combination of the $\mathcal{W}_\mu^3$ and $\mathcal{B}_\mu$, coupling to electric charge. The Z is the name for the linear combination that is perpendicular to the photon. Particle physicists have a great deal of faith in the validity of the Standard model gauge theory after the finding of a gauge boson with the anticipated features of Z [11].

2.4.2 From SM to $SU(5)$

A great many clues point to the need for further unification, at least in the light of retrospect. One is that the hypercharges($\frac{1}{2}Y$) of 15 weyl fields of 1^{st} generation add up to zero i.e. $3.1. - \frac{2}{3} + 3.2.\frac{1}{6} + 3.1.\frac{1}{3} + 1.1.1 + 1.2. - \frac{1}{2} = 0$ and the fact is that $U(1)$ is a part of Lie algebra. So, it follows that Y must be traceless which is the generator of $U(1)$(sum of Y should be zero). And the list goes on... Therefore, it is the need of the hour to embed the SM into a larger gauge group to rule out known discrepancies [11].

But note that the candidates for the larger gauge group must be at least of rank ≥ 4 since the rank of the standard model is 4. Hence, the simple and smallest larger gauge group embedding SM is $SU(5)$ whose rank is 4 and has $N^2 - 1 = 5^2 - 1 = 24$ gauge bosons twice the usual gauge bosons. The extra gauge bosons having both flavor and color— known as X and Y — defy the baryon and lepton number while preserving $B - L$ conservation [12].

The fundamental representation of $SU(5)$ is formed by the 24 5 by 5 hermitian traceless matrices operating on the 5 objects designated by ψ^α

with $\alpha = 1, 2, ..., 5$. Now divide ψ^α into two sets: one set is ψ^i with $i = 1, 2, 3$ and the other is ψ^j with $j = 4, 5$. The $SU(5)$ matrices that operates on ψ^i and ψ^j define an $SU(3)$ and $SU(2)$ respectively. In fact, 8 of the 24 hermitian traceless matrices are Gell-Mann matrices producing an $SU(3)$, and 3 are Pauli matrices yielding an $SU(2)$. This describes the fitting of SU(3) and SU(2) into SU(5). The 5 by 5 hermitian traceless matrix of $SU(5)$ is

$$S = \frac{1}{2}Y = \begin{pmatrix} -\frac{1}{3} & & & & \\ & -\frac{1}{3} & & & \\ & & -\frac{1}{3} & & \\ & & & \frac{1}{2} & \\ & & & & \frac{1}{2} \end{pmatrix} \tag{2.17}$$

called the hypercharge $\frac{1}{2}Y$ which is the generator of $U(1)$. *Why Nature felt the need to include an additional* $U(1)$ *in* $SU(3) \times SU(2) \times U(1)$? We can now see that the cause may be grand unification: $SU(5)$ decomposes naturally into $SU(3) \times SU(2) \times U(1)$, not into $SU(3) \times SU(2)$ [11].

How Embedding is Done?

It is apparent that the fundamental representation of $SU(5)$ has dimension 5. This gauge group is complex and, therefore, has a complex conjugate representation $\bar{5}$ also, referred as anti-fundamental representation. Finding a SM subgroup of $SU(5)$ is necessary to embed the $SU(3)$, $SU(2)$, and $U(1)$ gauge groups in $SU(5)$. So, as a starting point, let's try to fit the LH fields given in (2.16). There are two options in (2.16), each with a total of 5 dimensions:

$$\left(\bar{3}, 1, \frac{1}{3}\right) \oplus \left(1, 2, -\frac{1}{2}\right) \tag{2.18}$$

as $3.1 + 1.2 = 5$ and

$$\left(\bar{3}, 1, -\frac{2}{3}\right) \oplus \left(1, 2, -\frac{1}{2}\right) \tag{2.19}$$

in view of the fact that $3.1 + 1.2 = 5$. Catch on the fact that the option in (2.19) is prohibited because the hypercharge S is not traceless i.e. $3.1. - \frac{2}{3} + 1.2.\frac{1}{2} = -1 \neq 0$. Consequently, this group can't be embedded in $SU(5)$. Anyway, the possibility in (2.18) is allowed as $3.1.\frac{1}{3} + 1.2. - \frac{1}{2} = 0$(traceless). Thus, it can be embedded into $SU(5)$ as shown below

$$\bar{5} \rightarrow \left(\bar{3}, 1, \frac{1}{3}\right) \oplus \left(1, 2, -\frac{1}{2}\right) \tag{2.20}$$

By taking conjugate of above representation, we get the fundamental representaion of $SU(5)$

$$5 \rightarrow \left(3, 1, -\frac{1}{3}\right) \oplus \left(1, 2, \frac{1}{2}\right) \tag{2.21}$$

Heading in right direction, indeed! The content of the left-handed fields in representation $\bar{5}$ is

$$\begin{pmatrix} d_r^c \\ d_g^c \\ d_b^c \\ e^- \\ \nu_e \end{pmatrix}$$

and for the right-handed fields in representation 5

$$\begin{pmatrix} u_r^c \\ u_g^c \\ u_b^c \\ e^c \\ v_e^c \end{pmatrix}$$

However, this explains 5 of the fields in (2.16) while the remaining 10 fields $\left(3,2,\frac{1}{6}\right) \oplus \left(\bar{3},1,-\frac{2}{3}\right) \oplus (1,1,1)$ must still be researched. For this, the next representation of $SU(5)$ has dimension $\frac{N(N-1)}{2} = \frac{5(4)}{2} = 10$ and is known as antisymmetric tensorial representation. This representation uses antisymmetric product technique to embed the remaining fields in 10 and $\bar{10}$. To determine the mechanism, we see that $10 = 5 \otimes_A 5$. Due to this, we may create these representations by multiplying the 5-dimensional left-handed fields subset as shown below

$$\begin{aligned}
10 &= 5 \otimes_A 5 \\
10 &\rightarrow \left[\left(3,1,-\frac{1}{3}\right) \oplus \left(1,2,\frac{1}{2}\right)\right] \otimes_A \left[\left(3,1,-\frac{1}{3}\right) \oplus \left(1,2,\frac{1}{2}\right)\right] \\
10 &\rightarrow \left(3,1,-\frac{1}{3}\right) \otimes_A \left(3,1,-\frac{1}{3}\right) \oplus \left(3,1,-\frac{1}{3}\right) \otimes_A \left(1,2,\frac{1}{2}\right) \oplus \left(1,2,\frac{1}{2}\right) \otimes_A \left(1,2,\frac{1}{2}\right) \\
10 &\rightarrow \left(3 \otimes_A 3,1,-\frac{1}{3}-\frac{1}{3}\right) \oplus \left(3,2,-\frac{1}{3}+\frac{1}{2}\right) \oplus \left(1,2 \otimes_A 2,\frac{1}{2}+\frac{1}{2}\right) \\
10 &\rightarrow \left(3 \otimes_A 3,1,-\frac{2}{3}\right) \oplus \left(3,2,\frac{1}{6}\right) \oplus (1,2 \otimes_A 2,1)
\end{aligned}$$

We know that

$$3 \otimes 3 = \bar{3}_a \oplus 6_s \tag{2.22}$$

and

$$2 \otimes 2 = 1_a \oplus 3_s \tag{2.23}$$

Therefore, the antisymmetric representation 10 is given as

$$10 \rightarrow \left(\bar{3}, 1, -\frac{2}{3}\right) \oplus \left(3, 2, \frac{1}{6}\right) \oplus (1, 1, 1) \tag{2.24}$$

The content of this representation is

$$\begin{pmatrix} 0 & u_b^c & -u_g^c & d_r & u_r \\ -u_b^c & 0 & u_r^c & d_g & u_g \\ u_g^c & -u_r^c & 0 & d_b & u_b \\ -d_r & -d_g & -d_b & 0 & e^c \\ -u_r & -u_g & -u_b & -e^c & 0 \end{pmatrix}$$

We can get the respresentation of right-handed fields by taking the conjugate of 10

$$1\bar{0} \rightarrow \left(3, 1, \frac{2}{3}\right) \oplus \left(\bar{3}, 2, -\frac{1}{6}\right) \oplus (1, 1, -1) \tag{2.25}$$

Lo and behold! The $\bar{5}$ and 10 representations of $SU(5)$ are ideal fits for the known fermion fields of a particular generation. With this, all the fermions are embedded into $SU(5)$ with respresentations: $\bar{5}$,10 for LH fields ,and 5,$1\bar{0}$ for RH fields. It is evident now that the generator of $SU(5)$ is hypercharge which is traceless. That's why sum of the hypercharges of the 15 Weyl fields is 0(discussed at the start).

2.4.3 Embedding $SU(5)$ into $SO(10)$

We have witnessed that in the $SU(5)$ theory, the 15 Weyl-fields containing all the fermions are placed into $\bar{5}$ and 10 representations which are irreducible and thus, signals flaw. Also, as per the principles of quantum field theory, all theories must pass a "health check" called freedom from anomaly, similar to a disease screening. In the case of the $SU(5)$ theory, the contributions of the $\bar{5}$ and the 10 precisely cancel each other out, indicating that unification must be continued to a larger gauge group(G).

It is generally agreed that $U(N)$ naturally fits into $SO(2N)$. It is worth mentioning here that there is an essential difference between $SO(2N)$ and $SO(N)$ that is the former has an extra complex representation knwon as spinorial representation, which is a more generalized version of Lorentz spinors. It can be understood implicitly by considering $SO(2N)$ as a set of linear transformations in which the scalar product of two real vectors $x = x_1, x_2, x_3, ..., x_n$ and $x' = x'_1, x'_2,'_3, ..., x'_n$ given as

$$xx' = \sum_{i=1}^{n} (x_i x'_i + y_i y'_i). \tag{2.26}$$

remains invariant. (**??**)e can develop two n-dimensional complex vectors, $u = x_i + \iota y_i$ and $u' = x'_i + \iota y'_i$, using these two real vectors where $i = 1, 2, 3, ..., n$. The group $U(N)$ is a subset of transformations applied to the complex vectors u and u' whose scalar product represented as

$$u(u')^* = \sum_{i=1}^{n} (x_i x'_i + y_i y'_i) + \iota \sum_{i=1}^{n} (x_i x'_i - y_i y'_i) \tag{2.27}$$

is also invariant. By observing equations (2.26) and (2.27), we infer that $U(N)$ leaves not only the $SO(2N)$ transformation invariant but also the

$\sum_{i=1}^{n}(x_i x_i' - y_i y_i')$ one. Hence, There is no doubt that the coordinates x_i and y_i rotate each other in the $2n$-dimensional space [11].

From above discussion, we conclude that $SO(10)$ model enables us to fit all the fermions in single irreducible representation called spinor representation as shown below

$$16 \;=\; 10 \oplus \bar{5} \oplus 1$$

Notably, it introduces a Weyl field that transforms as an $SU(5)$ singlet called the RH neutrino which is a much-needed feature in GUT models. The fact that fermions may convert into spinors in both spacetime and in internal symmetry space is another appealing aspect of $SO(10)$. Last but not the least, this model automatically exclude the anomaly.

2.5 Homotopy Theory

Homotopy theory is a fascinating branch of algebraic topology that explores the relationship between topological spaces and their continuous deformations. Put simply, homotopy theory has an intimate connection with geometry and topology, and allows physicists to categorize topological defects based on their unique characteristics.Homotopy theory and topological defects, though rooted in different domains of mathematics and physics, converge to illuminate the intricate topological tapestry of our universe. It introduces powerful algebraic invariants, such as homotopy groups, that encapsulate the topological information of a space relevant to the study of topological defects.

Using homotopy theory, we can not only analyze the type of defect that would arise from the breaking of a particular symmetry, but also determine whether the defect would be stable or not. The question here is, *How*?

Homotopy group	Defect	Topology of $\mathcal{M}$
$\Pi_0\mathcal{M} \neq 1$	Domain walls	Disconnected
$\Pi_1\mathcal{M} \neq 1$	Cosmic string	non-contractable loops
$\Pi_2\mathcal{M} \neq 1$	Monopoles	non-contractable 2-spheres
$\Pi_3\mathcal{M} \neq 1$	Textures	non-contractable 3-spheres

Table 2.2: Classification of topological defects on the basis of homotopy groups.

Remember, Kibble mechanism advocated that defects are associated order parameters or fields from one topological space — higher symmetry group $\mathcal{G}$ — to another with smaller symmetry group H which are not correlated. It is the topology of this coset space or vacuum manifold $\mathcal{M} = \frac{\mathcal{G}}{H}$ that helps us in the determination of type of defect. In simple words, we map the points of symmetry group $\mathcal{G}$ to smaller group H which should be non-trivial for the defect to produce. These mappings can be classified using homotopy classes or groups, which represent equivalence classes of continuous deformations or mappings and which correspond to distinct types of defects as described in the following Table.

2.6 Insight into $SO(10)$ Breaking

In this section, we will apply homotopy theory to the $SO(10)$ model by considering different symmetry breaking patterns and try to figure out which defects are possible. The reason behind specifically considering the $SO(10)$ model out of all is that it is one of the largest and most inclusive grand unified gauge group. Other reasons are

1. In $SO(10)$, all the fermions of a single generation are embedded into a

single representation, which is not the case in $SU(5)$.

2. $SO(10)$ allows for the inclusion of RH neutrinos, which are crucial for explaining the phenomenon of neutrino oscillation and generating neutrino masses through the seesaw mechanism.

3. The $SO(10)$ GUT framework can provide a natural explanation for proton decay, which is a crucial prediction of GUTs.

4. This model can solve the gauge hierarchy problem.

5. In this model, the Dimopoulos-Wilczek mechanism can lead to natural doublet-triplet splitting.

6. Some versions of $SO(10)$ GUT models offer a mechanism for explaining the observed baryogenesis in the universe.

Thus, $SO(10)$ is a captivating model for unraveling the complexities of particle physics and the fundamental nature of our universe.

Clap eyes on the fact that in the rest of the section, we will employ supersymmetric(SUSY) $SO(10)$ model rather than a non-supersymmetric one. The reasons are primary distinctions in symmetry breaking scale and the selection of intermediate symmetry models. It means that to gain agreement with the observed value of $\sin^2\theta_w$ and the gauge coupling constants extrapolated to high energies to reach roughly to $10^{15}GeV$, non-SUSY models must undergo one intermediary symmetry breaking. As opposed to this, SUSY $SO(10)$ models may directly break to the standard model in which supersymmetry breaks at 10^3GeV, anticipating the observed value of $\sin^2\theta_w$, and uniting the gauge coupling constants in a single point at $2 \times 10^{16}GeV$.

It is quite natural to raise the issue that, *Isn't there any effect on the formation of topological defects in non-SUSY theories by the presence of su-*

persymmetry? And the answer is negative. Because in non-SUSY theories, the connection of the vacuum manifold $\frac{G}{H}$ is necessary for the topological defects to generate after the SSB of a non-SUSY Lie group G to a non-SUSY Lie group H. Now in the case of superalgebra of non-Lie nature, it is known to us that the superalgebra is Lie admissible. Also, one may exponentiate the superalgebra's infinitesimal transformations to get a Lie superalgebra.

The Lie algebra has an algebraic covering known as the Lie admissible algebra. Such a covering maintains the Lie group's global structure while facilitating a Lie admissible infinitesimal behavior. The graded Lie algebra is Lie admissible, allowing for the extension of most of the Lie algebra theory to it with the proper modification. A linked (super-)Lie group structure in particular, preserves. Therefore, topological defects will emerge in SUSY models in the same way that they do in non-SUSY ones [13].

Using no more than one intermediate breaking scale which in our case will be $SU(5)$, we enumerate every symmetry breaking pattern starting from SUSY $SO(10)$ down to the standard model(SM) without involving Z_2 parity.

$$\begin{aligned}
&SO(10) \to SU(5) \times U(1)_\chi \to SU(3)_c \times SU(2)_L \times U(1)_Y \\
&SO(10) \to SU(5) \to SU(3)_c \times SU(2)_L \times U(1)_Y \\
&SO(10) \to SU(5) \times U(1)_X \to SU(3)_c \times SU(2)_L \times U(1)_Y \\
&SO(10) \to SU(3)_c \times SU(2)_L \times U(1)_Y
\end{aligned} \tag{2.28}$$

while the breaking patterns involving Z_2 symmetry are

$$\begin{aligned}
&SO(10) \to SU(5) \times U(1)_\chi \to SU(3)_c \times SU(2)_L \times U(1)_Y \times Z_2 \\
&SO(10) \to SU(5) \times Z_2 \times \to SU(3)_c \times SU(2)_L \times U(1)_Y \times Z_2 \\
&SO(10) \to SU(5) \times U(1)_X \to SU(3)_c \times SU(2)_L \times U(1)_Y \times Z_2 \\
&SO(10) \to SU(3)_c \times SU(2)_L \times U(1)_Y \times Z_2
\end{aligned} \tag{2.29}$$

In all the models mentioned above, supersymmetry breaks at $10^3 GeV$ — without taking into account how it breaks — and the SM is broken to $SU(3) \times U(1)_{em}$ by the standard Higgs mechanism. However, the symmetry breakings mentioned in (2.29), the Z_2 symmetry functions as matter parity and is unbroken all the way down to SM. It prohibits rapid proton decay and stabilizes the lightest supersymmetric particle(LSP), making it an excellent candidate for hot dark matter. For simplicity, we will use the following notations

$$\begin{aligned} 3_c 2_L 1_Y &\equiv SU(3)_c \times SU(2)_L \times U(1)_Y \\ 3_c 2_L 1_Y(Z_2) &\equiv SU(3)_c \times SU(2)_L \times U(1)_Y(\times Z_2) \end{aligned}$$

Remember one thing, we will discuss defect formation in generic way only and not give details about the possibility of different types of configurations. However, the explanation about the stability of defects will be considered. Lastly, in order to reduce $SO(10)$ rank by one unit, a pair pf Higgs field $(\varphi + \overline{\varphi})$ must get a VEV that is in the order of the GUT scale, which can occur in the $16 + \overline{16}$ or $126 + \overline{126}$ dimensional spinorial representations of $SO(10)$. And a pair of $126 + \overline{126}$ dimensional Higgs representation must be used to keep the Z_2 matter parity intact down to low energy. Note that the symmetry breaking caused by the $(\varphi + \overline{\varphi})$ fields takes place at the end of inflation, and any corresponding topological defects will not be inflated away.

Breaking via $SU(5) \times U(1)_\chi$:

Consider the following symmetry breaking patterns of $SO(10)$

$$\begin{aligned} SO(10) &\rightarrow SU(5) \times U(1)_\chi && (2.30) \\ &\rightarrow SU(3)_c \times SU(2)_L \times U(1)_Y \times U(1)_\chi && (2.31) \\ &\rightarrow SU(3)_c \times SU(2)_L \times U(1)_Y (\times Z_2) && (2.32) \end{aligned}$$

During the first symmetry breaking, $\pi_2 \left(\frac{SO(10)}{SU(5) \times U(1)_\chi} \right)$ is non-trivial. Thus, a monopole carrying $U(1)_\chi$ magnetic charge will be produced. In second phase transition achieved by the VEV of an $SU(5)$ 24-plet Higgs in 45-plet $SO(10)$, a monopole-antimonopole pair having $U(1)_\chi$ and $U(1)_Y$ charge is generated. Due to the orthogonality of the χ and Y directions, the $U(1)_\chi$ symmetry in (2.32) breaks to unity (or to Z_2 if $SU(3)_c \times SU(2)_L \times U(1)_Y \times U(1)_\chi$ is broken using a pair of $126 + \overline{126}$ Higgs fields). In this phase transition,

$$\pi_1 \left(\frac{SU(3)_c \times SU(2)_L \times U(1)_Y \times U(1)_\chi}{3_c 2_L 1_Y (Z_2)} \right) = \pi_0 (3_c 2_L 1_Y (Z_2)) = Z_2$$

which indicates the formation of cosmic strings possessing mass per unit length(μ) of $10^{32} GeV^2$ connecting monopole-antimonopole pair. The inflationary scenario is unable to resolve the monopole problem because monopoles emerging at both phase transitions are topologically stable. Therefore, these two models aren't consistent with the information on hand.

Breaking via $SU(5)$:

Consider $SO(10)$ breaking via $SU(5)$ as follows

$$\begin{aligned} SO(10) &\rightarrow SU(5) && (2.33) \\ &\rightarrow SU(3)_c \times SU(2)_L \times U(1)_Y && (2.34) \end{aligned}$$

The initial step of symmetry breaking does not result in the formation of any topological defects because both SO(10) and SU(5) are simply connected. Monopoles form by the breaking of $SU(5)$ to $3_c 2_L 1_Y$ because

$$\pi_2 \left(\frac{SU(5)}{3_c 2_L 1_Y} \right) = \pi_1(3_c 2_L 1_Y) = Z$$

These monopoles will have Y charge, $10^{17} GeV$ mass and is stable. Since the rank is reduced by one unit during the second step; the monopoles are produced at the end of inflation, dominating the energy density of universe. Therefore, this model clashes with the standard cosmology and proton lifetime data and thus, is also inconsistent.

Breaking via $SU(5) \times U(1)_X$:

Consider the following breaking chain of $SO(10)$ to flipped $SU(5)$

$$\begin{aligned} SO(10) &\rightarrow SU(5) \times U(1)_X \\ &\rightarrow SU(3)_c \times SU(2)_L \times U(1)_Y \\ &\rightarrow SU(3)_c \times U(1)_{EM} \end{aligned}$$

Here $U(1)_X$ contains part of $U(1)_Y$ and $U(1)_{EM}$ symmetries. Since

$$\pi_2\left(\frac{SO(10)}{SU(5)\times U(1)_X}\right) = Z$$

therefore, first step symmetry breaking leads to monopole formation. Furthermore, for the second phase transition

$$\pi_2\left(\frac{SU(5)\times U(1)_X}{3_c 2_L 1_Y}\right) = \pi_1(3_c 2_L 1_Y) = Z$$

again resulting in the formation of monopole. The monopoles formed are topologically stable, carry $B-L$ charge and possess mass $\geq 5\times 10^{17} GeV$. In the last stage of symmetry breaking, embedded cosmic strings are formed. A hybrid inflationary scenario for supergravity models could cure the monopole problem, as the inflaton field can couple to the Higgs needed to break SU(5)× U(1) as rank of flipped $DSU(5)$ is 5, forming embedded strings at the end of inflation. Therefore, the above model is quite interesting.

However the problem occurs when this model favors rapid proton decay and does not give mass to right handed neutrino. To address this issue, we will use $126 + \overline{126}$ Higgs field to break flipped $SU(5)$. During this phase transition, first homotopy group will be non trivial — $\pi_1\left(\frac{SU(5)\times U(1)_X}{3_c 2_L 1_Y (Z_2)}\right) = Z_2$ — resulting in the formation of stable Z_2 cosmic strings also with $\mu \sim 10^{32} GeV^2$.

Breaking via $SU(5)\times Z_2$:

Consider the symmetry breaking patterns as given below

$$\begin{aligned} SO(10) &\rightarrow SU(5)\times Z_2 \\ &\rightarrow SU(3)_c \times SU(2)_L \times U(1)_Y \times Z_2 \end{aligned}$$

Here the intact Z_2 symmetry is a subgroup of Z_4 centre of $SO(10)$. Note, at first step of breaking,

$$\pi_1\left(\frac{SO(10)}{SU(5)\times Z_2}\right) = \pi_0(SU(5)\times Z_2) = Z_2$$

Hence, stable cosmic strings are generated with $\mu \sim 10^{32}GeV^2 - 10^{38}GeV^2$. As the Z_2 symmetry is kept intact down to SM, these cosmic strings are topologically stable. Since $SO(10)$ has rank 5 and the rank of $SU(5)$ is 4, stable monopoles with mass $10617GeV$ will be formed at the end of inflation during the second symmetry breaking. Hence, this model conflicts with the established perception.

Breaking via $SU(3)_c \times SU(2)_L \times U(1)_Y$:

One may get the SM straight from the SUSY $SO(10)$ as follows

$$\begin{aligned} SO(10) &\rightarrow SU(3)_c \times SU(2)_L \times U(1)_Y \\ &\rightarrow SU(3)_c \times U(1)_{EM} \end{aligned} \tag{2.35}$$

or

$$\begin{aligned} SO(10) &\rightarrow SU(3)_c \times SU(2)_L \times U(1)_Y \times Z_2 \\ &\rightarrow SU(3)_c \times U(1)_{EM} \times Z_2 \end{aligned} \tag{2.36}$$

In (2.35) model, both steps of symmetry breaking produces monopoles because the second homotpy group(π_2) is non-trivial in both cases. They have mass of about $10^{17}GeV$, meaning that they will dominate the universe. In (2.36) model, fisrt phase transition produces cosmic strings as

$$\pi_1\left(\frac{SO(10)}{3_c 2_L 1_Y(Z_2)}\right) = \pi_0(3_c 2_L 1_Y(Z_2)) = Z_2$$

and they remain topologically stable even at low energy because Z_2 symmetry remains intact and have mass per unit length of $10^{32}GeV^2$. Monopoles arise during the grand unified phase transition once again as a result of the unbroken $U(1)_Y$ symmetry. They are topologically stable at low energy and have Y topological charge which might switch from Y to EM.

The possible clash with the accepted big-bang cosmology is once more not averted since monopoles emerge in both models at the end of inflation. With a superpotential of the type $\varphi + \overline{\varphi}$, one can attempt to inflate away the monopoles, but this needs the introduction of an intermediate scale. Therefore, the monopole overabundance problem remains unsolved or the simplicity of this symmetry breaking scheme is lost.

Chapter 3

Beyond Maxwell: The Quest for MMs

Magnetic monopoles are enigmatic and elusive hypothetical particles that acts as magnetic analog to an electric charge. Unlike ordinary magnets that have both north and south poles connected in pairs, MMs are singular and carry only one type of magnetic charge. Efforts to detect MMs have been ongoing for decades, and various theoretical and experimental approaches have been pursued. These include investigations in particle physics, cosmology, and condensed matter physics. Therefore, in this chapter, our prime focus will be the theory which shed light on the existence of MMs — **Dirac's theory** — with a look into soliton theory for better understanding as MMs are also referred as topological solitons.

3.1 Dirac's Theory

In the realm of theoretical physics, few ideas have captivated the imagination of scientists and researchers quite like the concept of MMs proposed by the British Physicist Paul Adrien Maurice Dirac in 1931 [14]. This theory repre-

sents an elegant and profound attempt to bridge the gap between EM forces and the tantalizing possibility of isolated magnetic charges. At the core of Dirac's theory lies the enigmatic "Dirac Quantization Condition (DQC)," a mathematical relationship that not only connects electric and magnetic charges but also offers a window into the deeper symmetries of the universe.

Dirac, renowned for his contributions to Quantum Mechanics (QM) and Quantum Field Theory (QFT), was struck by the apparent asymmetry — which at the time was described by Maxwell's equations — between electric charges and magnetic charges. While electric charges exist as separate entities, no isolated MMs had been observed. Dirac sought to reconcile this imbalance by postulating the existence of MMs. Dirac's groundbreaking insight is encapsulated in a profound manner as

$$\frac{qg}{4\pi} = \frac{1}{2}n. \tag{3.1}$$

here 'n' is an integer identified as a winding number (a topological interpretation). It goes without saying that DQC connects the electric charge quantization and the possible existence of magnetic monopoles. Bear in mind that DQC requires all magnetic charges to be integer multiples of the Dirac charge, represented by 'g_D' and is equal to

$$\begin{aligned} \frac{eg}{4\pi} &= \frac{1}{2}n, \\ g &= \frac{4\pi}{2e^2}en = \frac{137}{2}en, \\ &= 68.5en = ng_D. \end{aligned} \tag{3.2}$$

where $\alpha = \frac{4\pi}{e^2} = \frac{1}{137}$ and is known as fine-structure constant. We can also turn this argument around. Suppose there exists a MM of charge 'g_D' then

it is consistent for a particle with charge 'q' to exist only if

$$e^{\iota q g_D} = 1,$$

According to Euler's formula

$$e^{\iota\theta} = \cos\theta + \iota \sin\theta$$

Neglecting imaginary part due to the fact that MMs are real, we get

$$\begin{aligned} \cos(qg_D) &= 1, \\ qg_D &= 2\pi n, \\ q &= \frac{2\pi}{g_D} n = \frac{2\pi}{e}.\frac{2e^2}{4\pi} n, \\ q &= en \end{aligned} \tag{3.3}$$

Therefore the existence of MM implies quantization of electric charge [15].

Unlike electric charges, magnetic charges are always paired, with one being a north pole and the other being a south pole. And it is very hard to pair-produce the MMs arising from the intricate relationship between electric and magnetic charges dictated by the DQC. To have a deeper view to this, imagine a universe where particles can only carry one of the two potential charges — electric or magnetic — with possible values being 'q_j' and 'g_k' respectively. In such a case, the DQC has the form

$$\frac{q_j g_j}{4\pi} = \frac{1}{2} n_{jk}. \tag{3.4}$$

with n_{jk} being an integer. So, every electric charge 'q_j' needs to be a multiple of '$\frac{4\pi}{2g_j}$' for any given magnetic charge 'g_j' and vice versa. Assuming 'q_0' and

'g_0' as smallest electric and magnetic charges respectively, we have

$$q_j = n_j\, q_o \qquad , \qquad g_j = n'_j\, g_0 \tag{3.5}$$

This implies that

$$\frac{q_0\, g_0}{4\pi} = \frac{1}{2} n_0,$$

The interaction among two MMs can be calculated by squaring above equation

$$\frac{q_0^2\, g_0^2}{16\pi^2} = \frac{1}{4} n_0^2,$$

$$\begin{aligned} g_0^2 &= \frac{1}{4} n_0^2 . \frac{16\pi^2}{q_0^2} = q_0^2 \left(\frac{4\pi}{q_0^2}\right)^2 \frac{n_0^2}{4}, \\ &= q_0^2 \left(\frac{n_0}{2\alpha}\right)^2 . \end{aligned} \tag{3.6}$$

Equation (3.6) makes it clear that there exists very strong interaction among MMs due to the fact that the charge coupling is very small. Thenceforth, the magnetic monopoles will be significantly more challenging to pair-produce than the electrically charged particles [16].

Note that DQC can be derived by using both classical mechanics and quantum mechanics approaches. Following are the detailed, heuristic derivations of DQC from both aspects.

3.1.1 Semi-Classical Derivations

Lorentz Force Approach

Examining the motion of charged particle in a MM's field is one heuristic method for deriving the DQC. For this, consider a MM of strength 'g' is located at the origin. The magnetic field generated by this monopole at a

distance 'r' is expressed as

$$\vec{B} = \frac{g}{4\pi r^2}\hat{r}. \tag{3.7}$$

where $\hat{r}$ is radial unit vector. Now, let that a particle of charge 'q' possessing mass 'm' is in motion due to the magnetic field as shown in Figure 3.1. The motion of particle can be given by the following relation

$$\begin{aligned} \vec{F} &= q(\vec{v} \times \vec{B}), \\ m\ddot{\vec{r}} &= q(\dot{\vec{r}} \times \vec{B}), \end{aligned}$$

Pre-cross multiplying by $\vec{r}$

$$\begin{aligned} \vec{r} \times m\ddot{\vec{r}} &= q[\vec{r} \times (\dot{\vec{r}} \times \vec{B})], \\ \frac{d}{dt}\left(\vec{r} \times m\dot{\vec{r}}\right) &= q\left[\vec{r} \times (\dot{\vec{r}} \times \frac{g}{4\pi r^2}\hat{r})\right] = \frac{qg}{4\pi r^3}\left[\vec{r} \times (\dot{\vec{r}} \times \vec{r}\right], \end{aligned}$$

Since $\frac{\vec{r}\times(\dot{\vec{r}}\times\vec{r})}{r^3} = \frac{d\hat{r}}{dt}$, the above relation becomes

$$\frac{d}{dt}\left(\vec{r} \times m\dot{\vec{r}}\right) = \frac{d}{dt}\left(\frac{qg}{4\pi}\hat{r}\right),$$

$$\begin{aligned} \frac{d}{dt}\left(\vec{r} \times m\dot{\vec{r}}\right) - \frac{d}{dt}\left(\frac{qg}{4\pi}\hat{r}\right) &= 0, \\ \frac{d}{dt}\left(\vec{r} \times m\dot{\vec{r}} - \frac{qg}{4\pi}\hat{r}\right) &= 0. \end{aligned} \tag{3.8}$$

Hence, the total angular momentum is conserved and is given as

$$\vec{J} = \vec{r} \times m\dot{\vec{r}} - \frac{qg}{4\pi}\hat{r}. \tag{3.9}$$

Poincaré was the first to perceive that a vectorial integral of motion, arising

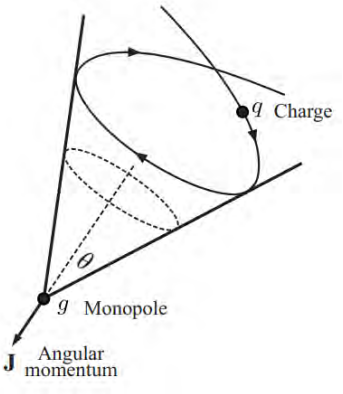

Figure 3.1: Dynamics of an electrical charge in motion within a magnetic monopole's field. This indicates that the charge travels in a cone with an angle θ along the axis $\vec{J}$ [17].

for a charge-MM system, is conserved and consists of a typical mechanical angular momentum besides an additional radial contribution($\frac{qg}{4\pi}\hat{r}$). But he failed to recognize that the conserved quantity is actually the system's total angular momentum(J) [18].

The conservation of $\vec{J}$ indicates that in the presence of q and g, the angular momentum is transferred back and forth between particle and field. By quantizing the above relation along radial direction, we get

$$J_r = \vec{J}.\hat{r} = -\frac{qg}{4\pi}. \tag{3.10}$$

We know that the total angular momentum is quantized and have half integral eigenvalues. Thus above equation becomes

$$\frac{qg}{4\pi} = \frac{1}{2}n \tag{3.11}$$

here 'n' is an integer which absorbs the minus sign. Equation (3.11) represents the DQC [16].

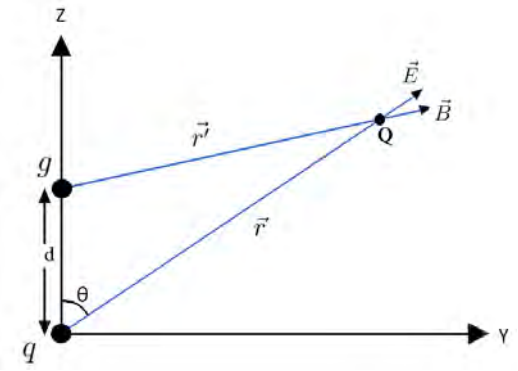

Figure 3.2: Thomson dipole configuration

Thomson Dipole Approach

In 1893, J.J. Thomson established that an electromagnetic field is related to the momentum density($\vec{P}$), which is propotional to a poynting vector. So, we can write the EM angular moemntum as

$$\vec{L}_{EM} = \int \vec{r} \times (\vec{E} \times \vec{B}) d^3r. \tag{3.12}$$

Here $\vec{E}$ is the elctric field produced by electric charge q, $\vec{B}$ is the magnetic field produced by magnetic monopole g. Both the charges are at rest, and are seperated by a finite distance denoted by d. This configuration, given in figure 3.2, was first considered by J.J.Thomson in the year 1904 and is now referred after his name as "Thomson dipole". He also pointed out that the mechanical and EM angular momenta are both conserved quantities, with the mechanical angular momentum being equal to 0 [18]. We know that

$$\vec{E} = \frac{q}{4\pi r^2}\hat{r} = \frac{q}{4\pi}\frac{\vec{r}}{r^3}. \tag{3.13}$$

and

$$\vec{B} = \frac{g}{4\pi r'^2}\hat{r'} = \frac{g}{4\pi}\frac{\vec{r'}}{r'^3}. \tag{3.14}$$

In this context, momentum density can be written as

$$\begin{aligned}\vec{P} &= \vec{E}\times\vec{B},\\ &= \frac{q}{4\pi}\frac{\vec{r}}{r^3}\times\frac{g}{4\pi}\frac{\vec{r'}}{r'^3},\\ &= \frac{qg}{(4\pi)^2}\left(\frac{\vec{r}\times\vec{r'}}{r^3r'^3}\right),\end{aligned}$$

From figure 3.2, we see that

$$\vec{r'} = \vec{r} - d\hat{z}. \tag{3.15}$$

We know that

$$\frac{1}{\mathtt{r}} = \frac{1}{\sqrt{r^2 + r'^2 - 2rr'\cos\theta}}. \tag{3.16}$$

This implies that

$$r'^3 = (r^2 + d^2 - 2rd\cos\theta)^{\frac{3}{2}}. \tag{3.17}$$

Substituting equations (3.15) and (3.17) in momentum density relation, we get

$$\begin{aligned}\vec{P} &= \frac{qg}{(4\pi)^2}\left(\frac{\vec{r}\times(\vec{r}-d\hat{z})}{r^3(r^2+d^2-2rd\cos\theta)^{\frac{3}{2}}}\right),\\ &= \frac{qg}{(4\pi)^2}\left(\frac{\overbrace{(\vec{r}\times\vec{r})}^{=0}+(\vec{r}\times\hat{z})(-d)}{r^3(r^2+d^2-2rd\cos\theta)^{\frac{3}{2}}}\right),\\ &= -\frac{qgd}{(4\pi)^2}\left(\frac{(\vec{r}\times\hat{z})}{r^3(r^2+d^2-2rd\cos\theta)^{\frac{3}{2}}}\right).\end{aligned} \tag{3.18}$$

Putting this value of $\mathcal{P}$ into equation (3.12)

$$\begin{aligned}\vec{L}_{EM} &= -\int \frac{qgd}{(4\pi)^2}\left(\frac{\vec{r}\times(\vec{r}\times\hat{z})}{r^3(r^2+d^2-2rd\cos\theta)^{\frac{3}{2}}}\right)d^3r,\\ &= -\frac{qgd}{(4\pi)^2}\int\left(\frac{\vec{r}\times(\vec{r}\times\hat{z})}{r^3(r^2+d^2-2rd\cos\theta)^{\frac{3}{2}}}\right)d^3r,\end{aligned}$$

Since

$$\vec{r}\times(\vec{r}\times\hat{z}) = \vec{r}(\vec{r}.\hat{z}) - \hat{z}(\vec{r}.\vec{r}) = r^2(\cos^2\theta - 1)\hat{z}.$$

Therefore

$$\begin{aligned}\vec{L}_{EM} &= -\frac{qgd}{(4\pi)^2}\hat{z}\int\left(\frac{r^2(\cos^2\theta-1)}{r^3(r^2+d^2-2rd\cos\theta)^{\frac{3}{2}}}\right)d^3r,\\ &= -\frac{qgd}{(4\pi)^2}\hat{z}\int\left(\frac{\cos^2\theta-1}{r(r^2+d^2-2rd\cos\theta)^{\frac{3}{2}}}\right)d^3r,\end{aligned}$$

We know that $d^3r = r^2\sin\theta dr d\theta d\varphi$, this implies that

$$\begin{aligned}\vec{L}_{EM} &= -\frac{qgd}{(4\pi)^2}\hat{z}\int\left(\frac{\cos^2\theta-1}{r(r^2+d^2-2rd\cos\theta)^{\frac{3}{2}}}\right)r^2\sin\theta dr\, d\theta\, d\varphi,\\ &= -\frac{qgd}{(4\pi)^2}\hat{z}\int\left(\frac{r(\cos^2\theta-1)}{(r^2+d^2-2rd\cos\theta)^{\frac{3}{2}}}\right)\sin\theta dr\, d\theta\, d\varphi,\end{aligned}$$

Let $v = \cos\theta \qquad \Longrightarrow \qquad dv = -\sin\theta\, d\theta$

This results in

$$\begin{aligned}\vec{L}_{EM} &= \frac{qgd}{(4\pi)^2}\hat{z}\int\left(\frac{r(v^2-1)}{(r^2+d^2-2rdv)^{\frac{3}{2}}}\right)dr\, dv\, d\varphi,\\ &= -\frac{qgd}{8\pi}\hat{z}\int_{-1}^{1}\int_{0}^{\infty}\left(\frac{r(1-v^2)}{(r^2+d^2-2rdv)^{\frac{3}{2}}}\right)dr\, dv, \qquad (3.19)\end{aligned}$$

Solving the r integral, we get

$$\begin{aligned}
\int_0^\infty \left(\frac{r}{(r^2+d^2-2rvd)^{\frac{3}{2}}}\right) dr &= \left[\frac{(rv-d)}{d(1-v^2)\sqrt{r^2+d^2-2rvd}}\right]_0^\infty, \\
&= \frac{r(v-\frac{d}{\infty})}{d(1-v^2)r\sqrt{1+\frac{d^2}{\infty}}} - \frac{0.v-d}{d(1-v^2)\sqrt{0+d^2-o}}, \\
&= \frac{v}{d(1-v^2)} + \frac{d}{d^2(1-v^2)}, \\
&= \frac{1}{d(1-v)}. \qquad (3.20)
\end{aligned}$$

Substituting this value in equation (3.19)

$$\begin{aligned}
\vec{L}_{EM} &= -\frac{qgd}{8\pi}\hat{z}\int_{-1}^{1}\left(\frac{1-v^2}{d(1-v)^{\frac{3}{2}}}\right) dv, \\
&= -\frac{qg}{8\pi}\hat{z}\int_{-1}^{1}(1+v)\,dv \;=\; -\frac{qg}{4\pi}\hat{z}. \qquad (3.21)
\end{aligned}$$

It is evident that quantization of the above EM angular momentum in radial direction yields DQC.

Saha's Approach

Using Thomson's EM angular momentum, M.N. Saha obtained the Dirac quantization condition in 1936 in a considerably rigorous way. In essence, he contends that angular momentum of any form in a quantum system should be a half integer, according to semi-classical theory. He genuinely thought of a neutron model where the enormous mass obtained by neutron to electron ratio was linked to the fact that it is a system comprising monopole-antimonopole pair [19].

Saha's model foresaw later MMs models that were proposed by Schwinger and others, despite the fact that it is not a plausible model for a neutron. To

derive Dirac quantization by Saha's approach, let's start by re-writing the Thomson's EM angular momentum

$$\vec{L}_{EM} = \int \vec{r} \times (\vec{E} \times \vec{B})\, d^3r.$$

Using $BAC - CAB$ rule, we get

$$\vec{L}_{EM} = \int \vec{E}(\vec{r}.\vec{B})\, d^3r - \int \vec{B}(\vec{r}.\vec{E})\, d^3r,$$

Putting value of $\vec{B}$ from equation (3.14)

$$\begin{aligned}
\vec{L}_{EM} &= \int \vec{E}(\vec{r}.\frac{g}{4\pi r^2}\hat{r})\, d^3r - \int \frac{g}{4\pi r^2}\hat{r}(\vec{r}.\vec{E})\, d^3r, \\
&= \int \vec{E}(r\hat{r}.\frac{g}{4\pi r^2}\hat{r})\, d^3r - \int \frac{g}{4\pi r^2}\hat{r}(r\hat{r}.\vec{E})\, d^3r, \\
&= \int \vec{E}\frac{g}{4\pi r}(\hat{r}.\hat{r})\, d^3r - \int \frac{g}{4\pi r}\hat{r}(\hat{r}.\vec{E})\, d^3r, \\
&= \int \vec{E}\frac{g}{4\pi r}(1)\, d^3r - \int \frac{g}{4\pi r}\hat{r}(\hat{r}.\vec{E})\, d^3r,
\end{aligned}$$

In index notation,

$$\begin{aligned}
\vec{L}_{EM} &= \int E^j \frac{g}{4\pi r}\delta^i_j\, d^3r - \int \frac{g}{4\pi r}\hat{r^i}(\hat{r^j}E^j)\, d^3r, \\
&= \frac{g}{4\pi}\int E^j \left(\frac{\delta^i_j - \hat{r^i}\hat{r^j}}{r}\right) d^3r, \qquad (3.22)
\end{aligned}$$

Consider

$$\begin{aligned}
\frac{\partial}{\partial r^j}\hat{r^i} &= \frac{\partial}{\partial r^j}\left(\frac{r^i}{r}\right), \\
&= \frac{r\left(\frac{\partial r^i}{\partial r^j}\right) - r^i\left(\frac{\partial r}{\partial r^j}\right)}{r^2},
\end{aligned}$$

$$\begin{aligned}
\frac{\partial}{\partial r^j}\hat{r^i} &= \frac{r\delta^i_j - r^i\left(\frac{\partial r}{\partial r^j}\right)}{r^2}, \\
&= \frac{r\delta^i_j - r\hat{r^i}\left(\frac{\partial r}{\partial r^j}\right)}{r^2}, \\
\implies &= \left(\frac{\delta^i_j - \hat{r^i}\hat{r^j}}{r}\right). \qquad (3.23)
\end{aligned}$$

Thus equation (3.22) becomes

$$\vec{L}_{EM} = \frac{g}{4\pi}\int E^j\left(\frac{\partial}{\partial r^j}\right)\hat{r^i}\, d^3r, \qquad (3.24)$$

Let

$$\begin{aligned}
\frac{\partial}{\partial r^j}\left(E^j\frac{g}{4\pi}\hat{r^i}\right) &= \frac{g\hat{r^i}}{4\pi}\frac{\partial E^j}{\partial r^j} + E^j\frac{\partial}{\partial r^j}\left(\frac{g}{4\pi}\hat{r^i}\right), \\
E^j\frac{\partial}{\partial r^j}\left(\frac{g}{4\pi}\hat{r^i}\right) &= \frac{\partial}{\partial r^j}\left(E^j\frac{g}{4\pi}\hat{r^i}\right) - \frac{g\hat{r^i}}{4\pi}\frac{\partial E^j}{\partial r^j}
\end{aligned}$$

So above equation can be written as

$$\begin{aligned}
\vec{L}_{EM} &= \int\frac{\partial}{\partial r^j}\left(E^j\frac{g}{4\pi}\hat{r^i}\right)\, d^3r - \int\frac{g\hat{r^i}}{4\pi}\frac{\partial E^j}{\partial r^j}\, d^3r, \\
&= \overbrace{\int\frac{\partial}{\partial r^j}\left(E^j\frac{g}{4\pi}\hat{r^i}\right)\, d^3r}^{=0} - \frac{g\hat{r^i}}{4\pi}\int\nabla.\vec{E}\, d^3r, \\
&= -\frac{g\hat{r^i}}{4\pi}\int\nabla.\vec{E}\, d^3r, \\
\because \vec{\nabla}.\vec{E} &= \rho = q\delta^3(\vec{r}), \\
\therefore \vec{L}_{EM} &= -\frac{g\hat{r^i}}{4\pi}\int q\delta^3(\vec{r})\, d^3r,
\end{aligned}$$

$$\begin{aligned}\vec{L}_{EM} &= -\frac{qg}{4\pi}\hat{r^i}\underbrace{\int \delta^3(\vec{r})\, d^3r}_{=1}, \\ &= -\frac{qg}{4\pi}\hat{r^i}. \end{aligned} \tag{3.25}$$

which, after quantization of radial component, leads to DQC.

Landau Theory Approach

In the annals of physics, the Landau Theory of Diamagnetism, conceived by the Soviet Physicist Lev Landau in the 1930s, occupies a significant place. This theoretical framework provides an elegant explanation for the intriguing behavior of charged particles in the presence of external magnetic fields. A crucial component of this theory is the concept of Landau levels — quantized energy states that emerge due to the interplay of quantum mechanics and magnetic fields — which provides a rigorous and elegant description of how charged particles, such as electrons, navigate within a magnetic field.

Now, if MMs are real, it is quite natural to comprehend magnetic version of Landau levels. Therefore, consider a parallel plate capacitor lying in the xy-plane. The homogenous electric field produced by this capacitor can be denoted as

$$\vec{E} = E\hat{k}$$

Before proceeding further, let me mention here that in this particular topic, we will start by not using natural units and substitute at the end. Suppose a magnetic monopole of strength 'g' having mass 'm' is placed in the electric field between the plates of the capacitor. What happens is that the MM starts orbiting perpendicular to the electric field in a circle of radius 'r' with some velocity given by 'v' under the influence of Lorentz force. This Lorentz

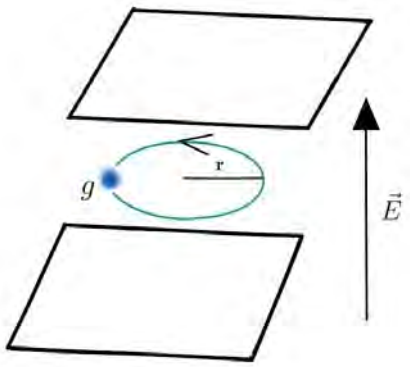

Figure 3.3: Motion of MM between the plates of a parallel-plate capacitor under the influence of electric field.

force is counterbalanced by the centrifugal force [20]. So,

$$\begin{aligned} F_E &= F_c, \\ gE\frac{v}{c} &= \frac{mv^2}{r}, \\ E &= \frac{mvc}{gr}. \end{aligned} \tag{3.26}$$

According to Landau theory, the allowed energy levels for monopole are

$$\mathcal{E}_n = \hbar\omega\left(n+\frac{1}{2}\right) = h\nu\left(n+\frac{1}{2}\right). \tag{3.27}$$

here $n = 0, 1, 2, 3, ...$ and ν can be derived by re-arranging (3.26) as

$$\frac{v}{r} = \frac{gE}{mc},$$

We know that

$$v = r\omega \quad \Longrightarrow \quad \omega = \frac{v}{r}$$

Thus, above equation results

$$\omega = \frac{gE}{mc}, \tag{3.28}$$

Sinec $\omega = 2\pi\nu$, therefore

$$\begin{aligned} 2\pi\nu &= \frac{gE}{mc}, \\ \nu &= \frac{gE}{2\pi mc}. \end{aligned} \tag{3.29}$$

As the MM orbits due to Lorentz force, it possesses kinetic energy which can equate the quantized energy of MM. Therefore

$$\begin{aligned} \frac{1}{2}mv^2 &= h\nu\left(n+\frac{1}{2}\right), \\ \frac{1}{2}mv^2 &= h\frac{gE}{2\pi mc}\left(n+\frac{1}{2}\right), \\ \frac{1}{2}mv^2 &= h\frac{g}{2\pi mc}\frac{mvc}{gr}\left(n+\frac{1}{2}\right), \\ mvr &= \hbar(2n+1), \\ \because \vec{J} = \vec{r}\times\vec{p} \quad \Longrightarrow \quad J_z &= mvr \\ \Longrightarrow J_z &= \hbar(2n+1) \end{aligned} \tag{3.30}$$

This equation represents quantization of angular momentum in the Z-direction. If we write the elctric field relation given in (3.26) in terms of J_z, we will have quantization condition for electric field as shown below

$$E = \frac{mvc}{gr},$$

Multiplying and dividing by 'r'

$$\begin{aligned} E &= \frac{mvrc}{gr^2}, \\ &= J_z\frac{c}{gr^2} = \frac{\hbar c}{gr^2}(2n+1). \end{aligned}$$

In natural units

$$E = \frac{1}{gr^2}(2n+1). \tag{3.31}$$

We know that the relation of electric field between the plates of a parallel plate capacitor having charge density σ is

$$\begin{aligned} E &= \sigma, \\ \because \sigma = \frac{q}{A} &= \frac{q}{\pi r^2} \\ \therefore E &= \frac{q}{\pi r^2} \end{aligned} \tag{3.32}$$

Putting this value in (3.31)

$$\begin{aligned} \frac{q}{\pi r^2} &= \frac{1}{gr^2}(2n+1), \\ \frac{qg}{\pi} &= 2\left(n+\frac{1}{2}\right), \\ \frac{qg}{4\pi} &= \frac{1}{2}\left(n+\frac{1}{2}\right), \end{aligned}$$

Clap eyes on the aspect that there still remains some charge at n = 0 for the reason that monopole has zero point energy. However, when radius 'r' approaches zero, both the area of the plate under consideration and the charge must contract to zero. In order to enforce the requirement that the lowest energy state have no charge, we subtract the vacuum effect as

$$\begin{aligned} \frac{qg}{4\pi} &= \frac{1}{2}\left(n+\frac{1}{2}-\frac{1}{2}\right), \\ \frac{qg}{4\pi} &= \frac{1}{2}n. \end{aligned} \tag{3.33}$$

which is just the DQC.

3.1.2 Quantum Mechanical Derivations

Analysis of the quantization of a particle's motion in a certain EM field leads to a thorough derivation of the DQC. When the EM field is quantized as is customary when there is no MM present, the EM field tensor $F^{\mu\nu}$ is written in the context of the four-vector potential as

$$F^{\mu\nu} = \partial^{\mu} A^{\nu} - \partial^{\nu} A^{\mu}. \tag{3.34}$$

where $A^{\mu} = (\varphi, \vec{A})$. Similarly, the electric and magnetic fields can also be written in terms of A_{μ} as

$$\vec{E} = -\vec{\nabla}\varphi - \frac{\partial \vec{A}}{\partial t}. \tag{3.35}$$

and

$$\vec{B} = \vec{\nabla} \times \vec{A}. \tag{3.36}$$

which in results satisfies the relation

$$\partial_{\mu} G^{\mu\nu} = 0$$

If a particle moves in an EM field, the Schrodinger's equation is given by the following relation

$$\left[\frac{1}{2m}(\vec{p} - q\vec{A})^2 + q\varphi\right] \Psi = \iota \frac{\partial \Psi}{\partial t}.$$

This Schrodinger's equation for EM field remains invariant under the following gauge transformation

$$\begin{aligned} \vec{A}(\vec{r}) &\longrightarrow \vec{A}(\vec{r}) + \vec{\nabla}\chi(\vec{r}) \\ \Psi(\vec{r}) &\longrightarrow e^{\iota q \chi} \Psi \end{aligned}$$

where $\chi(\vec{r})$ is an arbitrary gauge function and $e^{\iota q\chi}$ is element of gauge transformation.. One fact worth mentioning here is that the parameter χ's range is small if charge(q) is quantized in terms of some basic quanta e, in which case $\chi = 0$ and $\chi = 2\pi$ produce the same gauge transformation. It is important to distinguish between the compact one-parameter group, denoted by $U(1)$, and the non-compact one-parameter group, denoted by $\mathcal{R}$, which appears when the parameter range spans the whole real line and q is not quantized. Therefore, MM needs a small $U(1)$ group. In contrast, MMs exist in theories wherever there is a compact $U(1)$ group [21].

This means that A^{μ}, which serves as the fundamental dynamical variable in quantization, is extremely important. However, it is not possible for the vector potential to exist everywhere in the presence of MM. By proposing the idea of a string, Dirac overcomes this challenge. You are probably thinking, "***how***? "For this, let the magnetic field of a MM follows relation

$$\vec{B} = \frac{g}{4\pi r^2}\hat{r}. \tag{3.37}$$

In case of any closed surface including origin, we have

$$g = \oint \vec{B}.d\vec{S}.$$

By Gauss' divergence theorem

$$\begin{aligned} g &= \int \vec{\nabla}.\vec{B}\, dV, \\ g &= \int \vec{\nabla}.\vec{\nabla}\times\vec{A}\, dV, \\ g &= 0. \end{aligned}$$

It is obvious that $\vec{B}$ cannot be expressed everywhere as $\vec{\nabla}\times\vec{A}$ since the

above integral would be equal to zero in that case. On the other hand, we may define the $\vec{A}$ such that, everywhere on the line that exists between the origin and infinity, B is provided by $\vec{\nabla} \times \vec{A}$ [16].

Jackson's Treatment:

Think of a MM as either a single particle at the end of a string of dipoles or the tip of a tightly wound solenoid that extends to infinity. The vector potential of this magnetic dipole is given as

$$\begin{aligned} \vec{A}_{dip}(\vec{\mathtt{r}}) &= \frac{\vec{m} \times \hat{\mathtt{r}}}{\mathtt{r}^2}, \\ &= \frac{\vec{m} \times \vec{\mathtt{r}}}{\mathtt{r}^3}. \end{aligned} \tag{3.38}$$

Note that $\vec{\mathtt{r}}$ is the seperation vector given as

$$\vec{\mathtt{r}} = \vec{r} - \vec{r'}. \tag{3.39}$$

where $\vec{r}$ represents field point, $\vec{r'}$ is the source point and $\vec{m}$ denotes the magnetic dipole moment. Let an infinitesimally small magnetic dipole moments '$d\vec{m}$' at a point $\vec{r'}$ create the line of dipoles, which is a string whose vector potential is

$$\begin{aligned} d\vec{A} &= \frac{d\vec{m} \times \vec{\mathtt{r}}}{\mathtt{r}^3}, \\ \because \frac{\vec{\mathtt{r}}}{\mathtt{r}^3} = \frac{\hat{\mathtt{r}}}{\mathtt{r}^2} &= -\vec{\nabla}\left(\frac{1}{\mathtt{r}}\right), \\ \therefore d\vec{A} &= -d\vec{m} \times \vec{\nabla}\left(\frac{1}{\mathtt{r}}\right). \end{aligned} \tag{3.40}$$

We know that

$$d\vec{m} = g\, d\vec{l'}.$$

with 'g' being the magnetic charge and '$d\vec{l'}$ be a line element. So,

$$\begin{aligned} d\vec{A} &= -g\, d\vec{l'} \times \vec{\nabla}\left(\frac{1}{\mathtt{r}}\right), \\ \implies \vec{A} &= -g \int d\vec{l'} \times \vec{\nabla}\left(\frac{1}{\mathtt{r}}\right), \end{aligned}$$

Since

$$\begin{aligned} \vec{\nabla} \times \left(\frac{d\vec{l'}}{\mathtt{r}}\right) &= \frac{\mathtt{r}(\vec{\nabla} \times d\vec{l'}) - d\vec{l'}\overbrace{(\vec{\nabla} \times \mathtt{r})}^{=0}}{\mathtt{r}^2}, \\ &= \frac{1}{\mathtt{r}}(\vec{\nabla} \times d\vec{l'}), \\ \because \vec{A} \times \vec{B} = -\vec{B} \times \vec{A}. & \\ \therefore \vec{\nabla} \times \left(\frac{d\vec{l'}}{\mathtt{r}}\right) &= -d\vec{l'} \times \vec{\nabla}\left(\frac{1}{\mathtt{r}}\right). \end{aligned}$$

Thus above equation becomes

$$\vec{A} = g\vec{\nabla} \times \int \frac{d\vec{l'}}{\mathtt{r}}. \tag{3.41}$$

Keep in mind that this potential is already in Coulomb gauge($\vec{\nabla}.\vec{A} = 0$). Thus the curl of this potential gives

$$\vec{\nabla} \times \vec{A} = \vec{\nabla} \times \left(\vec{\nabla} \times \int_L \frac{g\, d\vec{l'}}{\mathtt{r}}\right),$$

Using $BAC - CAB$ rule

$$\begin{aligned} \vec{\nabla} \times \vec{A} &= \vec{\nabla}\left(\vec{\nabla}. \int_L \frac{g\, d\vec{l'}}{\mathtt{r}}\right) - \int_L \frac{g\, d\vec{l'}}{\mathtt{r}}(\vec{\nabla}.\vec{\nabla}), \\ &= g\vec{\nabla} \int_L \left(\vec{\nabla}.\frac{g\, d\vec{l'}}{\mathtt{r}}\right) - g \int_L \nabla^2 \left(\frac{1}{\mathtt{r}}\right). \end{aligned} \tag{3.42}$$

Consider 1^{st} integral

$$\begin{aligned}\int_L \vec{\nabla}.\left(\frac{d\vec{l'}}{\mathtt{r}}\right) &= \int_L \vec{\nabla}\left(\frac{1}{\mathtt{r}}.d\vec{l'}\right), \\ &= \int_L \frac{\hat{\mathtt{r}}}{\mathtt{r}^2}.d\vec{l'}, \\ &= \int_L \mathtt{r}^{-2}\, d\mathtt{r}, \\ &= -\frac{1}{\mathtt{r}}. \end{aligned} \tag{3.43}$$

Now consider the 2^{nd} integral

$$-\int_L \nabla^2\left(\frac{1}{\mathtt{r}}\right) = 4\pi\int_L \delta^3(\vec{\mathtt{r}})d\vec{l'}. \tag{3.44}$$

as $\nabla^2\left(\frac{1}{\mathtt{r}}\right) = -4\pi\delta^3(\vec{\mathtt{r}})$

Substituting these values into equation (3.42)

$$\begin{aligned}\vec{\nabla}\times\vec{A} &= g\vec{\nabla}\left(-\frac{1}{\mathtt{r}}\right) + g4\pi\int_L \delta^3(\vec{\mathtt{r}})d\vec{l'}, \\ \vec{\nabla}\times\vec{A} &= \frac{g}{\mathtt{r}^2}\hat{\mathtt{r}} + 4\pi g\int_L \delta^3(\vec{\mathtt{r}})d\vec{l'}, \end{aligned} \tag{3.45}$$

To have a clearer picture, it can be written as

$$\begin{aligned}\frac{g}{\mathtt{r}^2}\hat{\mathtt{r}} &= \vec{\nabla}\times\vec{A} - 4\pi g\int_L \delta^3(\vec{\mathtt{r}})d\vec{l'}, \\ \vec{B}_{Mon} &= \vec{\nabla}\times\vec{A} - \vec{B}_{String}. \end{aligned} \tag{3.46}$$

with

$$\vec{B}_{Mon} = \vec{\nabla}\times\vec{A}. \tag{3.47}$$

$$\vec{B}_{String} = 4\pi g\int_L \delta^3(\vec{\mathtt{r}})d\vec{l'}. \tag{3.48}$$

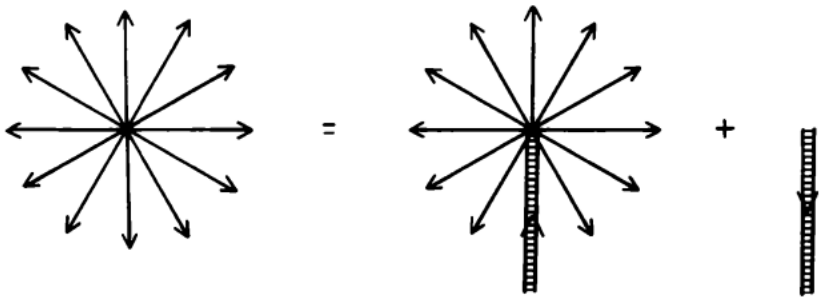

Figure 3.4: Pictorial representation of (3.49) [16].

As a particular application, consider a field that results from an indefinitely long, thin solenoid positioned along the negative Z-axis, with the positive pole of strength 'g' at the origin. Thus, $d\vec{l'} = dz'\hat{k}$. So, equation (3.45) can be modified as

$$\begin{aligned}
\vec{\nabla} \times \vec{A} &= \frac{g}{\mathtt{r}^2}\hat{\mathtt{r}} + 4\pi g\delta(x)\delta(y)\overbrace{\left[\int_{-\infty}^{0}\delta(z-z')dz'\right]}^{=\Theta(-z)}\hat{k}, \\
&= \frac{g}{\mathtt{r}^2}\hat{\mathtt{r}} + 4\pi g\delta(x)\delta(y)\Theta(-z)\hat{k}, \\
\Longrightarrow \vec{\nabla} \times \vec{A} &= \frac{g}{4\pi\mathtt{r}^2}\hat{\mathtt{r}} + g\delta(x)\delta(y)\Theta(-z)\hat{k},
\end{aligned}$$

Thus the field due to MM is given as

$$\vec{B}_{Mon} = \frac{g}{4\pi\mathtt{r}^2}\hat{\mathtt{r}} = \vec{\nabla} \times \vec{A} - g\delta(x)\delta(y)\Theta(-z)\hat{k}. \tag{3.49}$$

Here $\Theta(z)$ is a step function that can't be defined at $z = 0$. Note that Dirac string is actually the line which solenoid occupies. Equation (3.49) means that monopole field can be represented by a vector potential together with a string as shown in Fig. 3.4. With the exception of string singularity on the line $\theta = \pi$, the solution is valid everywhere. It is evident that using the standard definitions, the solenoid's vector potential $\vec{A}$ may be written in

terms of polar angle and azimuthal angle [16] in the following way

$$\begin{aligned} \vec{A}(r,\theta,\varphi) &= \int \frac{d\vec{m}\times\vec{\mathtt{r}}}{\mathtt{r}^3}, \\ \because d\vec{m} = g d\vec{z'}. & \\ \therefore \vec{A}(r,\theta,\varphi) &= g\int \frac{d\vec{z'}\times\vec{\mathtt{r}}}{\mathtt{r}^3}, \end{aligned}$$

$$\begin{aligned} &= g\int \frac{dz'\mathtt{r}\sin\theta}{\mathtt{r}^3}\hat{\varphi}, \\ &= g\int_{-\infty}^{0} \frac{dz'\sin\theta}{\mathtt{r}^2}\hat{\varphi}. \end{aligned} \tag{3.50}$$

According to law of cosines

$$\mathtt{r}^2 = r^2 + z'^2 - 2rz'\cos\theta.$$

Thus above equation can be re-written as

$$\vec{A}(r,\theta,\varphi) = g\int_{-\infty}^{0} \frac{dz'\sin\theta}{(r^2+z'^2-2rz'\cos\theta)}\hat{\varphi},$$

Multiplying and dividing by r, we get

$$\vec{A}(r,\theta,\varphi) = g\int_{-\infty}^{0} \frac{r\sin\theta}{(r^2+z'^2-2rz'\cos\theta)^{\frac{3}{2}}}dz'\hat{\varphi},$$

By solving the integral, we will get

$$\vec{A} = \frac{g}{4\pi r}\left(\frac{1-\cos\theta}{\sin\theta}\right)\hat{\varphi}. \tag{3.51}$$

which is singular along the negative Z-axis. Unambiguously, if we take the curl of equation (3.51) subjected to condition $\sin\theta \neq 0$, we will just have the

MM field as shown

$$\begin{aligned}
\vec{\nabla}\times\vec{A} &= \vec{\nabla}\times\left[\frac{g}{4\pi r}\left(\frac{1-\cos\theta}{\sin\theta}\right)\hat{\varphi}\right], \\
&= \frac{1}{r^2\sin\theta}\begin{vmatrix} \hat{r} & r\hat{\theta} & r\sin\theta\hat{\varphi} \\ \frac{\partial}{\partial r} & \frac{\partial}{\partial\theta} & \frac{\partial}{\partial\varphi} \\ 0 & 0 & \frac{g}{4\pi r}(1-\cos\theta) \end{vmatrix}, \\
&= \frac{1}{r^2\sin\theta}.\frac{g}{4\pi}\left[\frac{\partial}{\partial\theta}(1-\cos\theta)\right]\hat{r}, \\
&= \frac{g}{4\pi r^2}\hat{r} = \vec{B}. \qquad (3.52)
\end{aligned}$$

This is true because the differentiation process avoids the singularity caused by $\sin\theta = 0$. A MM and a magnetized string are the final two objects with which an electric charge will interact if it interacts with this potential. According to Dirac, the charge 'q' should never come into contact with the singular field $\vec{B}_{String}$ since there can be no other interaction except with the MM. In light of this, he hypothesized the dissipation of wave-function down the string. However, this condition is undoubtedly debatable because it would imply that the string doesn't actually exist. This is often refferred as "Dirac veto" hypothesizing the prohibition of contact between the electric charge and the string.

Dirac himself stated, "You must have the monopoles and the electric charges occupying distinct regions of space drawn anywhere subject to the condition that they must not pass through a region where there is electric charge present." To put it simply, Dirac string is not observable and the vector potential given in equation (3.51) is not specific to the solenoid field. The ability of the string to be moved about can be demonstrated by employing an appropriate gauge transformation [17]. For this, consider the gauge

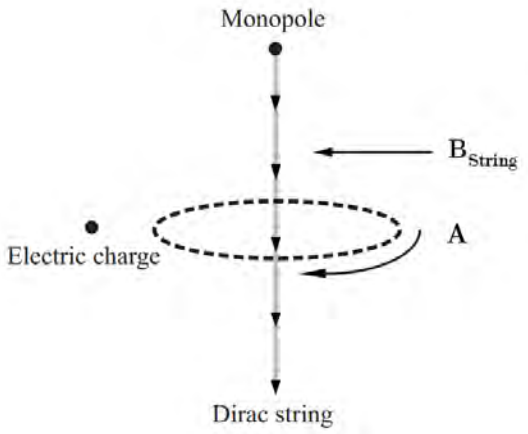

Figure 3.5: Dirac veto configuration [17].

transformation

$$\vec{A}' \longrightarrow \vec{A} + \vec{\nabla}\chi. \tag{3.53}$$

where χ is a non-singular, single-valued function of position. As a result, both the Dirac string and the $\vec{\nabla} \times \vec{A}$ terms in equation (**??**) must stay the same. To show that the location of Dirac string is independent, re-write equation (3.46) as

$$\vec{B}_{Mon} = \vec{\nabla} \times \vec{A} + \vec{h}(\mathcal{C}, \vec{r}).$$

where $\vec{h}(\mathcal{C}, \vec{r})$ gives the contribution of string along some curve $\mathcal{C}$ going from origin to infinity, having flux of strength 'g' as

$$\vec{h}(\mathcal{C}, \vec{r}) = 4\pi\, g \int \delta^3(\vec{r}) d\vec{l}'. \tag{3.54}$$

Consider an additional string $\mathcal{C}'$ that follows curve $\mathcal{C}$ from origin to infinity. Let ζ represent the curve $-\mathcal{C}'$ which is drawn in the opposite direction of $\mathcal{C}'$. By assuming that $\mathcal{C}'$ only deviates from $\mathcal{C}$ over a limited range, or by applying the appropriate transformations to what happens at infinity, we may regard this as a closed path. Let $\Omega(\vec{r})$ represent the solid angle that a

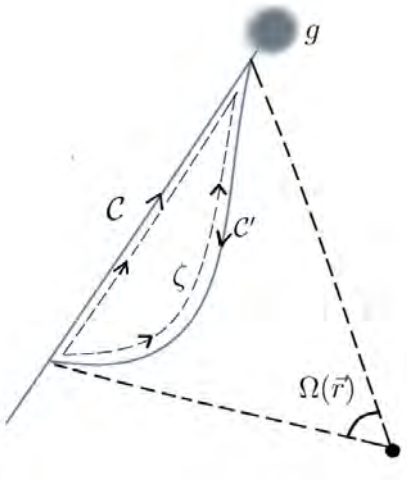

Figure 3.6: Representation of Dirac string connected with MM.

specific surface ζ occupies at $\vec{r}$. Different selections for the spanning surface will result in values of $\Omega(\vec{r})$ that varied by multiples of 4π, but they will all provide the same value for $\vec{\nabla}\Omega$ [16].

For two different curves $\mathcal{C}$ and $\mathcal{C}'$, the respective vector potentials would be $\vec{A}$ and $\vec{A}'$. Thus the extended gauge transformation can be calculated by integrating equation (3.41) along the closed curve $C = \zeta - \mathcal{C}_r$ as

$$\vec{A}' - \vec{A} = g\,\vec{\nabla} \oint_C \frac{d\vec{l'}}{\mathtt{r}},$$

Using Stokes' theorem

$$\vec{A}' - \vec{A} = \vec{\nabla} \times \left[\vec{\nabla} \times \left(\int_S \frac{g d\vec{a'}}{\mathtt{r}} \right) \right],$$

By $BAC - CAB$ rule

$$\begin{aligned}
\vec{A'} - \vec{A} &= \vec{\nabla}\left(\vec{\nabla}.\int_S \frac{g\vec{da'}}{\mathtt{r}}\right) - (\vec{\nabla}.\vec{\nabla})\int_S \frac{g\vec{da'}}{\mathtt{r}}, \\
&= g\vec{\nabla}\int_S \vec{\nabla}\left(\frac{1}{\mathtt{r}}\right).\vec{da'} - g\int_S \vec{\nabla}^2\frac{1}{\mathtt{r}}\vec{da'}, \\
&= g\vec{\nabla}\int_S \frac{\vec{\mathtt{r}}}{\mathtt{r}^3}.\vec{da'} + 4\pi g\int_S \delta^3(\vec{\mathtt{r}})\vec{da'},
\end{aligned}$$

The 1^{st} term represents solid angle

$$\Omega(\vec{r}) = \int_S \frac{\mathtt{r}}{\mathtt{r}^3}.\vec{da'}. \tag{3.55}$$

Thus,

$$\begin{aligned}
\vec{A'} - \vec{A} &= g\vec{\nabla}\Omega(\vec{r}) + 4\pi g\int_S \delta^3(\vec{r})\vec{da'}, \\
\implies \vec{A'} - \vec{A} &= \frac{g}{4\pi}\vec{\nabla}\Omega(\vec{r}) + g\int_S \delta^3(\vec{r})\vec{da'},
\end{aligned} \tag{3.56}$$

The contribution of delta integral vanishes at any point $\vec{r}$, but not on the surface S, so we can drop it off and have

$$\begin{aligned}
\vec{A'} - \vec{A} &= \frac{g}{4\pi}\vec{\nabla}\Omega(\vec{r}), \\
\vec{A'} &= \vec{A} + \frac{g}{4\pi}\vec{\nabla}\Omega(\vec{r}).
\end{aligned} \tag{3.57}$$

The gauge transformation seen in equation (3.53), where $\chi = g\Omega$, is brought to mind by the fact that $\vec{A'}$ and $\vec{A}$ are linked by a function's gradient. The important thing to remember in this situation is that the solid angle Ω experiences a discontinuous fluctuation of 4π when the observation point(q) crosses the surface S [17] . As a result, the gauge function χ on ζ is multi-valued

and poorly defined for $\vec{r}$. Therefore

$$\vec{\nabla} \times \vec{A'} = \vec{\nabla} \times \vec{A} = \vec{B}. \tag{3.58}$$

except on the two strings. Think of a small loop that surrounds any point on ζ. Using Stokes' theorem, we can determine the flux of $\vec{\nabla} \times (\vec{A'} - \vec{A})$ along ζ as

$$\begin{aligned} \int_S \vec{\nabla} \times (\vec{A'} - \vec{A}).d\vec{a'} &= \int_{\mathcal{C}_r} (\vec{A'} - \vec{A}).d\vec{l'}, \\ &= \frac{g}{4\pi} \int_{\mathcal{C}_r} d\Omega = g. \end{aligned} \tag{3.59}$$

Using equation (3.54), we get

$$\begin{aligned} \vec{\nabla} \times (\vec{A'} - \vec{A}) &= \vec{h}(\mathcal{C}, \vec{r}) - \vec{h}(\mathcal{C}', \vec{r}), \\ \Longrightarrow \vec{B} &= \vec{\nabla} \times \vec{A} + \vec{h}(\mathcal{C}, \vec{r}) = \vec{\nabla} \times \vec{A'} + \vec{h}(\mathcal{C}', \vec{r}). \end{aligned}$$

It can be seen from this that the Dirac string is moved by the gauge transformation. The string's random location proves it is not tangible or as said, "The Dirac string is a gauge artifact [16]."

Aharonov Bohm Effect Approach:

For a long time, physicists believed that the vector potential $\vec{A}$ is a mathematical object which is introduced just to reproduce a magnetic field. Until 1959 when Yakir Aharonov and David Bohm gave the famous Aharonov-Bohm effect. It is a quantum interference phenomenon that demonstrates how the EM vector potential, which is usually considered non-observable in classical physics, can have measurable effects on the quantum phase of charged particles. This effect highlights the significance of gauge potentials

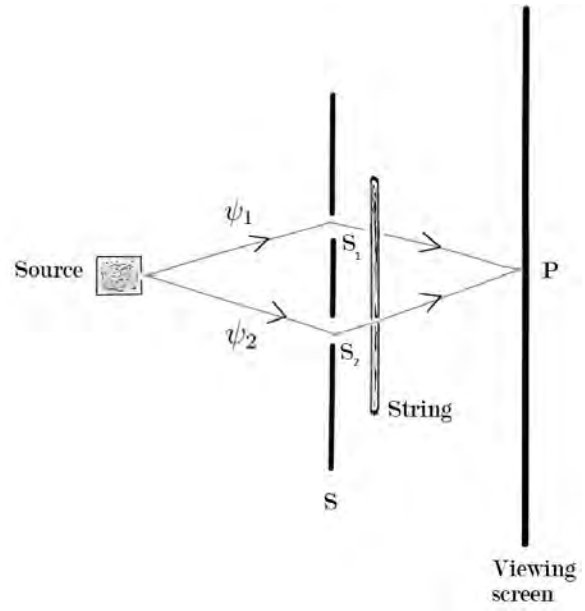

Figure 3.7: Aharanov-Bohm effect with Dirac string.

and their impact on the wave-functions of charged particles, even when those particles do not directly interact with the EM fields i.e. $\vec{B} = 0$.

It becomes apparent that DQC and Aharonov-Bohm effect exhibit commonalities. The Aharonov-Bohm effect involves a long solenoid, while the DQC involves semi-infinite string. Henceforth, one may contemplate Dirac string as a solenoid of Aharonov-Bohm effect and explore the plausibility of confirming the ambiguity of Dirac string and can also derive DQC through this approach [17].

For this, consider a source of electric charges. The rays of charges emitted by source pass through a screen(S) with two slits S_1 and S_2. We designate the wave-functions of the two rays of charges that pass through the slits as ψ_1 and ψ_2. These rays of charges are then detected at point 'P' on the viewing screen. Let a Dirac string is placed between the viewing screen and the screen with slits such that it lies in between the two slits as shown in Fig. 3.7. In the absence of the Dirac string, the wave-function of charges

coherently combine, resulting in probability density($\mathcal{P}$) given by relation

$$\mathcal{P} = |\psi_1 + \psi_2|^2. \tag{3.60}$$

However, in the presence of Dirac string, the string potential($\vec{A}_{String}$) causes each of the wave-functions ψ_1 and ψ_2 to acquire a phase. In this case, the wave-function of charges can be written as

$$\begin{aligned} \psi &= \left| e^{\iota q \int_1 \vec{A}_{String}.d\vec{l}} \psi_1 + e^{\iota q \int_2 \vec{A}_{String}.d\vec{l}} \psi_2 \right|^2, \\ &= e^{\iota q \int_c \vec{A}_{String}.d\vec{l}} |\psi_1 + \psi_2|^2, \end{aligned}$$

Using Stokes' Theorem, we get

$$\begin{aligned} \psi &= e^{\iota q \int_c \vec{\nabla} \times \vec{A}_{String}.d\vec{s}} |\psi_1 + \psi_2|^2, \\ &= e^{\iota q \frac{g}{4\pi} \int_c \frac{\hat{r}}{r^2}.d\vec{a}} |\psi_1 + \psi_2|^2, \end{aligned}$$

By applying Gauss' divergence theorem, we get

$$\begin{aligned} \psi &= e^{\iota q \frac{g}{4\pi}.4\pi} |\psi_1 + \psi_2|^2, \\ &= e^{\iota q g} |\psi_1 + \psi_2|^2. \end{aligned} \tag{3.61}$$

where

$$e^{\iota q \int_c \vec{A}_{String}.d\vec{l}} = e^{\iota q \int_1 \vec{A}_{String}.d\vec{l}} + e^{\iota q \int_2 \vec{A}_{String}.d\vec{l}}.$$

If $e^{\iota q g} = 1$ – which results in DQC – the Dirac string's effect would not be detectable. When this happens, the probability density will be the same given in equation (3.60), which indicates that the Dirac string has no effect on the interference pattern. In essence, if the DQC is satisfied, the Dirac string is undetectable. Reversing the logic, we may say that the Dirac string

is not observable if the DQC is true [17].

3.2 Solitons in Field Theory

After the development of QFT in early 1970s, the solutions of classical field equations are regarded as candidate for new particles, later named "**Solitons**." They have finite energy, are localized in space, and do not emit radiation during decay. This unusual stability is attributed to its topology. It should be noted that their quantization results in the emergence of new particle in QFT, not in perturbation theory.

What exactly does it imply to suggest that solitons resemble particles? We find that the solutions of classical field equations have a classical energy in terms of relativistic field theory. So, we can denote the soliton's mass 'm' in context of rest frame energy. Due to its relativistic nature, we can perform a Lorentz boost to produce a moving soliton which establishes relationship between energy and momentum in the form

$$E^2 - \vec{p}.\vec{p} = m^2.$$

This corresponds to another characteristic of a soliton that is Lorentz invariance. This provides support for considering solitons to be particles together with the notion that they are localized.

Due to their distinct features, solitons are distinct from the particles that appear in perturbative quantum fields. They, it turns out, have a topological nature distinct from the classical vacuum. Therefore, they cannot be considered perturbatively, at least not naively. Examples are kinks(in $1D$), vortices(in $2D$), monopoles or skyrmions(in $3D$), etc. Non-relativistic solitons do exist as well, however they are often not classified as particles.

Examples of their appearance include defects in solids and domain walls in ferromagnetic materials, both of which are not of our concern [22].

Conclusively, a soliton is — in an explicit manner — non-trivial, non-dissipative, finite energy solution of field equation and a subset of kinks. The difference between solitons and kinks is that solitons don't interfere in response to collision with other solitons, but kinks do. The presence of at least two degenerate minima in the potential energy is a prerequisite for both soliton and kink solutions to a field equation due to which the energy of kinks and solitons remain bounded [23].

You may ask, *What's the point of discussing solitons here*? Answer is, "To comprehend how the topology of space-time interacts with physical processes, finite energy solutions are essential." In simple words, in the framework of gauge theories such as electromagnetism, MMs can be considered as solitonic solutions to certain field equations. In this approach, the investigation of solitons in field theories sheds light on the behavior of topological defect and its consequences for particle physics.

Thus, a deeper knowledge of these types of solutions is crucial since it might aid in the identification of novel physical phenomena. In this context, two different scalar theories will be often examined:

1. $\lambda\varphi^4$ Theory

2. Sine-Gordon Theory

Note that for scalar field theories, the standard Lagrangian density is often given as

$$\mathcal{L} \;=\; \frac{1}{2}(\partial_\nu\varphi)^2 - U(\varphi).$$

We will describe here $\lambda\varphi^4$ theory in detail while the other one will be briefly

discussed in appendix B.

3.2.1 $\lambda\varphi^4$ Theory

To talk about MMs in non-abelian gauge theory, we usually consider $\lambda\varphi^4$ theory in $1+1$ dimensions. The Lagrangian density for $\lambda\varphi^4$ theory has the relation

$$\mathcal{L} = \frac{1}{2}(\partial_\nu\varphi)^2 + \frac{1}{2}\mu^2\varphi^2 - \frac{\lambda}{4}\varphi^4. \tag{3.62}$$

with λ being the dimensionless coupling constant, μ representing mass per unit length – while both depend on temperature(T)– and $U(\varphi)$ is potential energy equivalent to

$$U(\varphi) = -\frac{1}{2}\mu^2\varphi^2 + \frac{\lambda}{4}\varphi^4. \tag{3.63}$$

There is a global Z_2 symmetry in this Lagrangian density which will be evident by mapping $\varphi \longrightarrow -\varphi$. The corresponding Lagrangian can be expressed by the relation

$$L = \int \mathcal{L}dx = \int \left[\frac{1}{2}(\partial_\nu\varphi)^2 + \frac{1}{2}\mu^2\varphi^2 - \frac{\lambda}{4}\varphi^4\right] dx. \tag{3.64}$$

The Hamiltonian density can be written as

$$\begin{aligned} \mathcal{H} &= \frac{1}{2}(\partial_\nu\varphi)^2 + U(\varphi), \\ \mathcal{H} &= \frac{1}{2}(\partial_\nu\varphi)^2 - \frac{1}{2}\mu^2\varphi^2 + \frac{\lambda}{4}\varphi^4. \end{aligned} \tag{3.65}$$

and the Hamiltonian will be

$$\begin{aligned} H = \int \mathcal{H}dx &= \int \left[\frac{1}{2}(\partial_\nu\varphi)^2 - \frac{1}{2}\mu^2\varphi^2 + \frac{\lambda}{4}\varphi^4\right] dx, \\ &= \int \left[\frac{1}{2}(\partial_0\varphi)^2 + \frac{1}{2}(\partial_x\varphi)^2 - \frac{1}{2}\mu^2\varphi^2 + \frac{\lambda}{4}\varphi^4\right] dx. \end{aligned} \tag{3.66}$$

We know that classically, the potential will be conserved and as a consequence, the 1^{st} term in above equation becomes zero. Thus, the classical energy density could be described as

$$\mathcal{E} = \frac{1}{2}(\partial_x \varphi)^2 + U(\varphi). \tag{3.67}$$

with

$$\begin{aligned} U(\varphi) &= -\frac{1}{2}\mu^2\varphi^2 + \frac{\lambda}{4}\varphi^4, \\ &= \frac{\lambda}{4}\left[\left((\varphi^2)^2 - 2\frac{\mu^2}{\lambda}\varphi^2\right) - \left(\frac{\mu^2}{\lambda}\right)^2 + \left(\frac{\mu^2}{\lambda}\right)^2\right], \end{aligned}$$

$$U(\varphi) = \frac{\lambda}{4}\left[\left(\varphi^2 - \frac{\mu^2}{\lambda}\right)^2 - \left(\frac{\mu^2}{\lambda}\right)^2\right], \tag{3.68}$$

Since $\left(\frac{\mu^2}{\lambda}\right)^2$ is a constant which doesn't play any role in potential and as a result in Equation of Motion(EoM). Therefore, it can be neglected and the above equation can be written as

$$\begin{aligned} U(\varphi) &= \frac{\lambda}{4}\left[\varphi^2 - \left(\sqrt{\frac{\mu^2}{\lambda}}\right)^2\right]^2, \\ U(\varphi) &= \frac{\lambda}{4}(\varphi^2 - c^2)^2. \end{aligned} \tag{3.69}$$

where $c = \pm\sqrt{\frac{\mu^2}{\lambda}}$. Due to the fact that $(\partial_x\varphi)^2$ can't be a negative term, the condition for minimal energy density will be

$$\partial_x \varphi = 0 \tag{3.70}$$

with the constant value of φ will be determined by directly minimizing $U(\varphi)$

[16]. Since the coupling constant(λ) is positive, $U(\varphi)$ has the following two bounds:

Case-1: If $\mu^2(T) = c(T - T_c)$ then for $\mu^2 > 0$, the Lagrangian in equation (3.62) describes an ordinary scalar field theory. The classical ground state configuration in this case is given as

$$\begin{aligned} U(\varphi) &= 0 = \frac{\lambda}{4}(\varphi^2 - c^2)^2, \\ \Longrightarrow \varphi &= \pm c = \pm\sqrt{\frac{\mu^2}{\lambda}}. \end{aligned} \tag{3.71}$$

Thus the ground state energy becomes

$$\begin{aligned} \mathcal{E} &= \frac{1}{2}\overbrace{(\partial_x\varphi)^2}^{=0} + U(\varphi), \\ \mathcal{E} &= \frac{\lambda}{4}(\varphi^2 - c^2)^2 = \frac{\lambda}{4}(c^2 - c^2)^2, \\ \Longrightarrow E &= 0. \end{aligned} \tag{3.72}$$

Case-2 If $\mu^2(T) = c(T - T_c)$ then for $\mu^2 < 0$ (replace μ^2 by $-\mu^2$), the Lagrangian in equation (3.62) becomes

$$\mathcal{L} = \frac{1}{2}(\partial_\nu\varphi)^2 + \frac{1}{2}(-\mu^2)\varphi^2 - \frac{\lambda}{4}\varphi^4,$$

$$\mathcal{L} = \frac{1}{2}(\partial_\nu\varphi)^2 - \frac{1}{2}\mu^2\varphi^2 - \frac{\lambda}{4}\varphi^4. \tag{3.73}$$

with

$$U(\varphi) = \frac{1}{2}\mu^2\varphi^2 + \frac{\lambda}{4}\varphi^4 = \frac{\lambda}{4}\left[\left(\varphi^2 + \frac{\mu^2}{\lambda}\right)^2 - \underbrace{\left(\frac{\mu^2}{\lambda}\right)^2}_{=0}\right], \tag{3.74}$$

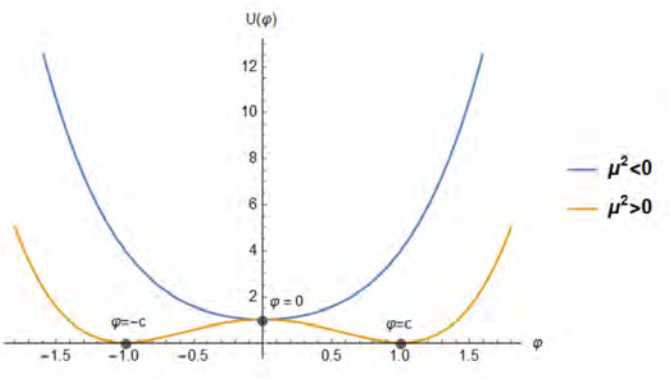

Figure 3.8: Effective potential for both possible bounds.

$$\begin{aligned} U(\varphi) &= \frac{\lambda}{4}(\varphi^2 + c^2)^2 = \frac{\lambda}{4}[\varphi^2 - (-c^2)]^2, \\ \Longrightarrow \varphi &= \pm(-c) = \pm\sqrt{\frac{-\mu^2}{\lambda}}. \end{aligned} \tag{3.75}$$

Clearly, the ground state energy is non-vanishing and the two possible values in (3.75) correspond to the two possible vacua.

From Fig. 3.8, we can infer that the extremum at $\varphi = 0$ is a local maxima of the potential(instead of minima) and is unstable. This potential will be minimized when φ has a constant, non-zero values which, in this case, is given by equation (3.75). At either minima, the Z_2 symmetry is spontaneously broken. Hence, it is evident that this Lagrangian has an internal Z_2 symmetry under $\varphi \longrightarrow -\varphi$.

We are interested in the time independent finite energy solution of EoM that can be derived by using variational principle as

$$\delta L = \delta \int \left[\overbrace{\frac{1}{2}(\partial_0\varphi)^2}^{=0} + \frac{1}{2}(\partial_x\varphi)^2 - U(\varphi) \right] dx = 0,$$

Replacing φ by x and x by t, we have

$$\delta L = \delta \int \left[\frac{1}{2} \left(\frac{dx}{dt} \right)^2 - U(x) \right] dx = 0, \tag{3.76}$$

Classical Mechanics tells us that the energy of moving particle is conserved which means that

$$\frac{1}{2} \left(\frac{dx}{dt} \right)^2 + [-U(x)] = 0, \tag{3.77}$$

which is related to explicit static solution of field theory as

$$\begin{aligned} \frac{1}{2} \left(\frac{d\varphi}{dx} \right)^2 + [-U(\varphi)] &= 0, \\ \frac{1}{2} \left(\frac{d\varphi}{dx} \right)^2 &= U(\varphi), \\ x &= \pm \int_{\varphi_0}^{\varphi} \frac{d\varphi}{\sqrt{2U(\varphi)}}. \end{aligned} \tag{3.78}$$

where $\pm$ sign indicates kink and anti-kink solutions, φ_0 is the value of φ at $x = o$ and can be any number between c and $-c$. The presence of this arbitrary parameter φ_0 is credited to translational invariance. Putting value of $U(\varphi)$ in above equation, we get

$$x = \pm \int_{\varphi_0=0}^{\varphi} \frac{d\varphi}{\sqrt{2\frac{\lambda}{4}(\varphi^2 - c^2)^2}}, \tag{3.79}$$

$$= \pm \sqrt{\frac{2}{\lambda}} \int_0^{\varphi} \frac{d\varphi}{(\varphi^2 - c^2)}, \tag{3.80}$$

By using method of partial fractions, we get

$$\begin{aligned} \frac{1}{(\varphi^2 - c^2)} &= \frac{\frac{1}{2c}}{(\varphi - c)} + \frac{-\frac{1}{2c}}{(\varphi + c)}, \\ &= \frac{1}{2c} \left[\frac{1}{(\varphi - c)} - \frac{1}{(\varphi + c)} \right]. \end{aligned}$$

Substituting this value in equation (3.80)

$$x = \pm\sqrt{\frac{2}{\lambda}}\int_0^{\varphi} d\varphi\left[\frac{1}{2c}\left(\frac{1}{(\varphi-c)}-\frac{1}{(\varphi+c)}\right)\right],$$

$$\begin{aligned} x &= \pm\frac{\sqrt{2}}{2c\sqrt{\lambda}}\left[\int_0^{\varphi}\frac{d\varphi}{\varphi-c}-\int_{\varphi_0}^{\varphi}\frac{d\varphi}{\varphi+c}\right], \\ x &= \pm\frac{\sqrt{2}}{2c\sqrt{\lambda}}\,ln\left(\frac{\varphi-c}{\varphi+c}\right), \\ c\sqrt{2\lambda}\,x &= ln\left(\frac{\varphi-c}{\varphi+c}\right), \end{aligned}$$

Since $c=\sqrt{\frac{\mu^2}{\lambda}}$, this implies that

$$\begin{aligned} \sqrt{2}\mu x &= ln\left(\frac{\varphi-c}{\varphi+c}\right), \\ \Longrightarrow e^{\pm\sqrt{2}\mu x} &= \frac{\varphi-c}{\varphi+c}, \\ e^{\pm\left(\frac{1}{2}\sqrt{2}\mu x+\frac{1}{2}\sqrt{2}\mu x\right)} &= \frac{\varphi-c}{\varphi+c}, \\ (\varphi+c)e^{\pm\frac{\mu}{\sqrt{2}}x} &= (\varphi-c)e^{\mp\frac{\mu}{\sqrt{2}}x}, \\ c\left(\frac{\varphi}{c}+1\right)e^{\pm\frac{\mu}{\sqrt{2}}} &= c\left(\frac{\varphi}{c}-1\right)e^{\mp\frac{\mu}{\sqrt{2}}}, \end{aligned}$$

Let $\pm\frac{\mu}{\sqrt{2}}x=a \quad\Longrightarrow\quad \mp\frac{\mu}{\sqrt{2}}x=-a$, then

$$\begin{aligned} \frac{\varphi}{c}e^{a}+e^{a} &= \frac{\varphi}{c}e^{-a}e^{-a}, \\ \frac{\varphi}{c}(e^{a}-e^{-a}) &= -(e^{a}+e^{-a}), \end{aligned}$$

Taking reciprocal on both sides

$$\frac{c}{\varphi}(e^{-a}-e^{a})=-(e^{-a}+e^{a}), \tag{3.81}$$

$$\begin{aligned}\varphi &= c\frac{(e^{a}-e^{-a})}{(e^{-a}+e^{a})} = c\tanh a,\\ &= c\tanh\left(\pm\frac{\mu}{\sqrt{2}}x\right).\end{aligned} \tag{3.82}$$

Thus, the finite energy solutions are

$$\varphi_{+} = c\tanh\left(\frac{\mu}{\sqrt{2}}x\right). \tag{3.83}$$

and

$$\varphi_{-} = c\tanh\left(-\frac{\mu}{\sqrt{2}}x\right) = -c\tanh\left(\frac{\mu}{\sqrt{2}}x\right). \tag{3.84}$$

where φ_{+} represents kink while φ_{-} represents anti-kink. Now, let's calculate the energy possessed by a single kink(or anti-kink). For this, we begin with the relation of energy density

$$\begin{aligned}\mathcal{E} &= \frac{1}{2}(\partial_x\varphi)^2 + U(\varphi),\\ \Longrightarrow \mathcal{E} &= 2U(\varphi) = \frac{\lambda}{2}(\varphi^2-c^2)^2.\end{aligned}$$

The total energy has thus the relation

$$E = \int \mathcal{E}dx = \int [2U(\varphi)]dx,$$

From equation (3.78)

$$\begin{aligned}E &= \int_{\varphi_0}^{\varphi}[2U(\varphi)]\frac{d\varphi}{\sqrt{2U(\varphi)}} = 2\int_{0}^{\pm c}[2U(\varphi)]^{\frac{1}{2}}\,d\varphi,\\ &= 2\int_{0}^{\pm c}\left[\frac{\lambda}{2}(\varphi^2-c^2)^2\right]^{\frac{1}{2}}d\varphi = \frac{2\sqrt{\lambda}}{\sqrt{2}}.\frac{c}{c}\int_{0}^{\pm c}(\varphi^2-c^2)\,d\varphi,\end{aligned}$$

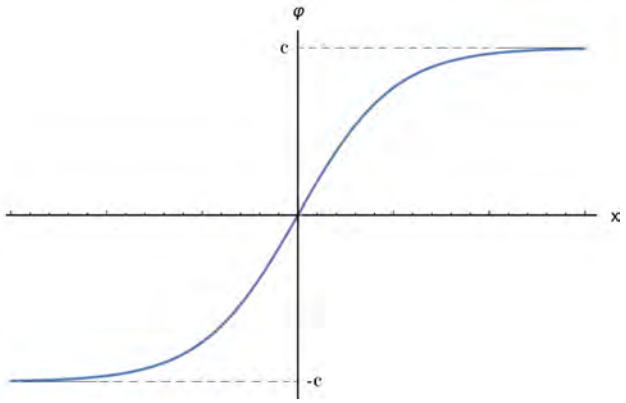

Figure 3.9: Demonstration of finiteness of energy.

$$\begin{aligned} E &= \frac{2\sqrt{\lambda}}{\sqrt{2}}.\frac{c\sqrt{\lambda}}{\mu}\left[\int_0^{\pm c}\varphi^2\,d\varphi - c^2\int_0^{\pm c}d\varphi\right] = \frac{4\lambda}{3\sqrt{2}\mu}.c^4, \\ &= \frac{2\sqrt{2}\mu^3}{3\lambda}. \end{aligned} \tag{3.85}$$

which is actually finite. It is quite apparent that when x approaches to $\pm\infty$, the kink solutions(φ_+) or anti-kink solution(φ_-) goes to zero of $U(\varphi)$. Mathematically,

$$\varphi \to \pm c \quad as \quad x \to \pm\infty$$

which is demonstrated in Fig. 3.9. Despite the fact that these solutions($\varphi_\pm$) are not the absolute minima of the potential energy, it can be demonstrated that they are stable with regard to petite perturbations. These finite-energy solutions to the EoM are interesting physically because they share certain characteristics with particles that have structure which are listed below:

1. A small, finite area of space contains all of its energy because these solutions($\varphi_\pm$) slightly diverge from the ground-state only in a small region near the origin.

2. Any velocity lower than unity can be used to move it. This is so because

the EoM is Lorentz invariant and we may use a Lorentz boost to get a solution with a velocity that is not zero [16].

3.2.2 Topological Conservation Laws

Physics comprises many conservation laws, Some of them are commonly known as topological or homotopic conservation laws. These laws are originated from well-defined SSB patterns discovered in the topology of the field manifold of solutions to a particular EoM rather than any symmetries possessed by a Lagrangian. Despite this, the symmetry properties of the Lagrangian are still crucial in theories with SSB, just as much as the symmetry characteristics of the ground-state configuration. It's worth noting that topological currents will also exist in any theory with degenerate minima [24].

The primary query at hand is, *What is the significance of homotopic conservation laws*? The answer is rooted in the observation that the stability of the finite energy solutions with respect to petite perturbations is attributed to its topological characteristics. Furthermore, this feature greatly assist in searching for stable finite-energy solutions to a specific EoM. Lastly, it can be easily adapted to more complex theories in higher dimensions, where explicit solutions are arduous to obtain [16].

So, now let's dig into the detail of topological property linked with finite energy solutions of $\lambda\varphi^4$ theory in one space and time dimensions. Finiteness of energy infer that

$$\begin{aligned} \varphi(\infty) - \varphi(-\infty) &= N(2c), \\ \implies \int_{-\infty}^{+\infty} \partial_x \varphi \, dx &= N(2c). \end{aligned} \tag{3.86}$$

where N is an integer and is a conserved quantum number which specify the

state of the system. Meaning that for ground state, it's value is 0. Similarly, $N = +1$ represents kink state while $N = -1$ corresponds to anti-kink state. For this conserved quantity, one can define a corresponding current as

$$\mathcal{J}_\mu(x) = \epsilon_{\mu\nu}(\partial^\nu \varphi). \tag{3.87}$$

where $\mathcal{J}_\mu(x)$ is called topological current which is different from Noether current and $\epsilon_{\mu\nu}$ is an anti-symmetric tensor having following properties

$$\epsilon_{\mu\nu} = -\epsilon_{\nu\mu} \qquad , \qquad \epsilon_{0\,1} = 1$$

This implies that

$$\partial^\mu \mathcal{J}_\mu(x) = \partial^\mu[\epsilon_{\mu\nu}(\partial^\nu \varphi)] = 0 \tag{3.88}$$

which means that topological current is a conserved quantity. According to the Noether theorem, if topological current is conserved, the conserved topological charge will be an integral of motion of the conserved current [23]. Mathematically,

$$\begin{aligned} \mathcal{Q} &= \int_{-\infty}^{+\infty} \mathcal{J}_0(x) = \int_{-\infty}^{+\infty} \partial_x \varphi \, dx, \\ \mathcal{Q} &= N(2c) \end{aligned} \tag{3.89}$$

This conservation speaks about the stability of kink solution or anti-kink solution. Meaning that kink, anti-kink and ground-state configurations cannot undergo transition into each other. In contrast to the typical Noether conservation laws, which derive from the theory's symmetry, this conservation law – referred as the topological conservation law – has a distinct origin since it holds independent of the EoM. This conservation law may be understood intuitively by imaging that an infinite amount of energy is required to trans-

late the kink or anti-kink configuration into the ground-state configuration because we have to penetrate the barrier around $\varphi = 0$ across an infinite range of x.

In the context of $(1 + 1)$ dimensions, there exist two unique points, $+\infty$ and $-\infty$, that make up the spatial infinities represented by set S. When it comes to $\lambda\varphi^4$ theory, the minima of the potential provided in equation (3.75) in also comprised of two distinct points which can be designated by set $\mathcal{M}_0$ as

$$\mathcal{M}_0 = \{\, \varphi : \; U(\varphi) = 0\} \tag{3.90}$$

In order to map points in S to $\mathcal{M}_0$, The requirement is that the asymtotic vacuum values of φ must go to zeroes of $U(\varphi)$ to ensure that the EoM has solutions possessing finite energy. Mathematically,

$$\lim_{x\to\pm\infty} \varphi(x) = \varphi \in \mathcal{M}_0 \tag{3.91}$$

For instance, the ground-state configuration maps both $\pm\infty$ to either c or $-c$. However, when it comes to kink configuration, $+\infty$ is mapped to c while $-\infty$ is mapped to $-c$. These mappings are important topologically, meaning that we cannot continuously transform one mapping into the other. This concept lies at the heart of topological conservation law. In short, we can conclude that for the topological solitons to exist, the theory under scope must contain degenerate minima and non-trivial topological features in order for these solitons to be topologically stable and of finite energy [16].

Chapter 4

A Comprehensive Overview of MMs

4.1 Theoretical Overview of MMs

There are various theoretical frameworks that had a significant impact on the field of physics and has inspired ongoing research into the possible existence of these elusive particles. Some scientists believe that magnetic monopoles could help explain certain phenomena, such as the quantization of electric charge and the behavior of cosmic rays, gravitational waves, etc. A number of theoretical models helps us in grasping the concept, structure and other information about MMs.

4.1.1 t'Hooft-Polyakov Monopoles

Dirac's theory on MMs proved that their existence do not preclude by quantum mechanics, which implies the quantization of electric charge. Infact, Dirac stated, "one would be surprised if Nature had made no use of it." Today we understand that the charge would still be quantized if the gauge

group $U(1)_{EM}$ is compact, which is possible by incorporating $U(1)_{EM}$ into a non-Abelian GUT group. This means that any GUTs with quantized charge include MMs. Also, though Dirac's theory is widely accepted, but it doesn't provide complete information about the characteristics of MM like mass, topology, structure, etc [15].

Motivated by this, two physicists Gerard 't Hooft and Alexander Polyakov — in 1974 — independently demonstrated that MMs arise in GUTs as solutions to the classical field equations. For this, they considered $SO(3)$ model, developed by Georgi and Glashow in 1972, due to its simplicity though experimental evidence rendered this model invalid due to the discovery of neutral-current phenomena. Remember that $SO(3)$ is isomorphic to $SU(2)_L$ and the symmetry breaking pattern is $SU(2)_L \sim SO(3) \rightarrow SO(2) = U(1)_{EM}$ [25, 26]. Thus, in the context of $SU(2)_L$ with isovector Higgs doublet $\vec{\varphi}$, the Lagrangian density can be written as

$$\mathcal{L} = -\frac{1}{4}F_{i\mu\nu}F_i^{\mu\nu} + \frac{1}{2}\mathcal{D}_\mu\vec{\varphi}\mathcal{D}^\mu\vec{\varphi} - U(\vec{\varphi}). \tag{4.1}$$

where $F_{\mu\nu}$ is the field tensor, $\mathcal{D}_\mu$ denotes covariant derivative and $U(\vec{\varphi})$ represents potential energy whose relations are as follows

$$\begin{aligned} F^i_{\mu\nu} &= \partial_\mu A^i_\nu - \partial_\nu A^i_\mu - e\epsilon^{ijk}A^j_\mu A^k_\nu. && (4.2)\\ (\mathcal{D}_\mu\varphi)^i &= \partial_\mu\varphi^i - e\epsilon^{ijk}A^j_\mu\varphi^k. && (4.3)\\ U(\vec{\varphi}) &= \frac{\lambda}{4}(\varphi^2 - c^2). && (4.4) \end{aligned}$$

where $i = 1, 2, 3$. The corresponding EoMs w.r.t $F_{\mu\nu}$ and φ are

$$\begin{aligned} (\mathcal{D}_\nu F_{\mu\nu})^i &= -e\epsilon^{ijk}\varphi^j(\mathcal{D}_\mu\varphi)^k. && (4.5)\\ (\mathcal{D}^\mu\mathcal{D}_\mu\varphi)^i &= -\lambda\varphi^i(\varphi^2 - c^2). && (4.6) \end{aligned}$$

The minimum of the potential provided in equation (4.4) can be designates as

$$\mathcal{M}_0 = \{\vec{\varphi} = \eta\,,\, \eta^2 = c^2\}. \tag{4.7}$$

For simplicity, we can write it as

$$\vec{\varphi} = \{0, 0, c\}. \tag{4.8}$$

Equation (4.8) is invariant under rotation around the $SO(2)$ transformation, pointing towards spherical symmetry. The unbroken $U(1)_{EM}$ symmetry corresponds to the EM interaction, with the massless gauge bosons representing the photon. In order to obtain a finite-energy solution, it is necessary that

$$\begin{aligned} &\vec{\varphi}(\vec{r})\,\epsilon\,\mathcal{M}_0 \qquad\qquad as \qquad\qquad \vec{r} \to \infty \\ &\qquad \Longrightarrow \varphi_i^{\infty} \quad = \eta_i = \quad c\hat{r}_i. \end{aligned} \tag{4.9}$$

The mapping provided in equation (4.9) is topologically stable and cannot be transformed continuously into the vacuum configuration [16]. To find out the explicit finite-energy solution for the spherically symmetric classical field equation mentioned above, we use the following ansatz

$$\begin{aligned} \varphi_a &= \frac{r^a}{er^2} H(cer). \\ A_a^i &= \epsilon_{iak} \frac{r^k}{er^2} [1 - K(cer)]. \\ A_a^0 &= 0. \end{aligned} \tag{4.10}$$

with H and K being the dimensionless functions. By using this ansatz, we

obtain the following relation for the energy

$$\begin{aligned} E &= \frac{4\pi c}{e}\int_0^\infty \frac{d\phi}{\phi^2}\left[\phi^2\left(\frac{dK}{d\phi}\right)^2+\frac{1}{2}\left(\phi\frac{dH}{d\phi}-H\right)^2\right. \\ &+ \left.\frac{1}{2}(K^2-1)^2+K^2H^2+\frac{\lambda}{4e}(H^2-\phi^2)^2\right]. \end{aligned} \tag{4.11}$$

where $\phi = cer$. The prerequisites for energy to be stationarity with regard to perturbations in H and K are

$$\phi^2\frac{d^2K}{d\phi^2} = KH^2+K(K^2-1). \tag{4.12}$$

$$\phi^2\frac{d^2H}{d\phi^2} = 2K^2H+\frac{\lambda}{e^2}H(H^2-\phi^2). \tag{4.13}$$

Following boundary conditions will be observed to derive the finite-energy solution

$$\begin{aligned} &H=0, \quad K=1 \quad as \quad r\to 0 \\ &H=1, \quad K=0 \quad as \quad r\to \infty \end{aligned} \tag{4.14}$$

By using these boundary conditions, one can get the solutions of H and K which do exist [15]. Thus, inference can be drawn that 't Hooft-Polyakov('tHP) monopoles naturally arise in GUTs. Salient features of the 'tHP solutions are:

1. It is observed that at large distances $K = 0$ as $r \to \infty$, so we have from equation (4.3)

$$\begin{aligned} F^i_{ab} &\sim \epsilon_{abc}\frac{r^c r^i}{er^4}, \\ &\sim -\frac{\vec{r}}{er^3} \sim \vec{B}. \end{aligned} \tag{4.15}$$

which indicates that the 'tHP solution behaves like a MM and for this reason, it is termed as "'tHP monopole." By comparing this relation with $\vec{B} = \frac{g\vec{r}}{4\pi r^3}$, we obtain the magnetic charge on 'tHP monopole which is equal to

$$g = \frac{4\pi}{e}. \tag{4.16}$$

To crunch up, we can say that 'tHP monopole carries two units of Dirac charge.

2. 'tHP theory gives a formula to calculate the mass of the MM

$$M_{Mon} = \frac{4\pi c}{e} f(\lambda/e^2). \tag{4.17}$$

which can be derived by solving equation (4.11). Here $f(\lambda/e^2)$ represented the value in the integral whose numerically calculated value is of the order of unity and c denotes the VEV of Higgs field. So, we can conclude that the mass of MM is of the order of SSB scale.

3. 'tHP monopole has a well-defined core unlike the point monopoles predicted by Dirac. This is due to the fact that when ϕ is large

$$K \to 0 \qquad , \qquad H \to \phi \tag{4.18}$$

This implies that

$$K \sim e^{-\phi} \cong e^{-Mr}. \tag{4.19}$$

$$H - \phi \cong e^{-\mu r}. \tag{4.20}$$

which are obtained by substituting the above mentioned boundary conditions in equations (4.13) and (4.13). Note that $\mu = c\sqrt{2\lambda}$ and $M \simeq ec$

which represents the masses of scalar bosons and gauge bosons respectively. This suggests that the masses of the associated particles govern how close a field approaches its asymptotic form. Since these masses dictate the 'tHP monopole's size, we may consider it to have a finite size.

4. Another interesting feature of 'tHP monopole can be shown by writing A_a^i as

$$A_a^i = \frac{1}{c^2 e}\epsilon^{abc}\varphi^b \partial^i \varphi^c.$$

Using this we can write the magnetic field tensor as

$$\begin{aligned} F_{ij} &= \partial_i A_j - \partial_j A_i - e(A_i A_j - A_j A_i), \\ &= \partial_i A_j - \partial_j A_i - (\text{additional terms}). \end{aligned} \tag{4.21}$$

which indicates that 'tHP monopole has no singularity, resulting in no requirement of Dirac string [16].

4.1.2 Nambu Monopoles

The MMs resulting from 'tHP theory are superheavy as they arise in GUTs. There was not a single theory that could explain the formation of mnopoles due to EW symmetry breaking until 1977 when Yoichiro Nambu has undertaken the task of describing monopole formation in Weinberg-Salam model. He got inspiration from Abrikosov-Neilsen-Olesen vortices found in Abelian Higgs model. In his study of the electroweak theory, Nambu observed that the theory contains vortex solutions that closely resemble the Abrikosov-Nielsen-Olesen vortices.

However, there is a significant difference between the two: the electroweak

string can terminate by placing an anti-monopole at the other end.. When the termination occurs, the magnetic flux that was previously trapped within the vortex is released through the termination point and then spreads out into space. This process gives the illusion of a MM. Furthermore, the magnetic flux is not the only physical quantity that is released during the termination; the energy density of the Higgs field is also released. For this, Nambu used the "isospinor" φ for the Higgs field given as

$$\varphi \sim \begin{pmatrix} \cos\frac{\theta}{2} \\ \sin\frac{\phi}{2}e^{\iota\phi} \end{pmatrix}. \tag{4.22}$$

From above expression. we can infer that along the negative z-axis, φ becomes ill-defined due to the absence of a limit for $\theta \to \pi$. To address this concern, Nambu introduced an assumption that the amplitude φ equates to zero when $\theta = \pi$. As a result, a semi-infinite string arises, spanning across the negative z-axis and culminating at the monopole placed at origin. This creates a striking resemblance to the meson string model.

To visualize it mathematically, consider the classical solutions in which the presence of a gauge field with a non-zero value of φ signifies that the system is in a state of minimum total energy. It means that potential energy $U(\varphi)$ is minimal resulting in

$$\mathcal{D}_\mu \varphi = 0. \tag{4.23}$$

For the case of isovector $\vec{\varphi}$ and gauge potential A_μ

$$\mathcal{D}_\mu \vec{\varphi} = \partial_\mu \vec{\varphi} - g\, A_\mu \vec{\varphi} = 0.$$

This tells us that $\vec{\varphi}.\vec{\varphi}$ is a constant. Thus above equation can be written as

$$\begin{aligned} \partial_\mu\vec{\varphi} - g\,A_\mu\vec{\varphi} &= a_\mu, \\ \partial_\mu\vec{\varphi}\times\vec{\varphi} - g\,A_\mu(\vec{\varphi}\times\vec{\varphi}) &= a_\mu\vec{\varphi}, \\ g\,A_\mu &= \vec{\varphi}\times\partial_\mu\vec{\varphi} + a_\mu\vec{\varphi}. \end{aligned} \tag{4.24}$$

where a_μ is an arbitrary constant. We know that the field tensor has the relation

$$\vec{F}_{\mu\nu} = \partial_\mu A_\nu - \partial_n u A_\mu + g A_\mu \times A_\nu.$$

Substituting equation (4.24), we have

$$\begin{aligned} \vec{F}_{\mu\nu} &= \partial_\mu\left[\frac{1}{g}\vec{\varphi}\times\partial_\nu\vec{\varphi} + a\nu\vec{\varphi}\right] - \partial_\nu\left[\frac{1}{g}\vec{\varphi}\times\partial_\mu\vec{\varphi} + a_\mu\vec{\varphi}\right] \\ &+ (\vec{\varphi}\times\partial_\mu\vec{\varphi} + a_\mu\vec{\varphi})\times\frac{1}{g}(\vec{\varphi}\times\partial_\nu\vec{\varphi} + a_\nu\vec{\varphi}), \\ \Longrightarrow &= \frac{1}{g}[(\partial_\mu\vec{\varphi}\times\partial_n u\vec{\varphi}) + (\partial_\mu a_\nu - \partial_\nu a_\mu)\vec{\varphi}], \\ &= \frac{1}{g}[(\partial_\mu\vec{\varphi}\times\partial_\nu\vec{\varphi}) + f_{\mu\nu}\vec{\varphi}. \end{aligned} \tag{4.25}$$

where $f_\mu\nu = \partial_\mu a_\nu - \partial_\nu a_\mu$. From this, we can have the value of $F_{\mu\nu}$ as

$$\begin{aligned} F_{\mu\nu} &= \vec{\varphi}.\vec{F}_{\mu\nu}, \\ &= \frac{1}{g}(\vec{\varphi}.\partial_\mu\vec{\varphi}\times\partial_\nu\vec{\varphi} + f_{\mu\nu}). \end{aligned} \tag{4.26}$$

In case of $SU(2)_L \times U(1)_Y$ model, we have Higgs iso-doublet φ. Thus, we will use scaled gauge fields given as

$$A_\mu = \iota\frac{\tau^a}{2}\vec{A}^a_\mu. \tag{4.27}$$

where $a = 1, 2, 3$. Thus, equation (4.1.2) can be re-written as

$$\begin{aligned} \mathcal{D}_\mu\varphi &= \partial_\mu\varphi - g\,A_\mu\varphi = 0, \\ 0 &= (\partial_\mu - g\iota\frac{\tau^i}{2}\vec{A}^i_\mu - \frac{\iota}{2}g'A^0_\mu)\varphi, \\ \Longrightarrow -\iota\partial_\mu\varphi &= (g\tau^i A^i_\mu + g'A^0_\mu)\varphi. \end{aligned}$$

Multiplying by $\varphi^\dagger$, we have

$$-\iota\varphi^\dagger\partial_\mu\varphi = gA^i_\mu(\varphi^\dagger\tau^i\varphi) + g'A^0_\mu(\varphi^\dagger\varphi). \tag{4.28}$$

Note that $\varphi^\dagger\varphi = 1$. Furthermore, the series of Fierz identities are given in appendix C. By implying these relations, equation (4.28) takes the form

$$gA^i_\mu + g'A^0_\mu(\varphi^\dagger\tau^i\varphi) = -\epsilon^i jk(\varphi^\dagger\tau^i\varphi)\partial_\mu(\varphi^\dagger\tau^k\varphi) - \iota(\varphi^\dagger\tau^i\varphi)(\varphi^\dagger\overleftrightarrow{\partial_\mu}\varphi). \tag{4.29}$$

We can divide this equation into two equations

$$\begin{aligned} gA^i_{\perp\mu} &= -\epsilon^i jk(\varphi^\dagger\tau^i\varphi)\partial_\mu(\varphi^\dagger\tau^k\varphi). \\ gA^i_{\parallel\mu} + g'A^0_\mu &= -\iota(\varphi^\dagger\overleftrightarrow{\partial_\mu}\varphi). \end{aligned} \tag{4.30}$$

with $A_\parallel$ and $A_\perp$ denoting, respectively, the parts that are parallel to $\varphi^\dagger\tau^i\varphi$ and perpendicular to it. These general solutions can be parametrized as

$$\begin{aligned} gA^i_{\perp\mu} &= -\epsilon^i jk(\varphi^\dagger\tau^i\varphi)\partial_\mu(\varphi^\dagger\tau^k\varphi). \\ gA^i_{\parallel\mu} &= \iota\xi(\varphi^\dagger\tau^i\varphi)(\varphi^\dagger\overleftrightarrow{\partial_\mu}\varphi). \\ g'A^0_\mu &= -\iota\eta(\varphi^\dagger\overleftrightarrow{\partial_\mu}\varphi). \end{aligned} \tag{4.31}$$

where $\eta + \xi = 1$. Same steps can be done for fields and the resultant equations

are

$$\begin{aligned} f_{\mu\nu} &= -2\iota(\partial_\mu\varphi^\dagger\partial_\nu\varphi - \partial_\nu\varphi^\dagger\partial_\mu\varphi). \\ g'F^0_{\mu\nu} &= \eta f_{\mu\nu}. \\ gF^i_{\mu\nu} &= -\eta f_{\mu\nu}(\varphi^\dagger\tau^i\varphi). \end{aligned} \tag{4.32}$$

This implies that

$$gF^i_{\mu\nu}(\varphi^\dagger\tau^i\varphi) + g'F^0_{\mu\nu} \equiv \sqrt{g^2+g'^2}F^Z_{\mu\nu}. \tag{4.33}$$

This equation tells us that the flux of the string is due to the Z-boson and can termed as Z-flux. By applying Gauss' divergence theorem on EM fields and Stoles' theorem on gauge fields, we witness that the flux due to $U(1)_Y$ is zero, while for $SU(2)_L$, its value is $-(4\pi/e)\cos\theta_{\mathcal{W}}\sin\theta_{\mathcal{W}}$. It's worth noting that the long-range fields behave quite differently along the string, with the $U(1)_Y$ portion exhibiting a return flux and the $SU(2)_L$ portion not. As a result, the poles are considered genuine $SU(2)_L$ monopoles of charge $4\pi/g$, which maintain their structural integrity due to their topological quantum number, provided they are spaced far enough apart

$$Q = \frac{4\pi\eta}{e}.$$

where $\eta = \sin^2\theta_{\mathcal{W}}$. Therefore, the magnetic charge carried by $SU(2)_L$ monopole is

$$Q = \frac{4\pi}{e}\sin^2\theta_{\mathcal{W}} \tag{4.34}$$

where $\theta_{\mathcal{W}}$ represents electroweak mixing angle. It is evident that the magnetic charge of the Nambu monopole has dependence on $\theta_{\mathcal{W}}$ [27].

4.2 Experimental Overview of MMs

The long theorized particles — MMs — continues to be a tantalizing mystery in the realm of physics. The ongoing experimental explorations to unmask the MMs fall into three catagories: production in accelerators, detecting them in cosmic rays or materials where they may be trapped, observing indirect signs astronomically.

4.2.1 Search at Colliders

Scientists around the globe have conducted many experiments using accelerators in an attempt to produce MMs. Despite thorough efforts at Tevatron, LEC, and HERA, no MMs have been found with masses less than $1\,TeV$. Therefore, several accelerators are currently trying to unveil the MMs at higher energies which are:

Monopole and Exotics Detector at the LHC(MoEDAL)

MoEDAL is a unique and innovative project at Large Hadron Collider(LHC) that aims to search for MMs which eluded us for decades. MoEDAL experiment employs Schwinger mechanism to generate MMs which involes the production of electrically charged-particles in a strong electric field via quantum tunneling. If MMs exist, they could also be produced through this mechanism in strong magnetic field due to EM duality. This approach has several advantages: absence of exponential suppression for monopole production, enhancement of production due to strong coupling and finite size of MMs, and calculation of production rate employing semi-classical techniques.

MoEDAL's strategy for finding MMs is its ingenious detectors. It employs an array of innovative detectors, known as MM trappers(MMT) and nuclear

track detectors. The strong magnetic field is produced by Pb-Pb heavy ion collisions so that monopole-antimonopole pairs are produced via Schwinger mechanism which get trapped in MMTs. Samples from the MMTs are sent using a superconducting coil to Superconducting Quantum Interference Device(SQUID), in which a signal triggers due to the magnetic charge of the trapped MMs. A recent experiment involved exposing the MoEDAL MMTs to $0.235\,nb^{-1}$ of Pb-Pb collisions and has established a new lower mass limit for MMs by eliminating monopoles with Dirac charges between $1g_D$ and $3g_D$ and masses up to $75\,GeV/c^2$ [28].

A Toroidal LHC ApparatuS(ATLAS)

ATLAS is an advanced particle detector that is one of the four major detectors located at LHC. While the Higgs boson discovery remains one of ATLAS's most celebrated achievements, its pursuits extend far beyond a single particle. The primary mission of ATLAS is to explore the subatomic world in unprecedented detail. It does so by analyzing new partcles and phenomena resulting from Drell-Yan mechanism or Photon Fusion mechanism for pair-production beyond the SM of particle physics.

ATLAS comprises various sub-detectors: inner tracking detectors including semiconductor detectors, transition radiation trackers, calorimeters of two types known as EM calorimeter and hadron calorimeter, and muon spectrometers, which work together to capture and record the properties of particles produced in collisions. Particles produced at LHC via hadron-hadron collision or photon fusion pass through the inner tracking detectors where the paths of charged particles is measured, while the calorimeters measure the energy of particles that interact with matter. The muon spectrometers are used to detect and measure the properties of muons, which are highly pene-

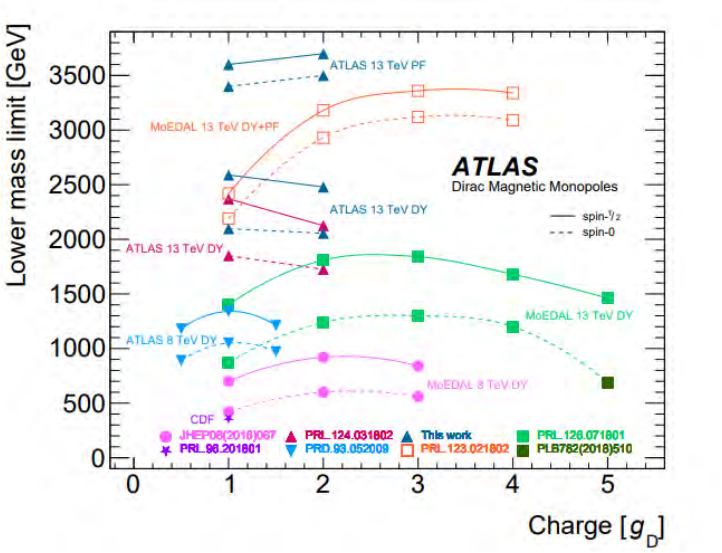

Figure 4.1: Comparison of ATLAS lower mass bounds with other LHC experiments [29].

trating particles that can travel through matter without being stopped. To manage the vast amount of data produced, ATLAS employs two-level trigger systme for the selection of events. In a recent run, for spin-0 and spin-$\frac{1}{2}$ MMs were examined with the aid of luminosity of 138 fb^{-1} of 13 TeV proton-proton collisions. Limitations were set on magnetic charges of 1 g_D and 2 g_D, and also on high-electric-charge objects with charges ranging from 20 to 100, and masses ranging from 200 GeV to 4000 GeV [29].

4.2.2 Indirect Astrophysical Imprints

The existence of MMs could have a significant impact on astrophysics, as they provide a potential means for searching and limiting their flux. The most notable impact would be on the galactic magnetic field, which currently has a strength of $3-6$ micro-gauss(μG). If there were an abundance of MMs with high magnetic charges in the universe, it could lead to the acceleration of proton decay, resulting energy depletion from the galactic field due to the

production of magnetic currents. The rate of dissipation would depend on the flux of the MMs, which could adversely effect the stability and energy balance of galaxies and stars. This, however, conflicts with observations of stable stars across the universe.

Thereby, the sustainability of the galactic field relies on the abundance of MMs in the universe not exceeding a specific limit known as the Parker bound, proposed by Eugene Parker. This limit is determined by the balance between dissipation and regeneration. When the MMs possess a mass greater than $10^{17}GeV$, the gravitational forces dominante their motion, rendering their effect weaker. However, for lighter MMs around $10^{17}GeV$ [30], the Parker bound is equal to

$$\phi \leq 10^{-15} cm^{-2} sec^{-1} sr^{-1}. \tag{4.35}$$

here sr represents the unit steradian. The extended Parker limit considers the survival of a small galactic field($M_{mon} \leq 10^{17}GeV$) [31] and reduces the flux bound to

$$\phi \leq 10^{-16} (M_{mon}/10^{17}GeV) cm^{-2} sec^{-1} sr^{-1}. \tag{4.36}$$

While magnetic monopoles remain hypothetical and have not been observed to date, the Parker Bound plays a crucial role in our understanding of the potential impact of these exotic particles on astrophysical phenomena.

One possible method for estimating the upper limit involves examining the overall mass of MMs present in the universe. Based on astronomical observations, it appears that matter particles account for approximately 31% of the total energy in the universe, and only 4.9% can be explained by known particles. This suggests that some or all of the remaining dark matter may

be MMs. If the mass of MMs is sufficiently low($< 10^{17}GeV$), then they would not be gravitationally bound to galaxies and would be distributed evenly throughout space. By observing the density of dark matter, it may be possible to estimate an upper limit for MMs equal to

$$\phi \leq 10^{-16}(M_{mon}/10^{16}GeV)(10^{-3}c/v)cm^{-2}sec^{-1}sr^{-1}. \tag{4.37}$$

where M_{mon} is the mass of a MM, v is their average speed, and c is the speed of light. This bound is only significant for heavy MMs, like that of GUT scale, due to the mass dependency. However, it is still competitive with other bounds on them.

4.2.3 Direct Searches in Cosmic rays and Materials

The search MMs in cosmic rays is an intriguing field of experimental physics which look for remnant GUT monopoles produced after SSB in the early universe. High-energy cosmic rays, which include protons and atomic nuclei, are continually bombarding Earth from various astrophysical sources like supernovae, black holes, and other cosmic phenomena. There have been several attempts to detect MMs in cosmic rays. A higher flux would increase the chance of a monopole cosmic ray hitting a detector.

Physicists have been using SQUIDs, which are extremely sensitive to changes in magnetic fields and can identify the passage of charged particles that would be anticipated to follow MMs. One similar experiment for MM detection was disclosed by Blas Cabrera in 1982. It took 151 days to track the current flowing through a superconducting ring. There was just one candidate detection found carrying $1g_D$ charge [32].

A few years later, in a configuration with two superconducting loops,

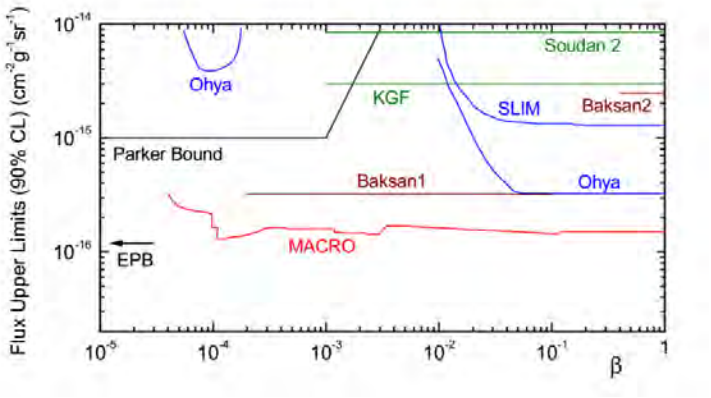

Figure 4.2: Flux bounds on MMs through different experiments [33].

Imperial College London observed yet another strange incident. However, they are thought to have been induced by other effects since subsequent tests were unable to duplicate them. However, they inspired physicists to create larger experiments like MACRO, AMANDA, Baksan, etc. that could place tighter bounds on the flux of MMs

shown in Fig. 4.2. These investigations also set the path for the present dark matter studies by allowing us to hunt for other sorts of particles in cosmic rays.

Monopoles may have been stuck in Earthly matter since the planet has been exposed to cosmic radiation for billions of years. There have been unsuccessful attempts to use SQUID to analyze samples of moon rock, meteorites, seawater, and iron ores to detect MMs trapped inside them [34].

4.3 MMs in Condensed Matter Systems

Despite decades of scientific pursuit and ingenious experiments, the enigmatic monopoles continue to evade direct detection, challenging our understanding of EM and igniting curiosity in the minds of physicists and researchers alike.

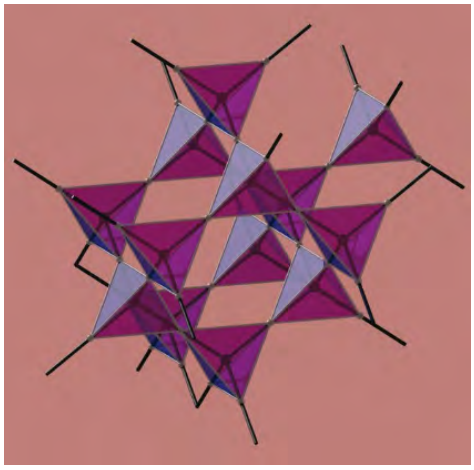

Figure 4.3: Pyrochlore lattice structure of spin ice [35].

As the quest for these elementary particles persists, an extraordinary narrative unfolded — the concept of emergent monopoles. There are condensed matter systems in which some particles mimics MMs. A thorough detail is given below.

4.3.1 MMs in Spin Ice

Electrically charged particles like protons and electrons are very common in nature. However, despite extensive research and experimentation, no elementary particles with a net magnetic charge have ever been observed. To approach this problem from a different angle, scientists have been exploring the possibility of realizing MMs as emergent particles rather than elementary ones. This led to the discovery of spin ice — a class of exotic magnetic materials — whose behavior resembles with a free gas of MMs. $Dy_2Ti_2O_7$ and $Ho_2Ti_2O_7$ are the examples of these magnetic materials, indicating certain rare-earth elements in its composition. The defining feature of spin ice materials is their crystal lattice structure, which is referred to as the pyrochlore lattice. In this lattice, the magnetic dipoles are arranged in a $3D$ network

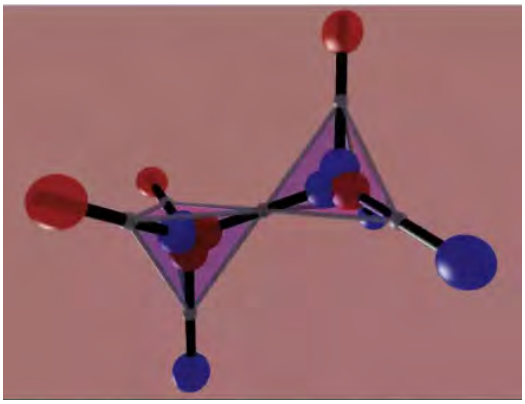

Figure 4.4: Dumbbell configuration of spins in the lattice [35].

of interconnected tetrahedra as seen in Fig. 4.3. Each corner-sharing tetrahedron is composed of four magnetic moments located at its vertices. These moments can be represented as Ising spins [35].

The spins in spin ice materials follow a set of rules known as "ice rules," which are analogous to the rules governing the arrangement of hydrogen and oxygen atoms in water ice. For this reason, these exotic magnets are termed as spin ice. These rules dictate that for every tetrahedron in the pyrochlore lattice, two spins must point into the tetrahedron, while the other two must point out. It is so because this arrangement of spins helps to minimize energy as $Q = 0$ and leads to correlated spin behavior. Therefore, spins at each vertex can thought of as two pairs connected by a dumbbell as demonstrated in Fig. 4.4. The length of the dumbbell is carefully chosen so that each magnetic moment must be situated at the center of the lattice [36].

The ice rule will be violated when the system is excited due to the reason that the flipping of a single spin causes one site in the pyrochlore lattice to acquire a positive magnetic charge while a neighboring site acquires a negative magnetic charge, thus $Q = \pm\frac{2\mu}{d}$. This behavior is depicted in Fig. 4.5. By flipping the nearby spins, these magnetic charges can propagate

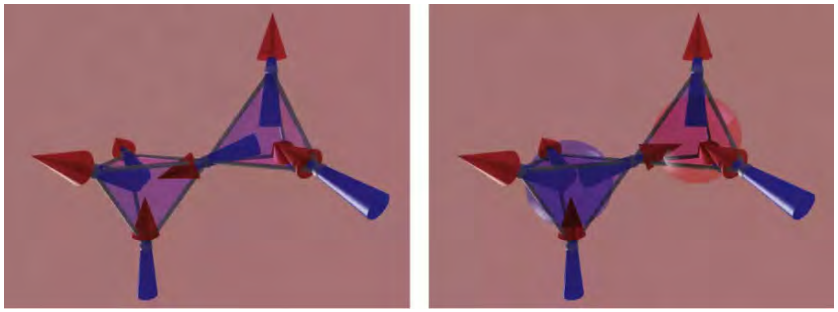

Figure 4.5: Formation of positive and negative magnetic charges in the lattice [35].

through the crystal lattice [35].

The result of these frustrations in the system in the emergence of monopole-antimonopole pair, shown in Fig. 4.6b, which differs from the usual MMs pair witnessed at the end of a tightly wound solenoid in the sense that its motion is not constrained and can move freely inside the crystal lattice due to the flipping of nearby spins as shown in Fig. 4.6a. This flipping results into the creation of a string of flipped dipoles which is analogous to Dirac string. Nevertheless, it is important to note that these Dirac strings are physical. Thus, the MMs do not adhere to the DQC [36].

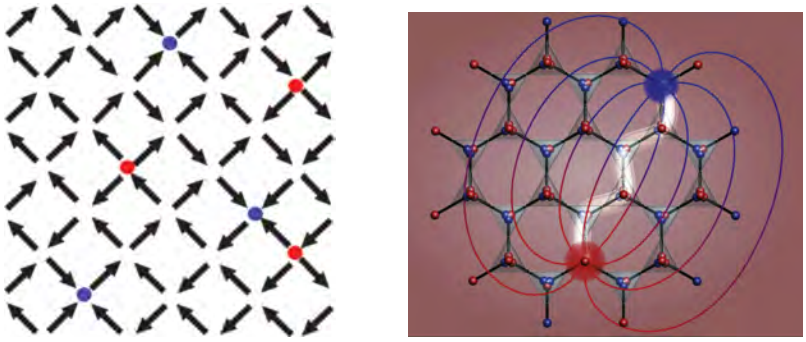

(a) (b)

Figure 4.6: Emergence of MMs in spin ice in (4.6a) $2D$ (4.6b) $3D$ [37, 35].

Scientists have been able to experimentally verify the existence of magnetic charge in spin ice. In a study conducted by Bramwell in 2009, MM

current emerging from them was also detected using the magnetic material $Dy_2Ti_2O_7$. The study also revealed Coulomb-like $\frac{1}{r^2}$ interactions among the MMs, along with measuring the magnetic conductivity of $Dy_2Ti_2O_7$ and the charge of these emergent quasi-particles [38].

Chapter 5

Composite Monopole Structure in SM

5.1 Background

The quest for MM is still ongoing, with scientists yet to find any solid evidence. Various experiments have been conducted, and more are underway, all in the pursuit of their elusive discovery. The absence of conclusive proof for MMs doesn't necessarily negate their existence. One of the key challenges in experimental verification is the mass of the MMs. Because the mass of the MM remains uncertain and varies depending on the model used, with estimates ranging from the GUT scale to the electroweak(EW) scale. Hence, there is the possibility that the masses of MMs exceed the capabilities of current experiments or that they interact feebly with ordinary matter.

Theoretical advancements, specifically the development of new particle physics models and a deeper comprehension of the early universe, may offer guidance for future experimental searches and provide valuable insight into the mass and characteristics of MMs. The best model will be the one in which

the MMs are produced due to the breaking of EW symmetry, implying their mass around the EW scale of roughly $250\,GeV$, — in few TeV range — an energy range that modern particle accelerators can currently reach.

It is mentioned before that in any theory, symmetry breaking in a particular way can produce MMs through Kibble mechanism, but only if the second homotopy group is non-trivial. However, it is widely accepted that finite energy MMs in the SM are not topologically stable. The problem is that in EW symmetry breaking of the SM, the vacuum manifold in the gauge group $\frac{SU(2)_L \times U(1)_Y}{U(1)_{EM}}$ is a three-sphere($\Pi_2(S^3) = 0$), not a two-sphere($\Pi_2(S^2) \neq 0$) which is the requirement for the formation of MMs. Be aware that adding more matter or scalar fields to the SM has no impact on this outcome. Nevertheless, the SM and its extensions, such as GUTs, include intriguing composite topological structures.

Scientists have been fascinated by the idea of MM since 1931, when Dirac proposed a point-like Abelian $U(1)_Y$ monopole with a semi-infinite string — a gauge artifact [14]. Later on, Wu-Yang extended the concept to non-Abelian monopole by expanding the gauge group to $SU(2)_L$. In 1974, A. t'Hooft and G. Polyakov independently showed that $SU(2)_L$ Higgs doublet offers a finite-energy MM solution to exist as a topological soliton [25, 26]. However, the electroweak sector of the SM fails to explain these t'Hooft-Polyakov monopoles because it utilizes the Higgs field in the fundamental representation rather than the adjoint representation [39].

Within the EW theory, Y. Nambu discovered another type of EW monopoles of a different type — vortex solutions — in the Abelian Higgs field model. In this model, a monopole is attached to an anti-monopole via a neutral, physical string [27]. For this reason, the $U(1)$ bundle would be trivial, implying that MM configuration predicted by Nambu doesn't has spherical symmetry

[39].

Inference could be drawn that ***MMs just don't exist in SM but the reality is other way around.*** Since the EW unification still preserves the $U(1)_{EM}$ validating the presence of Dirac monopoles, so it can infer that they may not be stable in the EW theory and must be mutated to another monopole. This is why, it is very reasonable to anticipate the existence of EW monopoles to necessitates the correctness of SM. Although it is widely believed that the discovery of Higgs particle is the final straw for testing the correctness of SM. However, it's not finished until the last whistle blows — discovery of EW monopoles [40].

In 1997, the search of MMs entered into new phase when Y.M. Cho and D. Maison have presented an overlooked topological scenario that provides the justification for the occurrence of MMs in EW theory. They proposed that the Weinberg-Salam model could well be interpreted as CP^1 model with the normalized Higgs doublet field acting as the CP^1 field with additional hypercharge $U(1)$. As a result, the Higgs field is allowed to have non-trivial second homotopy group($\Pi_2(CP^1) = Z$), opening up the possibility of non-Abelian topological monopoles existence in EW theory [41].

Furthermore, within the SM, $U(1)_Y$ takes on a non-trivial form which results in Abelian monopoles. This unique hybrid monopoles permits the existence of EW monpoles. However, the Cho-Maison EW monopole is flawed due to divergence at origin caused by $U(1)_Y$ point singularity, despite the $SU(2)_L$ gauge field being completely regular. This singularity results in the monopole carrying infinitely large energy at the classical scale, rendering its mass arbitrary [40].

5.2 Finite-energy MMs in SM

While the Cho-Maison solution is not inherently problematic, but predicting finite-energy MMs in EW theory is desirable due to its experimental implications. Some proposed solutions involve modifying the Lagrangian, but this may lead to the introduction of unknown physics at energies above the electroweak scale and a non-negligible uncertainty in the monopole mass. In the presence of unknown physics, MM solution arise from both the real Higgs triplet and Higgs doublet [42, 43].

Utilizing current knowledge to elucidate the intricacies of MM in SM until a breakthrough in physics is achieved is of utmost significance. In this regard, the EW-right-handed neutrino(ν_R) model, postulated by P.Q. Hung, is a physically-driven model that mandates the incorporation of a real triplet to uphold the Custodial Symmetry. This model entails non-sterile ν_Rs with masses equivalent to the EW scale, which are involved in a seesaw mechanism for light neutrinos that can be tested at colliders.

According to this model, ν_Rs couple to a complex Higgs triplet(χ^*) and gain Majorana masses(M_R) proportional to EW scale which is approximately $246\,GeV$. The neutrinos' non-sterile nature requires a minimum M_R of $46\,GeV$ to be consistent with the Z-boson width implying $\langle\chi^*\rangle = \nu_m \propto \Lambda_{EW}$. However, the presence of non-sterile ν_Rs would significantly impact the W- and Z-boson verified mass relationship in the SM. To solve this, a real Higgs triplet($\tilde{\xi}$) is introduced with $\langle\tilde{\xi}\rangle = \langle\chi^*\rangle = v_m$, creating a custodial symmetry in the EW-ν_R model [44]. This $\tilde{\xi}$ with $Y = 0$ predicts finite-energy MM of EW scale by solving the standard Euler-Lagrange equation.

5.2.1 Prediction of MM in EW-ν_R Model

In order to achieve finite-energy monopole configuration, the Higgs field must approach its minima, which take the form of a sphere in a $3D$ internal space represented by S^2. Essentially, this means that a 3-dimensional spatial sphere is mapped to the sphere of the vacuum manifold(S^2). In homotopy theory, this process is depicted by the second homotopy group(Π_2) for $3D$ space and $\Pi_2(S^2) = Z$, where $Z = 0, 1, 2, ...$ The initial value of $Z(n = 0)$ is the winding number, which corresponds to the trivial vacuum manifold with no monopole, whereas $n = 1$ leads to the first non-trivial solution, and so forth.

This results into topologically stable monopole because it requires an infinite amount of energy to undergo transition from the configuration $n = 1$ to $n = 0$. In this case, the Higgs vacuum manifold takes the shape of S^2 sphere. One specific example of this is the Georgi-Glashow model $SO(3) \sim SU(2)$ with a real Higgs triplet $\tilde{\xi} = (\tilde{\xi}_0, \tilde{\xi}_1, \tilde{\xi}_2)$. In this model, the vacuum manifold is $\tilde{\xi}_0^2 + \tilde{\xi}_1^2 + \tilde{\xi}_2^2 = v_{Mon}^2$, corresponding to S^2, and the model is able to accommodate a topologically stable monopole.

In the context of EW-ν_R model, there are several types of Higgs fields. These include a real triplet field($\tilde{\xi}$), a complex triplet field(χ^*), four complex doublet fields denoted by φ_i^{SM} and φ_i^M where $i = 1, 2$, which interact respectively with the SM and mirror fermions. Additionally, there are Higgs singlet fields represented by φ_S, which although important for various reasons, but do not play any role in the MM solution. It's worth noting that the proper vacuum alignment ensures that the custodial symmetry is maintained, which means that $\langle\tilde{\xi}\rangle = \langle\chi^*\rangle = v_{Mon}$.

The vacuum manifold of the SM will be a 3-sphere if it's composed of solely a complex doublet defined by $\varphi_1^2 + \varphi_2^2 + \varphi_3^2 + \varphi_4^2 = v^2$. This results into $\Pi_2(S^3) = 0$, indicating no monopole production in SM. However, if we

introduce a complex triplet which contains six real components, the vacuum manifold will be a 5-sphere, leading to $\Pi_2(S^5) = 0$. While real $SU(2)_L$ triplet has $\Pi_2(S^2) = 0$, which enunciates that SM with real triplet predicts topologically stable monopoles. Therefore, the vacuum manifold of the EW-ν_R model has non-trivial second homotopy group as evident from the following relation

$$\begin{aligned} \Pi_2(S_{vac}) &= \Pi_2(S^2) \oplus \Pi_2(S^5) \oplus \Pi_2(S^3_{SM_i,M_i})_{i=1,2} \\ \Pi_2(S_{vac}) &= \Pi_2(S^2) = Z \end{aligned} \tag{5.1}$$

which is typical topological justification for a 'tHP MM to exist. Therefore, within the EW-ν_R model, a topologically stable MM solution arises and establishes an intriguing link between the MM solution and the masses of light neutrino [45].

5.2.2 Charge Quantization via Topology

Let's begin with writing the Lagrangian for $SU(2)$ real triplet which is

$$\mathcal{L} = -\frac{1}{4}(\mathcal{W}^3_{\mu\nu})^2 + \frac{1}{2}(D_\mu \tilde{\xi})^2 - U(\tilde{\xi}). \tag{5.2}$$

where $\mathcal{W}^3_{\mu\nu}$ represents the field strength of $SU(2)$ gauge bosons and is given as

$$\mathcal{W}^3_{\mu\nu} = \partial_\mu \mathcal{W}^3_\nu + \partial_\nu \mathcal{W}^3_\mu - \frac{1}{v^3_{Mon}\, g}\epsilon^{ijk}\tilde{\xi}_i \partial_\mu \tilde{\xi}_j \partial_\nu \tilde{\xi}_k.$$

By using topological argument, one can write the topological current as

$$k_\mu = \frac{1}{2}\epsilon^{\mu\nu\sigma\rho}\partial_\nu \mathcal{W}^3_{\sigma\rho}. \tag{5.3}$$

This implies that

$$\partial^{\mu} k_{\mu} = \partial^{\mu} \left(\frac{1}{2} \epsilon^{\mu\nu\sigma\rho} \partial_{\nu} \mathcal{W}^{3}_{\sigma\rho} \right) = 0.$$

is a conserved quantity. And according to Noether theorem, conserved topological current leads to conserved topological charge as

$$g_{Mon} = \int k_0 \, d^3x = \frac{1}{g} \int \sqrt{\vec{g}} \, d^2\sigma = \frac{4\pi n}{g}.$$

where $\vec{g} = det\,(\partial^{\beta} \acute{\xi}_i \partial^{\gamma} \acute{\xi}_i)$ with $\acute{\xi}_i = \tilde{\xi}_i / v_{Mon}$ and g denotes the weak coupling which has relation $e = g \sin\theta_{\mathcal{W}}$. This equation gives us the charge quantization by the analysis of topology which is

$$\frac{g \, g_{Mon}}{4\pi} = n. \tag{5.4}$$

If we put $n = 1$, we will have

$$g^{0}_{Mon} = \frac{4\pi}{g} = \frac{4\pi}{e} \sin\theta_{\mathcal{W}}. \tag{5.5}$$

the value of unit magnetic charge in which $\theta_{\mathcal{W}}$ denotes the weak mixing angle. This consideration point out that

$$g^{n}_{Mon} = n \, g^{0}_{Mon}. \tag{5.6}$$

which means that total number of MMs given by the $SU(2)$ Higgs field will be equal to or greater than 2. By squaring equation (5.5) and comparing with the standard DQC, we get $\sin^2\theta_{\mathcal{W}} = \frac{1}{4}$.

5.2.3 Mass and Size of MM

According to 'tHP theory, the mass of the monopole can be calculated by using the relation

$$M_{Mon} = \frac{4\pi v_{Mon}}{g} f\left(\frac{\lambda}{g^2}\right). \tag{5.7}$$

where λ represents $\tilde{\xi}$ self-coupling. The following bound for mass of the MM is obtained

$$\simeq \ 890\,GeV \ - 3\,TeV. \tag{5.8}$$

by taking the lowest value, which corresponds to $v_{Mon} \sim 45.5\,GeV$ and $f = 1$(when $\lambda = 0$), and the highest value, which corresponds to $v_{Mon} \sim 87\,GeV$ and $f = 1.78$(when $\lambda = \infty$).

The monopole is characterized by a core with a radius of R_c approximately $10^{-16}\,cm$, which is almost a thousand times smaller than the radius of a proton. Inside the core, virtual $W^{\pm}$ and Z particles exist, while far from the core, the monopole acts like a Dirac MM [45]. Moreover, the Z-magnetic field, which is of short-range, becomes less significant compared to the long-range magnetic field present inside the core having size $(gv_{Mon})^{-1}$. In this paradigm, there aren't any long-range magnetic fluxes that would connect a MM with an anti-MM; instead, just the long-range actual magnetic field is observed beyond the core. This presumption suggests that the MMs aren't confined with their anti-MMs [36].

5.2.4 Ensuring Charge Quantization via Dirac's criterion

DQC is another litmus test, apart from topology, to check the validity of a model. The typical method for determining the DQC is to observe an

electron's movement around the Dirac string attached to a point-like MM. Note that the current solution of MM doesn't propose any string. This may lead some to believe that topological quantization arising from the homotopy theory is more than enough to ensure the consistency of the model.

Nevertheless, it is important to keep in mind that the DQC is a universal condition that can be derived from consistency conditions that extend beyond the confines of the monopole center. It remains unaffected by the specifics of the monopole solution and whether or not it features an attached string. Consequently, the DQC must always be enforced to maintain the consistency of a theory, even if it is already satisfied.

Since, there are several approaches to derive DQC, but we will use one classical approach and one quantum approach to verify that the EW-ν_R model is in conformity with the Dirac's theory. For this, our first consideration will be Thomson dipole configuration as shown in Fig. 5.1. We know that the electric field of a charged particle 'q' is given by

$$\vec{E} = \frac{e}{4\pi r^2}\hat{r}. \tag{5.9}$$

and the relation of the magnetic field for the first step breaking($SU(2)_L \times U(1)_Y \rightarrow U(1)_L \times U(1)_Y$), which is achieved by real Higgs triplet, can be derived as[45]

$$\begin{aligned} B_i &= -\frac{1}{2}\epsilon^{ijk}\mathcal{W}^3_{jk}, \\ \because \mathcal{W}^3_{bc} &= \epsilon^{ijk}\frac{\hat{r}_k}{gr^2}, \\ \Longrightarrow B_i &= \frac{1}{gr^2}\hat{r}_i = \frac{g_{Mon}}{4\pi r^2}\hat{r}_i. \end{aligned} \tag{5.10}$$

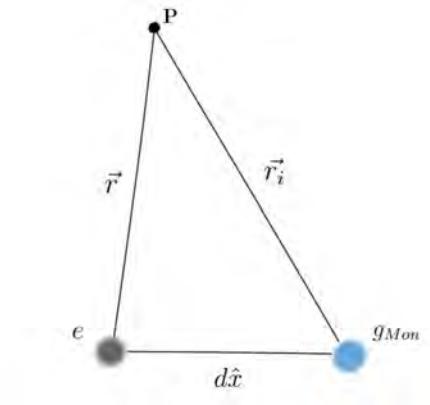

Figure 5.1: Charge and monopole configuration.

Hence, the EM angular momentum has the relation

$$\begin{aligned}
\vec{L}_{EM} &= \int \vec{r} \times (\vec{E} \times \vec{B}) d^3r, \\
&= \int \vec{r} \times \left(\frac{e}{4\pi r'^2} \hat{r'} \times \frac{g_M}{4\pi r_i^2} \hat{r}_i \right) d^3r, \\
&= \frac{e g_{Mon}}{(4\pi)^2} \int \left(\frac{\vec{r} \times (\vec{r} \times \vec{r_i})}{r^3 r_i^3} \right) d^3r,
\end{aligned}$$

It is evident from Fig. 5.1

$$\vec{r_i} = \vec{r} + d\hat{x}. \tag{5.11}$$

Also, we know that

$$\begin{aligned}
\frac{1}{\mathtt{r}} &= \frac{1}{\sqrt{r^2 + r'^2 - 2rr' \cos\theta}}, \\
\implies r_i^3 &= (r^2 + d^2 - 2rd\cos\theta)^{\frac{2}{3}}.
\end{aligned} \tag{5.12}$$

Substituting these values in equation (5.11), we have

$$\vec{L}_{EM} = \frac{e g_{Mon} d}{(4\pi)^2} \int \left(\frac{\vec{r} \times (\vec{r} \times \hat{x}}{r^3 (r^2 + d^2 - 2rd\cos\theta)^{\frac{2}{3}}} \right) d^3r.$$

By solving this integral, we get

$$\vec{L}_{EM} = \frac{eg_{Mon}}{4\pi}\hat{x}. \tag{5.13}$$

whose quantization along the radial direction leads us to DQC.

For the validation through quantum approach, we can draw an analogy between this monopole solution and an Abelian Wu-Yang monopole, which doesn't require a Dirac string. The monopole solution is based on Higgs breaking $SU(2)_L \times U(1)_Y \rightarrow U(1)_{EM}$, which differs from the conventional 'tHP monopole that is based on a Higgs triplet breaking the simple group $SU(2) \rightarrow U(1)$ as in the Georgi-Glashow model.

To compute the DQC, we often assume a closed loop 'l' that resides completely in the "equator region," which is the area where the two hemispheres — North(N) and South(S) — overlap, in the 3-space around the Wu-Yang monopole at the origin. The loop may be situated far away from the MM's center. If an electrically charged particle, like an electron with charge 'e', circulates the loop, then its wave function gains a phase

$$e^{\iota e \oint_l \vec{A}_{S,N}.d\vec{l}}. \tag{5.14}$$

where $\vec{A}_{S,N}$ denotes the EM potential in both hemispheres [36].

The flux in each hemisphere can be calculated by applying Stokes' theorem as

$$e \oint_l \vec{A}_N.d\vec{l} = e\int_{\sigma_N} (\vec{\nabla} \times \vec{A}_N).d\vec{\sigma}, \tag{5.15}$$

$$e \oint_l \vec{A}_S.d\vec{l} = -e\int_{\sigma_S} (\vec{\nabla} \times \vec{A}_S).d\vec{\sigma}, \tag{5.16}$$

$$\Longrightarrow e\int_{\sigma_N \cup \sigma_S} \vec{B}.d\vec{\sigma} = e\int_{\sigma_N} (\vec{\nabla} \times \vec{A}_N).d\vec{\sigma} - e\int_{\sigma_S} (\vec{\nabla} \times \vec{A}_S).d\vec{\sigma}. \tag{5.17}$$

From Gauss' divergence theorem, we have

$$\begin{aligned} e\int_{\sigma_N\cup\sigma_S}\vec{B}.d\vec{\sigma} &= e\int_V \vec{\nabla}.\vec{B}d^3r, \\ &= \frac{eg_{Mon}}{4\pi}\int_V\left(\vec{\nabla}.\frac{\hat{r_i}}{r^2}\right)r^2\sin\theta\,dr\,d\theta\,d\phi, \\ &= \frac{eg_{Mon}}{4\pi}.4\pi = eg_{Mon}. \end{aligned} \tag{5.18}$$

Irrespective of the topological argument, the requirement that the equation (5.18) have no effect on any physical observables entails the DQC.

5.2.5 Charge and Structure of MMs in SM

To complete the analysis, our final task is to determine if a pure EM monopole configuration can be produced in the SM. Without the $U(1)_Y$ sector, this is obviously impossible to happen. So, consider the complete EW breaking

$$\begin{aligned} SU(2)_c\times U(1)_Y &\rightarrow U(1)_Y\times U(1)_L \\ &\rightarrow U(1)_{EM} \end{aligned}$$

The first breaking is done using the $\tilde{\xi}$, while the later breaking involves all the other Higgs sectors(χ^*,$\varphi_i^{SM,M}$) of EW-ν_R model. This gives rise to new mass eigenstates $\mathcal{Z}_\mu$ and A_μ, not $\mathcal{W}_\mu^3$ due to the reason that $\mathcal{W}_\mu^3$ now comprises of Z-boson and photon fields. One can write the corresponding $SU(2)_L$ and $U(1)_Y$ gauge fields as

$$\begin{aligned} \mathcal{W}_\mu^3 &= A_\mu\cos\theta_{\mathcal{W}} - \mathcal{Z}_\mu\sin\theta_{\mathcal{W}}. \\ Y_\mu &= \mathcal{Z}_\mu\cos\theta_{\mathcal{W}} + A_\mu\sin\theta_{\mathcal{W}}. \end{aligned} \tag{5.19}$$

Due to the involvement of both Z-boson and photon, the MM can be termed as "γ-Z magnetic monopole". The magnetic field intensity, thus, takes the form

$$\begin{aligned} B_i^{\gamma Z} &= B_i^{\gamma}\sin\theta_{\mathcal{W}} + B_i^{Z}\cos\theta_{\mathcal{W}}, \\ &= \frac{\sin\theta_{\mathcal{W}}}{er^2}\hat{r}(\sin\theta_{\mathcal{W}} + e^{-M_Z r}\cos\theta_{\mathcal{W}}), \\ &= \frac{4\pi}{e}\sin^2\theta_{\mathcal{W}} + \frac{4\pi}{e}\sin\theta_{\mathcal{W}}\cos\theta_{\mathcal{W}}. \end{aligned} \tag{5.20}$$

which signify that the MM has both EM and Z magnetic flux, with Z magnetic flux appearing in a flux tube.. Note that at short distances, both $B_i^{\gamma} = \frac{1}{gr^2}\hat{r}_i$ and $B_i^{Z} = \frac{1}{gr^2}\hat{r}e^{-M_Z r}$ magnetic fields will be present, while at large distance from core, only the EM field dominates. The relation in equation (5.10) can be recovered by substituting $M_Z = 0$ and $\theta_{\mathcal{W}} = 0$ which will happen in the limit when VEVs of $\chi*$ and $\varphi_i^{SM,M}$ diappear [45].

It is worth mentioning here that the relation in (5.5) should be independent of the EW mixing angle for the MMs configuration in SM to possess spherical symmetry. To do this and to calculate the total MMs present in a configuration, we will consider Dirac monopole with charge

$$g_Y = \frac{12\pi}{g'}n. \tag{5.21}$$

while the charge due to $SU(2)_L$ Nambu monopoles, in the context of equation (5.5), is given as

$$g_L = \frac{4\pi}{g}n'. \tag{5.22}$$

For this reason, n' monopoles coming from $SU(2)_L$ has the net magnetic charge

$$g_L = g_{LZ}\cos\theta_{\mathcal{W}} + g_{LA}\sin\theta_{\mathcal{W}}. \tag{5.23}$$

while for n $U(1)_Y$ monopoles, it has the relation

$$g_Y = g_{LA}\cos\theta_{\mathcal{W}} - g_{LZ}\sin\theta_{\mathcal{W}} \tag{5.24}$$

The net magnetic charge on the MM configuration due to Z-boson and photon can, thus, be wriiten as

$$g_{Y+L}, Z = -\frac{12\pi}{g'}n\sin\theta_{\mathcal{W}} + \frac{4\pi}{g}n'\cos\theta_{\mathcal{W}}. \tag{5.25}$$

$$g_{Y+L}, A = \frac{12\pi}{g'}n\cos\theta_{\mathcal{W}} + \frac{4\pi}{g}n'\sin\theta_{\mathcal{W}}. \tag{5.26}$$

In order to guarantee the unhindered operation of the monopole configuration and prevent the emergence of anti-monopole formation, it is crucial to ensure that the configuration lacks any net Z magnetic charge. This is due to the fact that Z magnetic fields tend to become confined subsequent to the EW symmetry breaking, and a net Z flux would inevitably lead to the formation of a string. Therefore,

$$\begin{aligned} -\frac{12\pi}{g'}n\sin\theta_{\mathcal{W}} + \frac{4\pi}{g}n'\cos\theta_{\mathcal{W}} &= 0, \\ \because \sin\theta_{\mathcal{W}} = \frac{g'}{\sqrt{g^2+g'^2}} \quad , \quad \cos\theta_{\mathcal{W}} &= \frac{g}{\sqrt{g^2+g'^2}} \\ \implies -\frac{12\pi}{\sqrt{g^2+g'^2}}n + \frac{4\pi}{\sqrt{g^2+g'^2}}n' &= 0, \end{aligned}$$

This implies that

$$n' = 3n. \tag{5.27}$$

This equation tells us that there are three times more $SU(2)_L$ monopoles in the configuration in comparison to $U(1)_Y$ monopoles.

Now, to find the pure EM charge on this configuration, we will put the

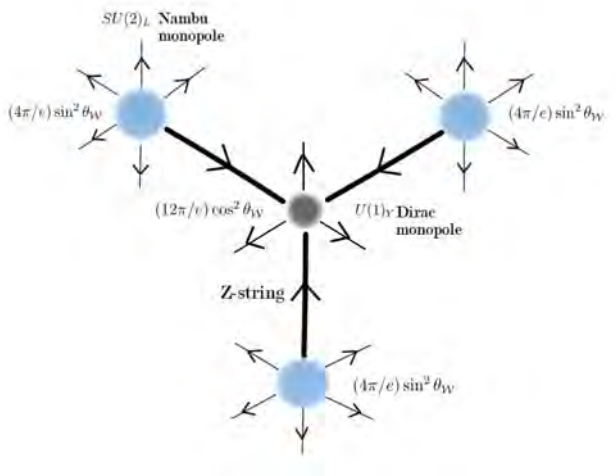

Figure 5.2: Necklace configuration in SM.

values of n' in equation (5.26),

$$\begin{aligned} g_{Y+L,A} &= \frac{12\pi}{g'} n\cos\theta_{\mathcal{W}} + \frac{12\pi}{g} n\sin\theta_{\mathcal{W}}, \\ \because e = g\sin\theta_{\mathcal{W}} = g'\cos\theta_{\mathcal{W}}, & \\ g_{Y+L,A} &= \frac{12\pi}{e} n\cos^2\theta_{\mathcal{W}} + \frac{12\pi}{e} n\sin^2\theta_{\mathcal{W}}, \\ &= \frac{12\pi}{e} n. \end{aligned} \tag{5.28}$$

From above relation, we can conclude that the MM configuration in the SM has minimum 6 unit of Dirac charge which has no dependence on the EW mixing angle [46]. The arrangement of these three $SU(2)_L$ Nambu monopoles and one $U(1)_Y$ Dirac monopoles in given in Fig. 5.2.

The magnetic charge on minimal $SU(2)_l$ Nambu monopole is $\frac{4\pi}{g}\sin\theta_{\mathcal{W}} = \frac{4\pi}{e}\sin^2\theta_{\mathcal{W}}$, while that of $U(1)_Y$ Dirac monopole is $\frac{12\pi}{g'}\cos\theta_{\mathcal{W}} = \frac{12\pi}{e}\cos^2\theta_{\mathcal{W}}$. These monopoles are linked with each other through Z-string having $\frac{4\pi}{g}\cos\theta_{\mathcal{W}}$ magnetic flux. From Fig. 5.2, we observed that this necklace configuration of MMs has singularity.

Conclusion

In the SM of particle physics, it is widely accepted that topologically stable monopoles cannot exist since the second homotopy group becomes trivial. Despite numerous proposed models attempting to address this issue, none have thoroughly explained the existence of homotopically stable, finite energy light monopoles. Recently, a model termed as "EW-ν_R model" has been proposed by P.Q. Hung which actually explains the possible existence of non-sterile RH neutrinos with EW scale masses.

Inspired by this, we have considered all the $SU(2)_L$ Higgs fields within the EW-ν_R model and discovered that it predicts the emergence of homotopically non-trivial monopole. We have also calculated the charge on this $SU(2)_L$ monopole which comes out to be equal to $\frac{4\pi}{e}\sin\theta_{\mathcal{W}}$, indicating dependence on EW mixing angle which is not acclamatory due to the fact that $\theta_{\mathcal{W}} \to 0$ for spherical symmetry to remain intact. Furthermore, this monopole is particularly enticing due to their mass falling in the TeV range and has a well-defined core.

It is important to emphasize that all of these explanations have been made through topological perspective. Therefore, to move a step further, we have validated the monopole generation in this model through the litmus test — DQC — using both classical and quantum approach. After thorough topological and theoretical validation, we tried to calculate the total number of MMs produced during the EW breaking and found out that there will be

three $SU(2)_L$ Nambu monopoles in the configuration alongside one $U(1)_Y$ Dirac monopole which are connected via Z strings. We have also observed that this configuration of composite monopoles has $\frac{12\pi}{e}$ magnetic charge, with no more dependence on $\theta_{\mathcal{W}}$, leading to a necklace configuration of MMs in SM.

Appendix A

Group Matrices

Any set of non-singular (invertible) $N \times N$ matrices which includes the unit matrix I and is closed under matrix multiplications, forms a group matrix.

A.1 Unitary Group $U(N)$

Unitary group is a set of complex matrices U satisfying,

$$UU^{\dagger} = I = U^{\dagger}U. \tag{A.1}$$

The number of independent parameters in $U(N)$ is

$$n = \frac{N(N+1)}{2} + \frac{N(N-1)}{2} = N^2. \tag{A.2}$$

Rank of unitary group is

$$Rank(U(N)) = N. \tag{A.3}$$

A.2 Special Unitary Group $SU(N)$

Special Unitary group is simply a unitary group with an additional condition that is,

$$det(U) = 1. \tag{A.4}$$

Number of independent parameters in $SU(N)$ is

$$n = N^2 - 1. \tag{A.5}$$

while the rank is given as

$$Rank(SU(N)) = N - 1. \tag{A.6}$$

Appendix B

Sine-Gordon Theory

B.1 Time-independent Finite Energy Solution

The Lagrangian density for Sine-Gordon theory is

$$\mathcal{L} = \frac{1}{2}(\partial_\nu \varphi)^2 - \frac{\mu^2}{\beta^2}(1 - \cos\beta\varphi). \tag{B.1}$$

with

$$U(\varphi) = \frac{\mu^2}{\beta^2}(1 - \cos\beta\varphi). \tag{B.2}$$

Since

$$\begin{aligned} x = \int dx &= \int_{\varphi_0}^{\varphi} \frac{d\varphi}{\sqrt{\frac{\mu^2}{\beta^2}(1-\cos\beta\varphi)}}, \\ &= \frac{\beta}{2\mu}\int_{\varphi_0}^{\varphi} \frac{d\varphi}{\sin\frac{\beta\varphi}{2}}. \end{aligned} \tag{B.3}$$

Let

$$t = \sin\frac{\beta\varphi}{2}, \tag{B.4}$$

$$d\varphi = \frac{2}{\beta}\frac{1}{\sqrt{1-t^2}}dt. \tag{B.5}$$

Putting these values in equation (B.3)

$$\begin{aligned} x &= \frac{\beta}{2\mu}\int_{t_1}^{t_2}\frac{1}{t}.\frac{2}{\beta}\frac{1}{\sqrt{1-t^2}}dt, \\ &= \frac{1}{\mu}\int_{t_1}^{t_2}\frac{dt}{t\sqrt{1-t^2}}. \end{aligned} \tag{B.6}$$

Also assume that

$$s = \sqrt{1-t^2}. \tag{B.7}$$

$$\implies dt = \frac{-\sqrt{1-t^2}}{t}ds. \tag{B.8}$$

Thus, equation (B.6) becomes

$$\begin{aligned} x &= \frac{1}{\mu}\int_{s_1}^{s_2}\frac{1}{t\sqrt{1-t^2}}.\frac{-\sqrt{1-t^2}}{t}ds = \frac{1}{\mu}\int_{s_1}^{s_2}-\frac{1}{t^2}ds, \\ &= \frac{1}{\mu}\int_{s_1}^{s_2}\frac{1}{s^2-1}ds, \\ &= \frac{1}{\mu}\int_{s_1}^{s_2}\frac{1}{(s+1)(s-1)}ds. \end{aligned}$$

This implies that

$$\begin{aligned} x &= \frac{1}{2\mu}\int_{s_1}^{s_2}\left(\frac{-1}{s-1}-\frac{1}{s+1}\right)ds, \\ &= \frac{1}{2\mu}ln\left|\frac{1-s}{1+s}\right|_{s_1}^{s_2}, \\ \implies e^{\pm 2\mu x} &= \frac{1-s}{1+s}, \end{aligned}$$

As we know $s = \sqrt{1-t^2}$ and $t = \sin\frac{\beta\varphi}{2}$. This implies that

$$\begin{aligned} s &= \sqrt{1-\sin^2\frac{\beta\varphi}{2}}, \\ s &= \cos\frac{\beta\varphi}{2}. \end{aligned}$$

Thus, above equation takes the form

$$\begin{aligned} e^{\pm 2\mu x} &= \frac{1-\cos\frac{\beta\varphi}{2}}{1+\cos\frac{\beta\varphi}{2}}, \\ \because 2\sin^2\frac{\theta}{2} = 1-\cos\theta \quad , \quad 2\cos^2\frac{\theta}{2} = 1+\cos\theta \therefore e^{\pm 2\mu x} &= \frac{2\sin^2\frac{\beta\varphi}{4}}{2\cos^2\frac{\beta\varphi}{4}}, \\ \varphi &= \frac{4}{\beta}\tan^{-1} e^{\pm\mu x} \end{aligned} \tag{B.9}$$

B.2 Energy of a Soliton

The energy of a single soliton has the relation

$$\begin{aligned} E &= \int_{\infty}^{\infty}\left[\frac{2\mu^2}{\beta}(1-\cos\beta\varphi)\right]^{\frac{1}{2}}, \\ &= \frac{\sqrt{2}\sqrt{2}\mu}{\beta}\int_0^{\frac{2\pi}{\beta}}\left(\frac{1-\cos\beta\varphi}{2}\right)^{\frac{1}{2}}\,d\varphi, \\ &= \frac{2\mu}{\beta}\int_0^{\frac{2\pi}{\beta}}\sin\frac{\beta\varphi}{2}\,d\varphi, \\ &= \frac{8\mu}{\beta^2}. \end{aligned} \tag{B.10}$$

which is a particle-like solution with a mass increasing as β decreases.

Appendix C

Fierz Identities

1. $\sum_i (\varphi^\dagger \tau^i \varphi)^2 = \varphi^\dagger \varphi$.
2. $\sum_i (\varphi^\dagger \tau^i \varphi)(\varphi^\dagger \tau^i \partial_\mu \varphi) = (\varphi^\dagger \varphi)(\varphi^\dagger \overleftrightarrow{\partial_\mu} \varphi)$.
3. $(\varphi^\dagger \tau^i \varphi)(\varphi^\dagger \overleftrightarrow{\partial_\mu} \varphi) - (\varphi^\dagger \varphi)((\varphi^\dagger \tau^i \overleftrightarrow{\partial_\mu} \varphi) = \iota \epsilon^i jk (\varphi^\dagger \tau^i \varphi) \partial_\mu (\varphi^\dagger \tau^k \varphi)$.

Bibliography

[1] Alejandro Gangui. Topological defects in cosmology. 10 (2001).

[2] Alamy. https://www.alamy.com/image229476608.html.

[3] Tanmay Vachaspati. Topological defects in cosmology. *arXiv preprint astro-ph/9401039*, (1994).

[4] Anupam Mazumdar and Graham White. Review of cosmic phase transitions: their significance and experimental signatures. *Reports on Progress in Physics*, 82(7):076901, (2019).

[5] Centre for Theoretical Cosmology. https://www.ctc.cam.ac.uk.

[6] Thomas WB Kibble. Topology of cosmic domains and strings. *Journal of Physics A: Mathematical and General*, 9(8):1387, 1976.

[7] Gia Dvali, Hong Liu, and Tanmay Vachaspati. Sweeping away the monopole problem. *Physical review letters*, 80(11):2281, 1998.

[8] Ajit M Srivastava. Topological defects in cosmology. *Pramana*, 53:1069–1076, (1999).

[9] Ruth Durrer. Topological defects in cosmology. *New astronomy reviews*, 43(2-4):111–156, (1999).

[10] David Griffiths. *Introduction to elementary particles*. John Wiley & Sons, 2020.

[11] Anthony Zee. *Group theory in a nutshell for physicists*, volume 17. Princeton University Press, 2016.

[12] Marina von Steinkirch. The gauge group su(5) as a simple gut. 2010.

[13] Rachel Jeannerot and Anne-Christine Davis. Constraining supersymmetric SO(10) models through cosmology. *Physical Review D*, 52(12):7220, 1995.

[14] Paul Adrien Maurice Dirac. Quantised singularities in the electromagnetic field. *Proceedings of the Royal Society of London. Series A, Containing Papers of a Mathematical and Physical Character*, 133(821):60–72, 1931.

[15] John Preskill. Magnetic monopoles. *Annual Review of Nuclear and Particle Science*, 34(1):461–530, 1984.

[16] Ta-Pei [0000-0002-1137-0969] Cheng and Ling-Fong [0000-0002-8035-3329] Li. *Gauge Theory of Elementary Particle Physics*. Oxford University Press, Oxford, UK, 1984.

[17] Ricardo Heras. Dirac quantisation condition: a comprehensive review. *Contemporary Physics*, 2018.

[18] Virendra Singh. Magnetic monopoles. Technical report, P00020071, 1993.

[19] MN Saha. On the origin of mass in neutrons and protons. *Indian J. Phys*, 10:141, 1936.

[20] Helmut J Efinger. An instructive model for the quantization of magnetic monopoles. *American Journal of Physics*, 37(7):740–741, 1969.

[21] E Gava, Antonio Masiero, Kumar Shiv Narain, Seifallah Randjbar-daemi, and Qaisar Shafi. *High Energy Physics And Cosmology-Proceedings Of The 1995 Summer School*, volume 12. World Scientific, 1997.

[22] Dexter Chua. Notes of lectures on Classical and Quantum Solitons given by N.S. Manton and D. Stuart, 2017.

[23] Hugo Laurell. A summary on solitons in quantum field theory, 2016.

[24] C von Westenholz. Topological and noether-conservation laws. In *Annales de l'IHP Physique théorique*, volume 30, pages 353–367, 1979.

[25] Gerardus t Hooft. Magnetic monopoles in unified theories. *Nucl. Phys. B*, 79(CERN-TH-1876):276–284, 1974.

[26] Alexander M Polyakov. Particle spectrum in quantum field theory. In *30 years of the Landau institute—selected papers*, pages 540–541. World Scientific, 1996.

[27] Yoichiro Nambu. String-like configurations in the weinberg-salam theory. *Nuclear Physics B*, 130(3):505–515, 1977.

[28] Bobby Acharya, Jean Alexandre, P Benes, Benedikt Bergmann, Sergio Bertolucci, A Bevan, Horea Branzas, Petr Burian, Michael Campbell, YM Cho, et al. Search for magnetic monopoles produced via the schwinger mechanism. *Nature*, 602(7895):63–67, 2022.

[29] ATLAS Collaboration. Search for magnetic monopoles and stable particles with high electric charges in $\sqrt{s}$ =13 tev pp collisions with the atlas detector, 2023.

[30] Eugene N Parker. The origin of magnetic fields. *The Astrophysical Journal*, 160:383, 1970.

[31] Michael S Turner, Eugene N Parker, and TJ Bogdan. Magnetic monopoles and the survival of galactic magnetic fields. *Physical Review D*, 26(6):1296, 1982.

[32] Blas Cabrera. First results from a superconductive detector for moving magnetic monopoles. *Physical Review Letters*, 48(20):1378, 1982.

[33] Arttu Rajantie. Magnetic monopoles in field theory and cosmology. *Philosophical Transactions of the Royal Society A: Mathematical, Physical and Engineering Sciences*, 370(1981):5705–5717, 2012.

[34] Hunmoo Jeon and Michael J Longo. Search for magnetic monopoles trapped in matter. *Physical review letters*, 75(8):1443, 1995.

[35] Claudio Castelnovo, Roderich Moessner, and Shivaji L Sondhi. Magnetic monopoles in spin ice. *Nature*, 451(7174):42–45, 2008.

[36] Kevin M Ellis. Magnetic monopoles: Quantization and quasiparticles, 2013.

[37] Robert J Aldus, Tom Fennell, Pascale P Deen, Eric Ressouche, Garret C Lau, Robert Joseph Cava, and Steven T Bramwell. Ice rule correlations in stuffed spin ice. *New Journal of Physics*, 15(1):013022, 2013.

[38] S Tetal Bramwell, SR Giblin, S Calder, R Aldus, D Prabhakaran, and T Fennell. Measurement of the charge and current of magnetic monopoles in spin ice. *Nature*, 461(7266):956–959, 2009.

[39] Romain Gervalle and Mikhail S Volkov. Electroweak multi-monopoles. *Nuclear Physics B*, 987:116112, 2023.

[40] YM Cho. Physical implications of electroweak monopole. *Philosophical Transactions of the Royal Society A*, 377(2161):20190038, 2019.

[41] YM Cho and D Maison. Monopole configuration in weinberg-salam model. *Physics Letters B*, 391(3-4):360–365, 1997.

[42] Kyoungtae Kimm, JH Yoon, and YM Cho. Finite energy electroweak dyon. *The European Physical Journal C*, 75:1–16, 2015.

[43] John Ellis, Nick E Mavromatos, and Tevong You. The price of an electroweak monopole. *Physics Letters B*, 756:29–35, 2016.

[44] PQ Hung. A model of electroweak-scale right-handed neutrino mass. *Physics Letters B*, 649(4):275–279, 2007.

[45] PQ Hung. Topologically stable, finite-energy electroweak-scale monopoles. *Nuclear Physics B*, 962:115278, 2021.

[46] George Lazarides, Qaisar Shafi, and Tanmay Vachaspati. Dirac plus nambu monopoles in the standard model. *Physical Review D*, 104(3):035020, 2021.